

SOIL DENSITY MODIFICATION WITH
FURROW OPENERS OF SIMPLE
GEOMETRIC SHAPE

By

GEORGE H. ABERNATHY

Bachelor of Science
New Mexico State University
Las Cruces, New Mexico
1952

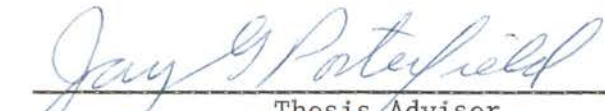
Master of Engineering
University of California
Davis, California
1956

Submitted to the faculty of the Graduate College of
the Oklahoma State University
in partial fulfillment of the requirements
for the degree of
DOCTOR OF PHILOSOPHY
May, 1967

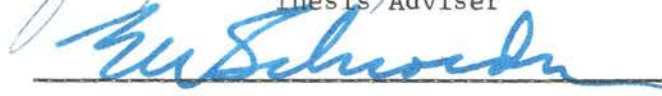
JAN 9 1968


SOIL DENSITY MODIFICATION WITH
FURROW OPENERS OF SIMPLE
GEOMETRIC SHAPE


Thesis Approved:




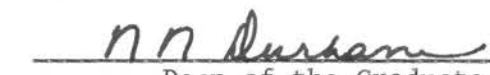
Thesis Adviser











Dean of the Graduate College

358287

PREFACE

A significant problem in the design of planting equipment is that the relationship of planter components to seed bed density is not known. To solve this problem, the effects of each component must be separately evaluated. Furrow openers of simple shape were chosen as the planter components to be studied.

Before the effect of furrow opener shape on seed bed density could be determined it was necessary to devise a method of measuring soil density using small samples. A method using gamma radiation decay rate, as suggested by Dr. J. F. Stone of the Agronomy Department, Oklahoma State University, proved to be satisfactory. The radiation method was used to determine the soil density patterns of nine furrow opener shapes as they passed through an artificial soil.

The author is indebted to all the advisory committee members at Oklahoma State University. These include Professor Jay G. Porterfield, Chairman, Dr. J. E. Garton, Professor E. W. Schroeder, Head, Agricultural Engineering Department, Dr. Stone and Professor J. V. Parcher, Civil Engineering Department. Many people at New Mexico State University gave the author considerable help, especially Dr. Marvin Wilson, Director, Agricultural Experiment Station. Others include Professor E. G. Hanson, Head Agricultural Engineering Department, and Dr. Morris Finkner, Department of Experimental Statistics.

TABLE OF CONTENTS

Chapter	Page
I. THE PROBLEM	1
Introduction.	1
Scope of Research	2
II. REVIEW OF LITERATURE	4
Effect of Soil Condition on Seedling Emergence and Plant Growth.	4
Soil Characteristics Affecting Tillage Research	11
Soil Response to Tillage Machinery.	14
Synthetic Soils for Tillage Research.	19
Density Measurement by the Gamma Radiation Technique.	24
III. THEORETICAL CONSIDERATIONS	27
Soil Compaction	28
Plastic Flow.	35
Fracture of Soil Beside Openers	42
IV. METHODS AND PROCEDURES	48
Apparatus	48
Soil Samples.	55
Opener Shapes	57
Sampling.	58
Density Measurement	63
Data Processing	67
V. RESULTS.	72
Density Patterns for the Various Soils	72
Results on "Artificial Fine" Soil	79
Comparison to Theoretical Models.	90
Evaluation of Slow Motion Films	95
Prediction Equations.	97
Effect of Furrow Compaction Wedges.	108
VI. SUMMARY AND CONCLUSIONS.	124
Suggestions for Future Work	128

	Page
LIST OF REFERENCES	130
APPENDIX A.	134

LIST OF TABLES

Table	Page
I. Summary of Decreased Density Zone Characteristics for Opener Face Angles on Artificial Fine Soil	80
II. Drag and Lift Forces for Various Opener Face Angles on Artificial Fine Soil	81
III. Comparison of Predicted and Observed Failure Angles.	93
IV. Effect of Wedge Displacement on Furrow Characteristics	114
V. Comparison of Observed and Calculated Maximum Pressures Under Furrow Compaction Wedges	115

LIST OF FIGURES

Figure	Page
1. Top View of the Unit Thickness Slice of Soil Used to Derive an Equation for Compaction Beside an Opener.	29
2. Model Used to Derive an Equation for Compaction Beside an Opener	29
3. Model Used to Derive an Approximate Expression for the Compaction Under a Furrow Bottom Wedge.	33
4. Two Dimensional Stresses Acting on a Cube of Soil	36
5. Mohr's Circle of Stresses Showing a Typical Failure Envelope for Soil	36
6. Stress Conditions for Plastic Flow Under a Planter Opener Using Mohr's Circle of Stresses	41
7. Loading Condition for the Derivation of the Rankine Passive Earth Pressure Formula.	43
8. Failure Block Predicted by the Rankine Theory	43
9. Diagram of the Coulomb Theory of Failure Behind a Rough Faced Retaining Wall.	45
10. Soil Failure Line Resulting from Pushing a Rough Faced Retaining Wall Against a Cohesive Soil.	45
11. Vertical Cross Sections of Those Openers Having Angularity in the Vertical Plane	47
12. Apparatus Used to Operate Test Furrow Openers Through Soil Samples	49
13. Strain Gage Recorder Used to Determine Forces Acting on Furrow Openers.	49
14. Strain Gage Transducer Used to Measure Drag and Lift Forces Acting on Experimental Openers	50
15. Sample Recording of Drag and Lift Forces Acting on a Planter Opener	52

Figure	Page
16. Force Transducer Clamped in Place to Calibrate for Drag Force	53
17. Soil Box Used to Prepare and Hold Test Specimen	53
18. Calibration Curve for Lift Force.	54
19. Calibration Curve for Drag Force.	54
20. Vertical and Horizontal Angles Used to Describe Test Openers	59
21. Furrow Bottom Compaction Wedges Used in the Experiment. . .	60
22. Cross Sectional Sampling Box.	62
23. Cross Sectional Samples Being Taken from a Soil Sample After an Opener has Passed Through.	62
24. Schematic Diagram of Equipment Used to Determine Soil Density by the Gamma Radiation Technique.	64
25. Cross Sectional Sample of Natural Soil in Jig for Gamma Radiation Density Measurement	65
26. Rate Meter and Hand Card Punch Used to Record Radiation Readings	65
27. Calibration Curve for Gamma Density Apparatus	66
28. Sample Data Sheet Showing Point Readings and Averages for a Section	68
29. Density Pattern in an Undisturbed Sample of Artificial Fine Soil	74
30. Density Pattern for Opener 0-82 1/2 in Artificial Fine Soil	76
31. Density Pattern of Opener 45-75 in Natural Medium Soil. . .	78
32. Effect of Opener Face Angle on Depth of the Reduced Soil Density Zone.	83
33. Effect of Opener Face Angles on Side Slope of the Reduced Soil Density Zone	84
34. Effect of Opener Face Angles on the Width of the Reduced Soil Density Zone	85
35. Effect of Opener Face Angle on Area of the Reduced Soil Density Zone.	87

Figure	Page
36. Effect of Opener Face Angles on Opener Drag Force	88
37. Effect of Opener Face Angle on Lift Force	89
38. Top View of Failure Block Orientation Necessary to Justify Rankine Solution of Furrow Wall Fracture	92
39. Effect of Opener Face Angles on Constant A of the Reduced Density Zone Boundary Equation	98
40. Effect of Opener Face Angles on Constant B of the Reduced Density Zone Boundary Equation	99
41. Effect of Opener Face Angles on Constant C of the Reduced Density Zone Boundary Equation	100
42. Effect of Opener Face Angle on the Depth of the Reduced Soil Density Zone	103
43. Effect of Opener Face Angles on the Boundary Slope of the Reduced Soil Density Zone	104
44. Effect of Opener Face Angles on the Width of the Zone of Reduced Soil Density	105
45. Effect of Opener Face Angles on Cross Sectional Area of the Reduced Soil Density Zone	106
46. Effect of Opener Face Angle on Drag Force	107
47. Effect of Opener Face Angle on Lift Force	109
48. Density Pattern for Compaction Wedge of 1/8 Inch in Artificial Soil	110
49. Density Pattern for Compaction Wedge of 3/16 Inch in Artificial Soil	111
50. Density Pattern for Compaction Wedge of 1/4 Inch in Artificial Soil	112
51. Density Pattern for Compaction Wedge of 1/8 Inch in Natural Soil	117
52. Density Pattern for Compaction Wedge of 3/16 Inch in Natural Soil	118
53. Density Pattern for Compaction Wedge of 1/4 Inch in Natural Soil	119

Figures	Page
54. Density Pattern for Compaction Wedge of 1/8 Inch in Remolded Natural Soil	121
55. Density Pattern for Compaction Wedge of 3/16 Inch in Remolded Natural Soil	122
56. Density Pattern for Compaction Wedge of 1/4 Inch in Remolded Natural Soil	123

CHAPTER I

THE PROBLEM

Introduction

Row crop production is widely practiced in American agriculture. Planting to obtain a satisfactory stand of plants is essential in row crop production culture. Engineers may contribute to successful stand establishment by designing equipment that will promote a favorable environment for seed germination and plant emergence. Failure to obtain satisfactory stands can, in many cases, be attributed to causes other than poor soil physical condition, but the planting equipment should do the best job possible under the existing conditions. Experimentation with crop planters has generally been of the "cut-and-try" procedure. This method has resulted in some improvement, but little information is available on the effect of planter components, such as openers and presswheels, on the soil physical conditions around the germinating seeds. Several investigators have performed research to determine the most favorable soil conditions for seed germination and emergence. They have considered such fundamental factors as moisture, soil density, temperature, aeration, and physical impedance in the seedbed. Intelligent application of this information requires quantitative knowledge about the effects of planter opener shape and the initial soil conditions on the final seedbed density pattern.

Scope of Research

Research under this project was limited to the effect of certain angular faced furrow openers on the density pattern of several soil medii. The only two variables were opener shape and soil condition. Operating speed and tool depth and width were constant throughout the experiment. No furrow closing devices or presswheels were used in the experiment.

The evaluation of opener effects on the density patterns of soil was on the basis of laboratory experiments. The final test of any agricultural machine or mechanism is the effect on the crop. For soil engaging tools this effect can be broken into two separate actions. First, the tool has some effect on soil properties. The change in soil properties in turn affects the crop. The overall effect of machine on crop can only be measured by field experiment. In this study, the only consideration was the effect of mechanisms on soil. Certain factors such as speed, depth, and soil condition are difficult to control in the field. Soil condition was difficult to control even in the laboratory, but speed and depth could be controlled; therefore, the laboratory method was selected.

There are certain advantages to working on this type of research in the laboratory. Photography can be used since light can be controlled more easily. Forces are easier to measure and record in the laboratory unless expensive field equipment is available, and soil samples can be handled with more facility.

The difficulty of controlling or even measuring soil condition in natural samples precluded their extensive use in this type of study.

A large portion of the research was conducted using an artificial mixture of sand, clay, and oil. Although the results may not be directly comparable to natural soils, the relationships established should be useful in narrowing the range of treatments that need to be tested on natural soils.

During the early stages of this research a satisfactory method of measuring soil density changes caused by planter openers was not available. Considerable effort was expended attempting to measure density in small volumes by the gravimetric method and by measuring resistance to penetration by a small needle. Using small sampling tubes it was impossible to consistently obtain samples of equal volume. The penetration resistance method was satisfactory in the large homogeneous portions of the cross section but near the boundaries failure cracks tended to form giving erroneously low readings. The gamma radiation technique, as explained in the procedure section, provided the accuracy and convenience required for this research.

CHAPTER II

REVIEW OF LITERATURE

In the literature reviewed, no specific reference was located on the measurement of soil density changes due to planter opener shape. Modified planter openers have been tried by several researchers (Abernathy, 1963; Anonymous, 1957; Holekamp, et al., 1962), but these experiments evaluated the crop response rather than the changes in soil physical properties. This chapter will cover some of the research related to the effect of planter opener shape on seedbed soil density. Some of these related areas are: effects of soil conditions on seeds and seedlings, soil factors affecting soil working machinery research, soil response to tillage machinery, experimental methods for soil machinery research, and density measurement techniques.

Effect of Soil Conditions on Seedling Emergence and Plant Growth

The mechanics of cotton seedling emergence have been discussed by Garner and Bowen (1963). The conditions necessary for organic growth are listed as: available water; proper temperature range, adequate oxygen; lack of inhibiting compounds such as carbon dioxide; light in some cases; and the lack of excessive mechanical impedance. These authors made an extensive review of research on the mechanics of seedling growth and combine this with their own experimental results to

describe seed germination and emergence as follows. The growth and emergence of cotton seedlings may be described in three phases. In the first phase, the root tip protrudes from the seed and grows the first forty millimeters mostly by elongation. In the second phase, the elongation takes place only at the root tip. The third phase consists of elongation at the root tip and in the hypocotyl, being most rapid just below the cotyledons.

Garner and Bowen have also reviewed soil mechanics theory to evaluate the forces encountered by seedlings. The work of Bekker (1961) was used to evaluate the force necessary for downward penetration. His equation related plate sinkage and pressure to certain soil characteristics.

The maximum force required for emergence of a plant from a homogeneous soil mass was represented by the familiar Mohr theory of rupture (Terzaghi and Peck, 1948). Compared to experimental results this calculation gave smaller resistances than the measured plant force, but more closely controlled experiments were needed to evaluate the difference.

The effect of soil compaction around seed has been evaluated by numerous authors. Triplett and Tesar (1960) planted seed at zero, one-fourth, one-half, and one-inch deep. They applied compaction pressures of zero, three, six, and twelve psi. All seeds so planted failed to germinate at a moisture tension of ten atmospheres when this was the total amount of moisture available for germination. In soils with higher original moisture contents, the high compaction pressures caused increased emergence except at the one-inch depth and twelve psi pressure. When the samples were irrigated after compacting the soil, the

compacted samples emerged better than uncompacted samples except at a depth of one-half and one inch.

Stout (1960) investigated the effects of compactions over seeds planted in soil with moisture content of 16 and 12 percent. Those in the compacted soil absorbed moisture faster in the first five hours, but later the seeds in the loose soil gained moisture at a more rapid rate. This would suggest that compact soil may retain moisture but that the soil does not readily yield this moisture to the seed when it is needed for germination.

Stout, Buchele, and Snyder (1961), reported that compacting soil may control the moisture and air available to seeds and produce mechanical resistance to penetration. They applied compaction pressures one-half, five, and ten psi. In the dry state, the lower compaction pressure gave better plant emergence than the higher pressures. Under abundant moisture conditions, seeds in the highly compacted soils emerged somewhat better. Soil compaction at the seed level was more effective in increasing emergence than was compaction at the soil surface. When surface compaction was used, emergence was improved by compacting soil at the seed level.

Morton and Buchele (1959) evaluated the factors affecting the force and energy requirements for emergence of seedlings. Soil samples with moisture contents of 12, 16, and 20 percent were compacted with pressures of one-half, one, two, four, eight, and sixteen psi. All finished samples were three inches thick. Mechanical plungers with diameters of 0.078, 0.106, 0.162, and 0.275 inches were pushed upward through the soil samples. Force and displacement were recorded. They concluded that emergence energy increased with compaction, high

initial moisture content and the amount of surface drying. Methods of reducing energy were listed as applying compaction at the seed level and maintaining high surface moisture. Small diameter plungers emerged with lower energy input than did large plungers.

The effect of seedbed compaction on soil drying rate has been evaluated by Johnson and Henry (1962). Test soil samples were obtained by screening an air-dried soil into various size ranges. Test samples were assembled in plastic containers, and in all samples the top three inches of soil could be separated for weighing. Corn seeds were placed two inches deep in each sample. The top one-half inch of soil in all samples was dry. Compaction pressures of zero and five psi were applied in five different patterns. Samples were aged in a controlled environment chamber with heat and wind to cause drying. Drying rate of the sample seedbeds was only slightly affected by the compaction treatments applied to small-sized granules. For larger granule size samples, compaction decreased the drying rate. The drying rate of the soil was found to be almost independent of the original moisture content and almost wholly dependent upon the size of aggregate in the seed bed. Larger aggregate dried at a faster rate than did small aggregate. Surface compaction appeared to reduce growth in the small granules. Where the compacted layer over the seed was allowed to dry, the seedlings had difficulty emerging. Where the compacted layer was kept at a relatively high moisture content, the soil strength was low and the plants were able to emerge adequately. Compacting soil at the seed level reduced the over-all drying rate; and, at low soil moistures, increased growth as compared to the plot without compaction.

Gill and Miller (1956) performed an experiment in which seeds were placed between a glass bead pack and a rubber diaphragm so that horizontal pressure could be applied to the diaphragm. At a confining pressure of 10 psi, they found germination and emergence to be related to the percent of oxygen available in the air which was supplied to the seeds. At confining pressures of 70 psi, no root growth occurred. Bailey (1963) in an experiment with corn seedlings in various media, such as glass beads, concluded that the seedling radical must have either large pores into which it can penetrate or it must be able to displace the soil in a manner similar to a penetrometer. He found that seedlings were unable to penetrate a pack of 38 micron glass beads when lateral pressures of 0.6 kilograms per square centimeter were applied.

Taylor and Gardner (1960) evaluated the penetrating ability of seven different crops by using waxes with various penetration resistances below the seeds. Using a standard penetrometer they conclude that at penetration numbers of 15.5 or harder, none of the seven crops were able to penetrate to a depth of one millimeter. At penetrations of 19.5 and softer, all crops were able to penetrate. Legumes did not penetrate the wax better than other crops. The failure of cotton to penetrate as well as several crops was attributed to the large diameter root tip, since other crops which produce the same large diameter root tips were also unable to penetrate. In a field experiment, Taylor and Gardner (1963) demonstrated that root penetration was decreased by high soil bulk densities and low moisture contents. In their experiment, aeration was not a cause of low root penetration because as moisture content increased aeration decreased and root penetration increased. Phillips and Kirkham (1962) demonstrated that density could cause

decreased length of corn roots. Aeration was not a problem in this case because sand and glass bead media at the same penetrometer readings also caused reduction in growth.

Jamison and Weaver (1952) in a study of penetrometers determined that on certain soils the penetrometer readings were related to porosity when the moisture contents of the two samples were consistent. In clay soil, penetrability was almost purely a function of moisture content. Veihmeyer (1948), in an experiment to determine the factors involved in the effect of soil compaction on root penetration, observed that soil samples settled by flooding resulted in densities of from 1.0 to 1.6 specific gravity. Roots of ordinary field crops did not penetrate soil in which the dry density exceeded 1.8 specific gravity. This experiment demonstrated the improbability that flood-irrigated soil can have sufficiently high density to cause failure of root penetration in the cultivated zone.

One further justification for soil compaction around the seed has been discussed by Matthes and Bowen (1962). They have written a general differential equation involving temperature differences and the diffusion coefficient to demonstrate that soil moisture content can be changed by vapor movement in the soil. They demonstrated that condensation and evaporation can be controlled by compacting certain locations in the soil. When the compacted area is on the cold side of a moist two-temperature system, condensation may occur in the compacted soil. This results from a decrease in the diffusion coefficient at the cold side of the system.

Compaction of soil beneath and around seeds has certain complicating factors. It is difficult to compact moist soil without producing

a certain amount of puddling. Puddling has not been well defined, but Beachar (1955) has discussed puddling generally. He concluded that puddling is not merely an increase in bulk density, but a combination of increased bulk density and a rearrangement of soil particles. Buehrar (1943) demonstrated that puddling can be detrimental to soil physical condition when it is done at moisture contents near the moisture equivalent, that is, field capacity. Tillage operations that would normally produce a puddled condition at the moisture equivalent were found to produce a friable soil condition when applied at moisture contents both higher and lower than field capacity.

The compaction of soil at various moisture contents has been investigated microscopically by Day and Holmgren (1952). Three different soils at numerous moisture contents were compressed and then impregnated with a plastic material. Sections were cut and microphotographs were taken. They concluded that at low moisture content the compaction force was resisted by transmittal of force between soil particles. At a moisture content of 29 percent inner-pore spaces tended to be filled by plastic deformation.

In summary, the effects of soil compaction around seeds has been studied by numerous investigators concerned with planting, germination and emergence. This review indicates that a firmly compacted base helps the plant as it pushes upward to emerge from the soil. A firm foundation has been observed to maintain moisture content over a longer period of time. There may be some question regarding the availability of the conserved moisture to seeds. Excess compaction below or above the seed may cause physical impedance of the growing seedling. Equilibrium of forces on the seedling must also be maintained. Despite

considerable research, more information is needed concerning optimum conditions of the soil below and above germinating seeds.

Soil Characteristics Affecting

Tillage Research

The most active period of agricultural engineering research on the soil characteristics affecting tillage was during the late 1920's and early 30's by Nichols and several others, at the National Tillage Machinery Laboratory in Auburn, Alabama. During this period, much effort was expended in attempting to describe soil strength with a single-valued index. This effort was unsuccessful and to date no single-valued constant can be used to describe soil strength.

In one of several early publications on the effects of soil characteristics on tillage, Nichols and Baver (1932) concluded that all of the soil factors needed to evaluate soil reaction could be determined from the Atterburg consistency limits. This information was useful because soil testing equipment was not available to those in the field. For most engineering work the soil constants are determined by testing. Nichols and Baver found that the soil factors affecting tillage most were internal angle of friction, compressive strength, cohesion, adhesion and soil to metal friction angle. These soil constants are in use today. The results that were obtained by a tillage tool were expressed in terms of fragmentation, arch action, compaction, or shear. In an early evaluation of the factors which affected the dynamic properties of soils, Nichols (1931) determined relationships between clay content and adhesion, cohesion, compression and shear. Using mixtures

of Cecil Clay and pure sand, he found that cohesion varied as the square of the clay content; adhesion, compression and shear strength varied as the first power of the clay content.

Wheeting (1936) has made a determination of static friction for six soils under different moisture conditions. For each soil, the maximum value of friction occurred at the wilting point. In this experiment a watch glass was used and at high values of normal force the watch glass sank into the soil tending to give somewhat misleading data. The most comprehensive report on soil to metal friction was by Nichols (1931). Using Cecil Clay and sand mixtures for soil he pulled a metal object over the surface to determine the coefficient of friction. He divided friction into four phases according to soil moisture content. In the first phase, compression occurred. The apparent friction was due to work being done on the soil and this increased as the square of the speed. The second phase occurred at a slightly higher moisture content and represented true friction. The force varied with the clay content in an increasing manner but was independent of speed. The third phase was adhesion which occurred above 16 percent moisture content for a non-plastic soil. The adhesive phase gave the highest values of friction. The fourth phase occurred at a very high moisture content when the water tended to lubricate the slider and friction decreased to the minimum value.

Soil shear strength was evaluated by Nichols (1932) using a synthetic mixture of Cecil Clay and pure sand. He determined shear strength by using a three-ring press with a moveable center ring. Displacement and force were continuously measured. Nichols concluded that shear was proportional to vertical pressure. Increased moisture

content up to the lower plastic limit caused increases in shear strength. Further increases in moisture content caused a decrease in shear strength. At moisture contents above the plastic limit, soils were found to fail in a viscous manner rather than in pure shear.

Bouyoucos (1932) determined the sticky point of a soil by pulling a metal disk away from a moist soil surface. He found that muck soils had zero stickiness. It was determined that the addition of sand to "sticky" soil samples did not decrease the stickiness, but that the addition of a muck soil did. Bouyoucos emphasized the difficulty of determining adhesion and metal-to-soil friction because the soil tended to stick to the surface of the metal and the evaluation was then a tension effect in the soil, or in the case of a sliding disk, was actually the soil-to-soil friction rather than soil-to-metal friction.

Payne (1956) lists, shear strength, soil-to-metal friction and bulk density as the constants affecting soil reaction to tillage tools.

Bailey and Weber (1964) evaluated methods of measuring soil shear strength in place. An annular grouser plate was found to give the most consistent results when compared to triaxial compression tests on the same soil. A similar device was used by Korayem and Reaves (1961). They also used a smooth annular plate on the rotating device to measure soil to metal friction. Shear strength has been shown by Rowe and Barnes (1961) to depend on the speed of shear failure. Siemans, Weber, and Thornburn (1964) report the same effect.

Hendrick and VandenBerg (1961) found that the tensile strength of Lloyd Clay briquettes was independent of load application rate. Briquettes loaded at the high rate, failed with less strain energy.

In conclusion, the most important soil characteristics affecting tillage research would appear to be shear strength as determined by the Coulomb constants; that is, cohesion and internal friction angle. Adhesion and soil-to-metal friction are important for all phases of soil-machinery research, but are generally difficult to evaluate since adhesion may prevent the measurement of soil-to-metal friction.

Soil Response to Tillage Machinery

If a planter furrow opener is to be designed to compact soil at the bottom of the seed furrow, it is necessary to predict the density that will result from a specific shape. Soehne (1958) has shown a relationship between soil moisture content, compaction pressure and porosity. For a heavy loamy soil he found the critical moisture content to be between 18 and 22 percent. At lower moisture contents the dry soil particles resisted compression and at higher moisture contents pore water resisted compression. Resistance to the plastic flow of soil around a plunger decreased 80 times as soil moisture content increased from 10 to 26 percent.

Soil compaction by planter openers may be comparable to the action of a soil penetrometer which has been investigated by Reaves and Nichols (1955). They described consolidation of soil in two phases. The first phase was the collapse of the random particle arrangement in loose soil. The second phase was rearrangement of solids into the voids. The later phase was theorized to be controlled by cohesion and frictional forces.

In addition to compaction, a furrow opener must make a slot in the soil into which seed of field crops can flow without restriction. For

large seeded crops such as cotton and corn, a slot three-quarters of an inch wide should be sufficient. Most planters have openers about one and one-quarter inches wide. It may be found that soil failure patterns around planter openers are predictable from soil mechanics theory and from the results of research on soil failures around tillage machinery.

Soil reaction to vertical and horizontal loads has been extensively studied by civil engineers. These studies provide information for the design of foundations and retaining walls to carry the expected loads with a minimum of construction expense. Analysis methods have been summarized in soil mechanics texts (Sowers and Sowers, 1958; Terzaghi and Peck, 1948). Failure surfaces in cohesive soils caused by the movement of a rough faced retaining wall toward the soil is described by a logarithmic spiral. The spiral is positioned with the origin in the soil near the back of the wall, with the exact location depending on the cohesive properties of the soil. The spiral surface extends from the bottom of the wall toward the soil until it becomes tangent to the plane $(45^\circ - \phi/2)$, where ϕ is the soil internal friction coefficient. For a smooth wall, the failure surface is described as a plane from the bottom of the wall extending upward toward the soil at an angle of $(45^\circ - \phi/2)$. Most research reports (Jumikis, 1956, Konder, 1963) agree with this theory, but some consider simple rupture surface shapes such as circular arcs (Anderson, 1946) adequate for engineering design.

Several authors whose work is reviewed below have explained failure patterns in front of tillage tools in terms of soil mechanics. This procedure may be justified for planter openers, but it is not

obvious that a direct thrust load duplicates the failure caused by a sliding wedge such as a runner opener.

The most comprehensive research on tillage tools has been done by Payne and Tanner (1959). They experimented with narrow and wide chisels with vertical angles from the direction of travel of 20 to 160 degrees. Chisels at all of these angles were found to cause a circular section of soil to break ahead of the chisel in the horizontal plane. A triangular block of soil was formed on the front of all chisels. At angles up to 90 degrees, the soil block appeared to move up the chisel as the tool was pulled through the field. At angles greater than 90 degrees, the soil block was observed to move downwardly and off the chisel. They have evaluated the shape of the semi-circular failures around the chisels. Measurements were made on the initial block that failed and the results were presented graphically in their report. Angles greater than 90 degrees were found to increase the draft necessary to operate the chisel.

Tanner (1960) evaluated chisels two inches wide at vertical angles of 20 to 132 degrees from the direction of travel. Using a one-sided box with a checkerboard pattern on the soil, he evaluated, through photography, the failure angles in the soil. For all of the angles included in this experiment, the soil adhered to the chisel and a cone-shaped block was pushed in front of the blade. The shape of the block and adhesion to the chisel caused an upward force to be exerted on the 90 degree angled chisel and at obtuse chisel angles. Compression of the one-half inch of soil below the chisel appears to be almost 50 percent of the original density of the soil showing that considerable compaction can inadvertently be done by tillage implements.

Failure planes in front of inclined chisels have been investigated by Siemans, Weber, and Thornton (1964). By using the principles of passive retaining wall failure as outlined by Terzaghi and Peck and summarized previously in this report, Siemans, et al., predicted the draft required to operate chisels. Spiral centers for the soil failure surfaces were assumed in their computation and the center that resulted in the minimum draft on the tillage tool was accepted as the true spiral center. For tools inclined less than 70 degrees from the horizontal the foregoing did not apply. For these angles a plane failure at an angle of $(45^\circ - \phi/2)$ was assumed. In this case, equilibrium for an individual block of soil was assumed and the resulting draft was computed by summing the forces of shear resistance, friction and weight in the horizontal and vertical planes. High-speed movies were correlated through oscillograph readings to relate draft and soil failure. Maximum force was found to occur at the same time a failure plane developed in the soil. For tool inclinations of 15 to 60 degrees the failure was observed to be a plane at approximately the predicted angle. Failure plane angle was not related to tool angle. For tool angles of 70 and 90 degrees, the bottom surface was curved and then became a plane as had been predicted on the basis of soil mechanics. In all cases, the measured failure plane was near the predicted value.

Speed did not have a linear effect on forces. The author demonstrated that acceleration forces did not explain the total gain in draft caused by increased speed. The explanation was given that at higher speed shear strength is increased causing a decrease in the failure surface angle. In this research, the angle of the resulting force on the chisel was computed, but since no allowances were made for

soil adhering to the face, these data seem ambiguous. Calculated and measured values of soil resistance forces did not agree well in this experiment seeming to indicate that more research is needed before a total account can be made of all the forces acting on plane chisels.

Rowe and Barnes (1961) evaluated the effects of speed and shear strength on the draft requirements of plane chisels. In soils with high clay contents calculated values of draft versus speed did not agree with observed results. Inclusion of an acceleration allowance did not improve the fit. When the shear strength increase due to speed of shearing was included in the calculated curves, agreement with the observed curves was good for this type of research. They concluded that increased soil shear strength at high speeds accounted for the draft increase.

The action of subsoilers in breaking up soil has been investigated by Nichols and Reaves (1958). They found that a soil wedge formed on the front of chisels and that the wedge was subject to plastic flow. When they designed a metal wedge to replace the accumulated soil, draft was reduced by about 25 percent. Soil blocks were observed to form in front of the chisel when the resistance to compression at the bottom of the soil block ahead of the chisel was greater than the shear value of the soil. At high moisture content, the failure tended to be a plastic flow rather than a series of shear failures as observed at lower moisture contents. No measurement of the resulting soil properties were made in this experiment.

Synthetic Soils for Tillage

Research

The first reference to the use of synthetic soils for tillage research found by this author, was by Nichols (1931). The synthetic soils used by Nichols were mixtures of Cecil clay and sand. Using these mixtures and various moisture contents, Nichols developed formulas for computing the shear strength of soils with various clay contents. Nichols also used the same artificial soil mixtures to determine the frictional properties of soil. These formulas are useful in explaining the concept of soil to metal friction. In recent tillage research projects, frictional properties have been evaluated by sliding the material to be tested over soil samples.

Korayem and Reaves (1961) have determined the frictional properties of certain artificial soils and evaluated the use of these artificial soils in a study of plane chisels. The mechanical characteristics needed for tillage research were assumed to be angle of internal friction, cohesion, soil-to-metal friction angle, and adhesion. In that research, the angle of internal friction and cohesion have been determined for various artificial soil mixtures. The ingredients in the artificial soil mixtures were bentonite and sand. The moistening agent used in these soils was ethylene glycol which does not evaporate rapidly at room temperatures, but it does diffuse into the air at a low rate. At normal room temperature it was satisfactorily stable for the period of time necessary for most tillage research. The constituents of soil were mixed by using a single-spindle beater. The mixture was arbitrarily called "saturated" when a glistening appearance of the soil

appeared and the materials felt wet to the touch. With zero clay content this occurred when 18 percent, by weight, of ethylene glycol had been added to the soil. When the mixture was 100 percent clay, the percent of ethylene glycol needed to cause saturation was 110 percent. Throughout this experiment the glycol content was less than 50 percent of saturation so that no ethylene glycol came out of solution.

The soil characteristics of cohesion and internal friction were evaluated on a triaxial test apparatus using standard techniques. Samples were prepared by tamping the artificial soil mixture lightly into a mold and then preconsolidating at a pressure of one kilogram per square centimeter for 15 minutes. The sample was then removed from the mold and placed in the triaxial test machine.

The conclusion from these triaxial tests was that artificial soils can be compounded using moistening agents such as ethylene glycol or oil to maintain constant soil strength factors over a considerable period of time. Artificial soils can be compounded to have characteristics similar to natural soils.

Selig and Rowe (1960) studied the engineering characteristics of a number of artificial soil mixtures to determine the variety of properties that could be obtained. They also commented on the stability of the mixtures. The soils were compounded using a variety of clay, silt, and sand materials. The moistening agents used were water, light mineral oil, and ethylene glycol. Several different mixtures of these ingredients were subjected to Atterburg limit tests, Harvard miniature compaction tests unconfined compression tests and triaxial compression tests.

Water and ethylene glycol moistened samples gave comparable Atterburg limits. Where oil was used, the limits varied radically as compared to the water moistened samples. The maximum density obtained by standard test increased for soil samples as average particle size increased. Optimum compaction moisture decreased as average particle size increased. Of the three moistening agents, water gave the highest dry density with the lowest moisture content. Ethylene glycol gave about 10 percent lower dry density at a 6 percent higher liquid content. Oil gave the lowest dry density and required the highest moistening agent content for optimum compaction.

The maximum unconfined compression strength was independent of the proportion of clay, silt, or sand but depended on moisture content. Maximum strength of clay samples occurred at higher moisture contents than mixtures of clay and sand or clay and silt. Ethylene glycol and oil reduced the unconfined strength compared to water and the points of maximum strength occurred at higher moistening agent contents.

Stability was judged best for the samples prepared with oil as the liquid. Such samples were stable for six months. Ethylene glycol was found to separate from the soil mixture.

The authors concluded that artificial soils should be useful and satisfactory for many types of research, but it does not appear that all soils can be duplicated by an artificial mixture.

Korayem and Reaves (1961) evaluated the use of artificial soil as a medium for model studies of tillage tools. The tools evaluated in this case were plane chisels operated in a laboratory soil tank. They conclude that artificial soil can be used to perform tillage research. It was observed, in the course of their experiment, that although the

binding agents had considerably lower cohesive properties than water, the familiar rupture planes did develop in the soil around the chisel, indicating that the action of the tillage tool was near that expected in a normal water-moistened soil.

Bailey and Weber (1964) used artificial soil to evaluate various methods of determining the shear strength of soils. The devices tested in their experiment were the annular grouser plate, the torsional shear head, and the triaxial apparatus. Two known clay soils were used with low and high viscosity oils. Their data show the soil with low viscosity oil to have cohesion varying from zero to about one psi for the 95 percent confidence limits and a friction angle of 37 to 42 degrees. For the high viscosity oil sample, the cohesion varied from 0.5 to 1.2 psi and the internal friction from 31 to 36 degrees. In this experiment the annular grouser plate was the only in-place device to yield data whose 95 percent confidence interval consistently overlapped or fell within the triaxial values. It was concluded from these data that the torsional shear head was less desirable as a means of evaluating soil shear strength than the annular grouser plate if triaxial tests are accepted as the standard.

Artificial soil has been used in a practical tillage experiment by Siemens, Weber, and Thornburn (1964). The soil used by these researchers was a known clay soil mixed with low viscosity oil at a rate of 10 percent by weight. This artificial soil remained stable for a period of six months allowing research to be carried on for a considerable period of time with no significant differences in the soil characteristics. The soil, as used in this experiment, was similar to a damp, coarse silt. The frictional properties of the soil were

determined by measuring the force required to slide a metal plate over the soil. The plate was constructed of the same material as the model tillage tool. Shear-strength properties were measured by the triaxial test machine and by direct shear tests. They found that the results of the two shear tests were very similar. The cohesion intercept was 0.8 psi and the internal friction angle was 36.5 degrees for both machines. For the soil used in this experiment, the angle of soil-to-metal friction was 24 degrees and the adhesion intercept was negligible.

Soil preparation in this experiment consisted of rototilling the soil twice, striking the surface with a blade to take out minor indentations and a variable number of roller passes to obtain different densities. All tool tests were made after six roller passes. The tools evaluated in this experiment were plane chisels with widths of two, three, four, and five inches operated at angles from the horizontal in the direction of travel of 15, 30, 50, 70, and 90 degrees. Soil failure surfaces were adequately predicted from soil mechanics theory showing that artificial soils can be subjected to standard failure analysis. The draft was not accurately predicted in this experiment, indicating that more research is needed to adequately explain the total action of tillage tools.

Mink, Carter, and Mayeux (1964) have used artificial soil to evaluate the effects of an air slide on soil-engaging tools. The soil used in this experiment was clay, sand, and low viscosity oil. The soil samples, through which chisels were to be drawn, were prepared by rotary tilling, striking level, and rolling with a 90-pound weight until the desired density had been obtained. The variations in draft, caused

by differences in soil conditions, were found to vary only 1.49 percent over a period of three months during the investigation.

The use of artificial soil to evaluate earth-moving equipment has been reported by Cohron (1961). The soil used by Cohron consisted of clay, sand, and low viscosity oil. Different proportions of these materials were used to produce a range of soils. The internal friction angle was varied by increasing the bulk density of the sample. This was also found to increase the cohesion of the soil, but had little effect on the friction of steel-on-soil. Cohron reports that the soils used in this experiment remained in stable condition for long periods of time and several months of research were possible without significant changes in the engineering properties of the soil. One of the problems raised by Cohron is that the artificial soils cover only a narrow range and that a greater variety of artificial soils are needed. The results of model studies on scraper-loader time showed that results obtained in the soil bin with artificial soil and an electronically-controlled model yielded more consistent data than did field observations of full-scale equipment operating on variable soil conditions. The ability of model testing to detect small differences was emphasized.

Density Measurement by the Gamma Radiation Technique

Certain radio-active elements emit energy in the form of gamma rays. Gamma rays are normally visualized as particles called photons since they can be counted by certain electronic devices. Photons are emitted from their source in all directions. As the photons pass through matter they lose energy and experience direction changes by

three mechanisms (Glasstone and Sesonske, 1963). These are, first, the photoelectric effect where the photon transfers all of its energy to an orbital electron of an atom. The displaced electron is normally replaced by a higher orbit electron with the emission of an X-ray photon of much less energy than the gamma ray photon. A second effect of matter on photons is the Compton interaction. Here the collision between the electron and the photon is elastic in nature and only part of the photon energy is transferred to the electron. In the collision, the photon changes in both direction and energy level. As the scattering angle increases the energy loss by the photon also increases. The third effect of matter on gamma rays is pair production. A photon is absorbed by the nucleus of an atom resulting in the formation of an electron - positron pair. This effect is important only at high photon energy levels.

It is seen from the foregoing that as a beam of electron passes through matter some of the photons will be absorbed, some will be scattered and others will lose energy. This effect is usually referred to as attenuation.

Attenuation is assumed to increase with radiation intensity, I , and with matter thickness, dx . Attenuation is defined as the change in intensity dI , and μ is the linear attenuation coefficient.

Then

$$dI = -\mu I dx \quad (2.1)$$

or

$$\frac{dI}{I} = -\mu dx.$$

The solution of which is

$$\log I = -\mu x + c. \quad (2.2)$$

When

$$x = 0$$

$$I = I_0$$

and

$$\log I_0 = c.$$

Therefore $\log I - \log I_0 = -\mu x. \quad (2.3)$

This equation is valid for a column of parallel gamma rays.

Davisson and Evans (1952) stated that a point source can be considered a collimated beam if the solid angle is not greater than 0.016 steradians. They used a set of lead shields to obtain such a beam to determine absorption coefficients. Smith and Dixon (1963) used a collimated beam of the same type to determine the direct absorption of soil samples. They used absorption data to develop equations applicable to soil density determination by the back-scatter technique.

Vomocil (1954) investigated the use of gamma rays to determine the density of soils in place. He pointed out that nearly all the elements in soil interact with gamma rays in a similar manner except hydrogen. Water is the principle source of hydrogen in the soil. Smith and Dixon were unable to detect any differences in readings due to water content changes normally found in soil. We could thus expect that a certain mass of soil and water would have a definite attenuating effect that is independent of composition on a gamma ray beam. For a known length of soil sample, the total attenuation depends on the soil density.

CHAPTER III

THEORETICAL CONSIDERATIONS

The movement of soil engaging tools such as planter openers or chisels through soil forces the displacement of particles in the path of the tool. Reaction and displacement of soil in the immediate vicinity of the tool probably depends on the shape of the tool and the physical characteristics of the soil. About five different mechanisms of soil failure can be visualized. First is elastic deformation where strain is linearly proportional to stress and the material returns to its original size and shape if the stress is removed. Second is compaction or consolidation where stress and strain may be linearly related but there is little or no recovery of the strain when the stress is removed. Third would be plastic failure where the material flows without change in volume. Fourth is granular flow where the soil gains in total volume during failure due to rearrangement of the particles. The fifth type of failure would be fracture. It is probable that soil failure around agricultural tools involves all of these; therefore, applicable theoretical analysis will be difficult if not impossible with presently available theories.

Despite the difficulty of analyzing failure mechanisms at all points in the soil around tools, it may be possible to construct some simple models that will approximate the results. Three modes of action caused by planter openers passing through soil will be proposed. These

include soil compaction beside and below openers, plastic or granular flow from beneath openers and soil fracture beside openers.

Soil Compaction

If the soil beside an angular-faced opener is compacted as the opener moves past, we may approximate the action as follows. Figure 1 is a top view of an angular-faced opener. Let us consider a vertical slice of soil beside the opener such as ABCD. As the opener moves forward, some soil in the area adjacent to the opener face will be displaced in a forward direction. However, the final compaction pattern will be two dimensional beside the opener; therefore, deflection in the direction of travel was not considered in the following development. The unit thickness slice of soil from Figure 1 is shown in Figure 2 in a plane normal to the direction of travel. Shear stresses on the front and rear surfaces of the slice are assumed to be equal and opposite; therefore, they need not be considered.

The unit thickness slice of soil appears as DCEF, where D and C refer to the same corners as in Figure 1. As the opener pushes the soil to the side, it exerts a maximum unit pressure P against the furrow wall. At some distance x beside the opener the applied pressure is balanced by a compressive stress σ and a portion of the triangularly distributed shear stress with a maximum value of S . At some distance L the stresses were assumed to become insignificant. At the point x , by summation of horizontal forces

$$Pd_0 = \sigma d_0 + Sx\left(1 - \frac{x}{2L}\right) . \quad (3.1)$$

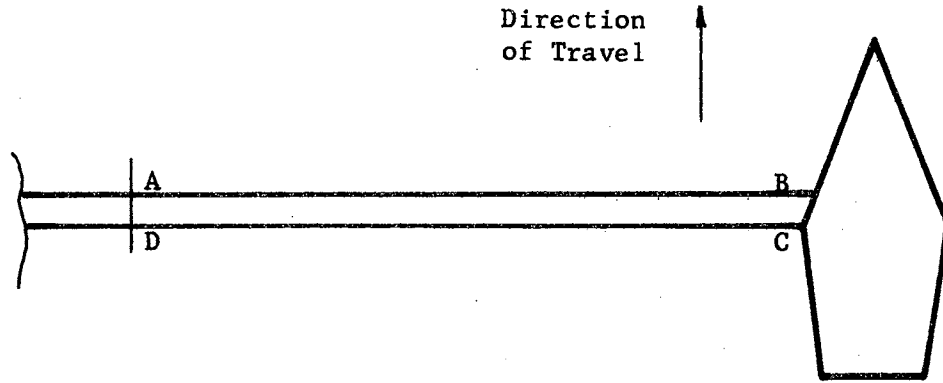


Figure 1. Top View of the Unit Thickness Slice of Soil Used to Derive an Equation for Compaction Beside an Opener

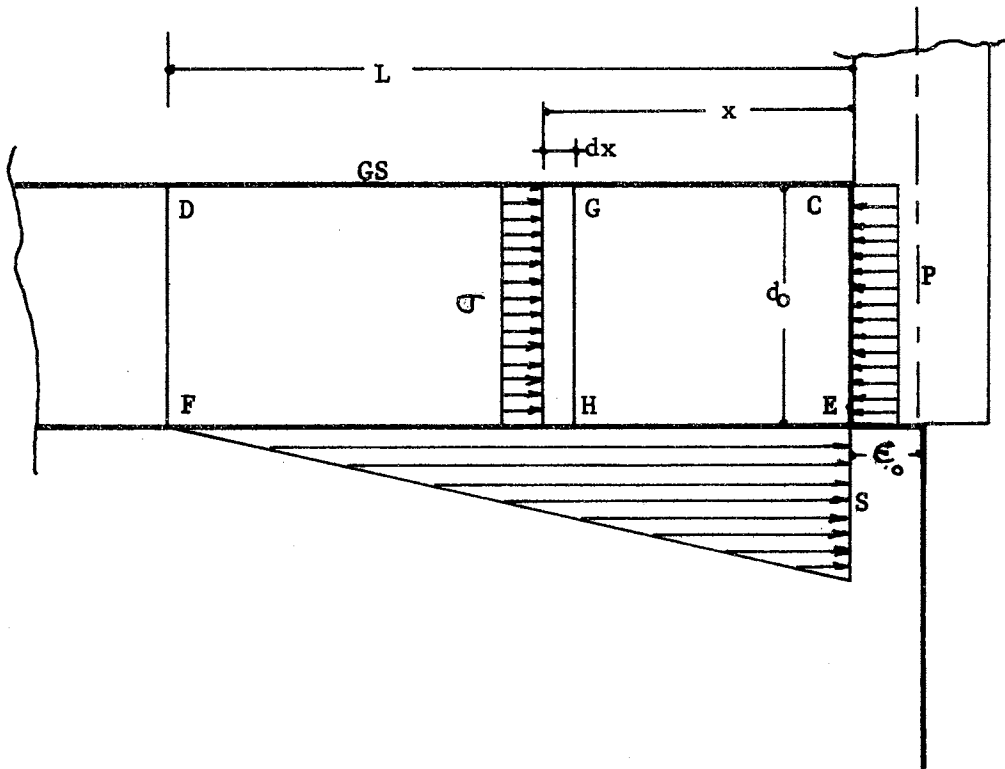


Figure 2. Model Used to Derive an Equation for Compaction Beside an Opener

For the thin layer of soil dx at point x the compressive stress is

$$\sigma = P - \frac{Sx}{d_0} \left(1 - \frac{x}{2L}\right) \quad (3.2)$$

Let compressive unit stress and unit strain be quadratically related so that

$$\delta = A\sigma - B\sigma^2 \quad (3.3)$$

In 3.3, δ is the unit strain, σ is the unit stress and A and B are constants to be evaluated by a soil test similar to a consolidation test. If the compaction of the thin layer dx is $d\epsilon$, then

$$d\epsilon = -\delta dx \quad (3.4)$$

Bringing in 3.3,

$$d\epsilon = - (A\sigma - B\sigma^2) dx \quad (3.5)$$

Substituting 3.2 in 3.5 yields

$$d\epsilon = -A \left[P - \frac{Sx}{d_0} \left(1 - \frac{x}{2L}\right) \right] dx + B \left[P^2 - \frac{2PSx}{d_0} \left(1 - \frac{x}{2L}\right) + \frac{S^2 x^2}{d_0^2} \left(1 - \frac{x}{L} - \frac{x^2}{4L^2}\right) \right] dx \quad (3.6)$$

Which can be solved by direct integration. Thus

$$\epsilon = xP(-A+BP) + \frac{x^2}{2} \left(\frac{SA}{d_0} - \frac{2PSB}{d_0} \right) - \frac{x^3}{3} \left(\frac{SA}{2d_0L} - \frac{PSB}{d_0L} - \frac{S^2 B}{d_0^2} \right) - \frac{x^4}{4} \left(\frac{S^2 B}{d_0^2 L} \right) + \frac{x^5}{5} \left(\frac{S^2 B}{4d_0^2 L^2} \right) + C$$

Where C is the constant of integration. At the point $x = 0$,

$\epsilon = \epsilon_0$ thus $C = \epsilon_0$ and

$$\epsilon = \epsilon_0 - xP(A-BP) + \frac{x^2 S}{2d_0}(A-2BP) - \frac{x^3 S}{3Ld_0} \left(\frac{A}{2} - BP - \frac{SBL}{d_0} \right) - \frac{x^4 S^2 B}{4d_0^2 L} \left(1 - \frac{x}{5L} \right) \quad (3.7)$$

In 3.7, ϵ represents the deflection of any vertical section in the soil out to the distance L where the deflection was assumed to be negligible. The maximum shear strength may be expressible by the well-known equation

$$S = c + \sigma \tan \phi \quad (3.8)$$

where

c = unit cohesion

σ = normal stress on the failure plane, and

ϕ = angle of internal friction.

For the entire soil block DCEF

$$\frac{SL^2}{2} = Pd_0$$

or

$$S = \frac{2Pd_0}{L^2} \quad (3.9)$$

But S cannot exceed the value given by 3.8 so for low shear strength soils, P must be small or L must be large.

Several assumptions were made in the course of this development that should be experimentally verified. If the surface of the soil is unconfined, it is doubtful that soil near the surface will be compacted unless the soil has high cohesion. This means that the linearly distributed compressive stress should be replaced by a more appropriate model. If a confining mechanism, such as a flat gauge shoe, were used

on the soil surface, the model might be more applicable especially for soils of low cohesion.

As the point x is moved from the centerline outward toward the point L , the shear stress along the bottom of the failure block balances ever greater portions of the force applied to the furrow wall. This action decreases the compressive force applied to each succeeding layer. One might expect that the compressive stress would be diminished most rapidly near the lower boundary. Again a more accurate compressive stress distribution would have to be determined experimentally.

This model would predict the maximum compaction to occur near the opener face. Plane layers would be compressed to diminishing densities as distance from the opener increased. No compaction would be expected in soil below the bottom of the opener.

A possible method of compacting soil in the seed furrow is to attach a sliding wedge to the bottom of the opener. Such a wedge would force the bottom of the furrow downward as the opener moved past. A simple but approximate solution to this problem may be formulated from an approximate bearing capacity method presented by Sowers and Sowers (1958). The bearing pressure exerted by a foundation on soil is assumed to be supported by a prism of soil with side slopes of two vertically to one horizontally. The model appears as Figure 3. If we consider a unit thickness slice of soil normal to the direction of travel, on which a maximum pressure P is exerted by the sliding wedge the pressure, σ , on some soil layer y distance below the furrow bottom is

$$\sigma(w_0 + y) = Pw_0 \quad (3.10)$$

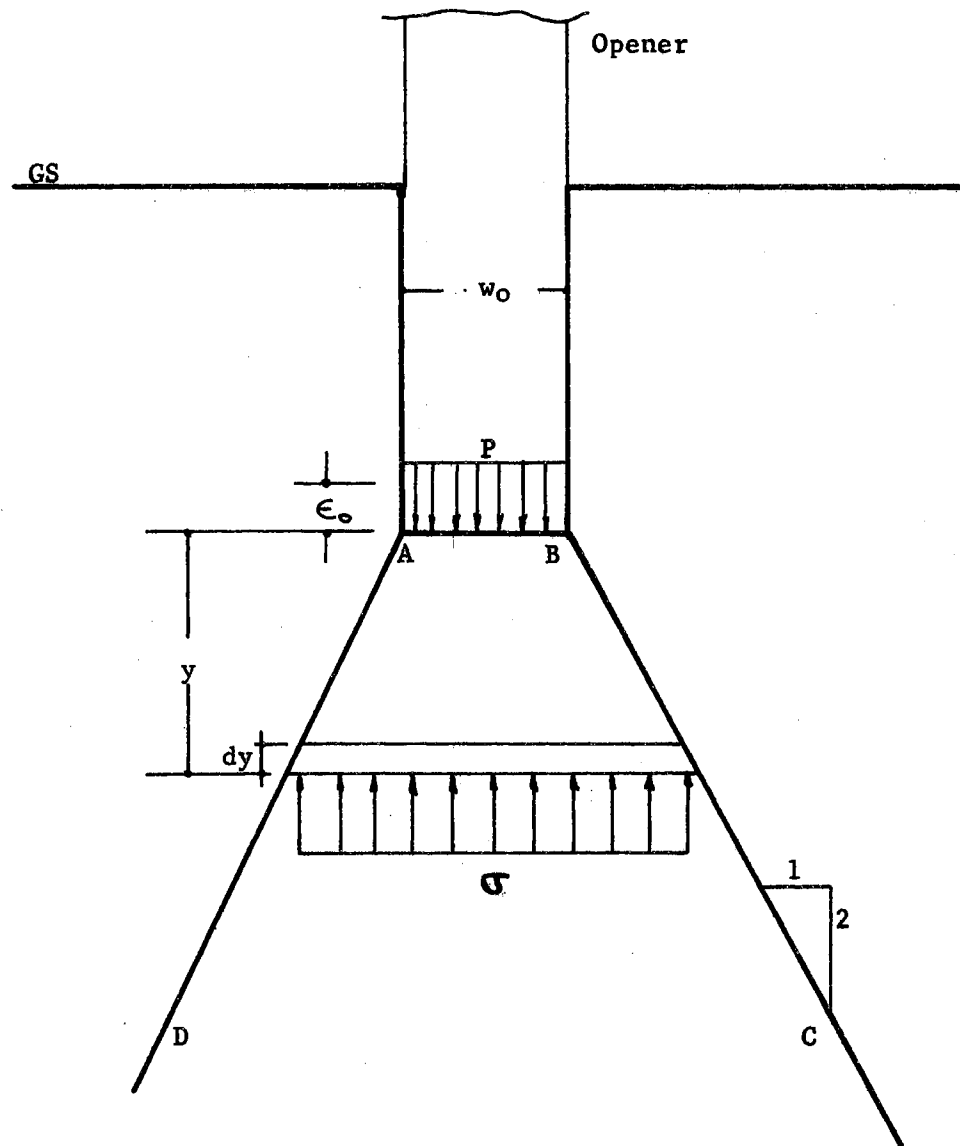


Figure 3. Model Used to Derive an Approximate Expression for the Compaction Under a Furrow Bottom Wedge

We consider an element dy at a depth of y . This layer will be compacted an amount $d\epsilon$ by the unit strain acting over length dy . Thus

$$d\epsilon = -\delta dy \quad (3.11)$$

If unit stress and unit strain are quadratically related as previously assumed in 3.3

$$\delta = A\sigma - B\sigma^2 \quad (3.12)$$

Solving for the stress on the thin layer in 3.10 and inserting the result in 3.12 and then into 3.11 we have

$$d\epsilon = \left(\frac{-APw_0}{(w_0+y)} + \frac{B P^2 w_0^2}{(w_0+y)^2} \right) dy \quad (3.13)$$

Which can be solved by direct integration resulting in

$$\epsilon = -APw_0 \log(w_0+y) - BP^2 w_0^2 \left(\frac{1}{(w_0+y)} \right) + C$$

where C is the constant of integration. Letting the maximum deflection ϵ_0 occur at the point $y = 0$,

$$C = \epsilon_0 + APw_0 \log(w_0) + BP^2 w_0^2$$

For any layer at depth y below the furrow bottom

$$\epsilon = \epsilon_0 + APw_0 \log\left(\frac{w_0}{w_0+y}\right) + BP^2 w_0^2 \left(1 - \frac{w_0}{w_0+y}\right) \quad (3.14)$$

To find the compaction of any finite layer, the deflection on each side of the layer can be calculated and the compaction determined by difference.

There are several limitations of the above development. The horizontal stress distribution is only approximated by the assumed prism of soil. Experimental results may dictate a different side slope of the prism. A more accurate distribution of compressive stresses can be calculated by the formulas of Boussinesq and Westergaard (Sowers and Sowers, 1958) based on elasticity. Introduction of a nonlinear stress-strain relationship in these equations creates formidable problems. At the present state of knowledge about planter openers, the more complicated analysis hardly seems justified. We can, however, notice that the general shape of an equal pressure line in the elastic analysis is bulb like. If bulb shaped-high density zones are found below planter openers, applicability of the elastic theory will have been demonstrated.

In the previous development, no allowance was made for plastic flow. Such flow, to be discussed in the next paragraph, would negate the derivation.

Plastic Flow

Regardless of the method used to calculate pressure distributions, compaction under a sliding wedge is limited by the pressure at which soil becomes plastic at the corners of the wedge. This can be evaluated as follows. Consider an elemental cube in the soil beneath an opener. The stresses acting on the cube are shown in Figure 4. By summation of forces on the upper portion of the cube, assuming a longitudinal dimension of one,

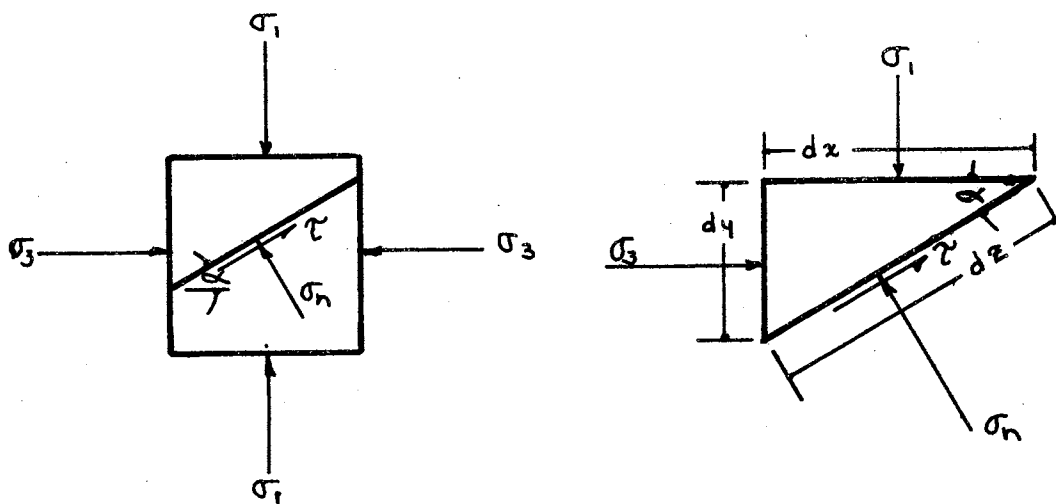


Figure 4. Two Dimensional Stresses Acting on a Cube of Soil

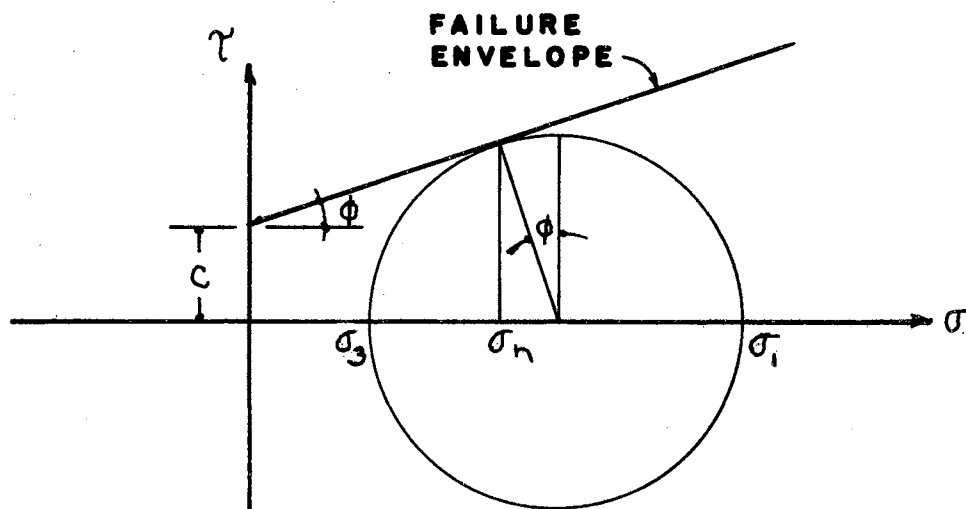


Figure 5. Mohr's Circle of Stresses Showing a Typical Failure Envelope for Soil

$$\begin{aligned}\sigma_3 dy - \sigma_n \sin \alpha dz + \tau \cos \alpha dz &= 0 \\ \sigma_1 dx - \sigma_n \cos \alpha dz - \tau \sin \alpha dz &= 0\end{aligned}\quad (3.15)$$

But

$$dy = dz \sin \alpha$$

$$dx = dz \cos \alpha$$

therefore

$$\begin{aligned}\sigma_n \sin \alpha - \tau \cos \alpha &= \sigma_3 \sin \alpha \\ \sigma_n \cos \alpha + \tau \sin \alpha &= \sigma_1 \cos \alpha\end{aligned}\quad (3.16)$$

Solving 3.16 by determinates

$$\sigma_n = \frac{\begin{vmatrix} \sigma_3 \sin \alpha & -\cos \alpha \\ \sigma_1 \cos \alpha & \sin \alpha \end{vmatrix}}{\begin{vmatrix} \sin \alpha & -\cos \alpha \\ \cos \alpha & \sin \alpha \end{vmatrix}}.$$

From which

$$\sigma_n = \frac{\sigma_3 \sin^2 \alpha + \sigma_1 \cos^2 \alpha}{\sin^2 \alpha + \cos^2 \alpha}.$$

Using half angle formulas

$$\sigma_n = \sigma_3 \left(\frac{1 - \cos^2 \alpha}{2} \right) + \sigma_1 \left(\frac{1 + \cos^2 \alpha}{2} \right)$$

from which

$$\sigma_n = \frac{\sigma_1 + \sigma_3}{2} + \left(\frac{\sigma_1 - \sigma_3}{2} \right) \cos 2\alpha \quad (3.17)$$

Finding shear stress from 3.16 by determinates

$$\tau = \frac{\begin{vmatrix} \sin \alpha & \sigma_3 \sin \alpha \\ \cos \alpha & \sigma_1 \cos \alpha \end{vmatrix}}{1}$$

so that

$$\tau = \sigma_1 \sin \alpha \cos \alpha - \sigma_3 \sin \alpha \cos \alpha .$$

Using half angle formulae

$$\tau = \sigma_1 \left(\frac{\sin 2\alpha}{2} \right) - \sigma_3 \left(\frac{\sin 2\alpha}{2} \right)$$

or

$$\tau = \left(\frac{\sigma_1 - \sigma_3}{2} \right) \sin 2\alpha . \quad (3.18)$$

Equations 3.17 and 3.18 are parametric equations of the familiar Mohr's circle of stress. For soil, the circle is limited in size by a maximum shear stress that increases as the principle stress increases. The general formula for the limiting shear stress in soil is

$$\tau = c + \sigma_n \tan \phi \quad (3.19)$$

where

c = Cohesion

σ_n = Normal stress on the shear plane, and

ϕ = Friction angle of the soil .

The foregoing is shown graphically in Figure 5. By the use of a half-angle formula Equation 3.17 can be written in the form,

$$\sigma_n = \sigma_3 + (\sigma_1 - \sigma_3) \cos^2 \alpha \quad (3.20)$$

Combining Equations 3.18, 3.19, and 3.20

$$\frac{\sigma_1 - \sigma_3}{2} \sin 2\alpha = c + (\sigma_3 + (\sigma_1 - \sigma_3) \cos^2 \alpha) \tan \phi \quad (3.21)$$

which simplifies to

$$\sigma_1 = \sigma_3 + \frac{\sigma_3 \tan \phi + c}{\sin \alpha \cos \alpha - \cos^2 \alpha \tan \phi} \quad (3.22)$$

Failure occurs when the circle becomes tangent to the failure envelope. At the point of tangency

$$2\alpha = \pi/2 + \phi \quad (3.23)$$

Using this relationship Equation 3.22 reduces to

$$\sigma_1 = \sigma_3 \left(\frac{1 + \sin \phi}{1 - \sin \phi} \right) + 2c \frac{\cos \phi}{1 - \sin \phi} \quad (3.24)$$

Using the identities

$$\tan^2 (45 + \phi/2) = \left(\frac{1 + \sin \phi}{1 - \sin \phi} \right) \quad (3.25)$$

and

$$\tan (45 + \phi/2) = \frac{\cos \phi}{1 - \sin \phi} \quad (3.26)$$

and letting

$$k = \tan (45 + \phi/2) \quad (3.27)$$

then

$$\sigma_1 = \sigma_3 k^2 + 2c k \quad (3.28)$$

Horizontal resistance to plastic flow is assumed to be provided by the overburden soil pressure. If the opener applies sufficient stress in the horizontal plane to overcome the vertical stress due to overburden, plastic flow is assumed to occur. The assumed loading condition is illustrated in Figure 6. The vertical stress on block 1 is assumed to be

$$\sigma_{III} = \gamma d \quad (3.29)$$

where

- σ_{III} = Vertical unit stress
- γ = Unit weight of soil, and
- d = Depth of the furrow.

In order that failure occurs in the soil beside the opener, the horizontal stress σ_I must satisfy the passive transfer equation

$$\sigma_I = \gamma dk^2 + 2ck . \quad (3.30)$$

Referring to block 2 we see that σ_3 is the minor principle stress resisting plastic expulsion from beneath the opener. It is equal to σ_I but in the opposite direction. The major principle stress is then

$$\sigma_1 = \sigma_3 k^2 + 2ck . \quad (3.31)$$

Bringing in σ_I from Equation 3.30 for σ_3

$$\sigma_1 = \gamma dk^4 + 2c(k^3 + k) . \quad (3.32)$$

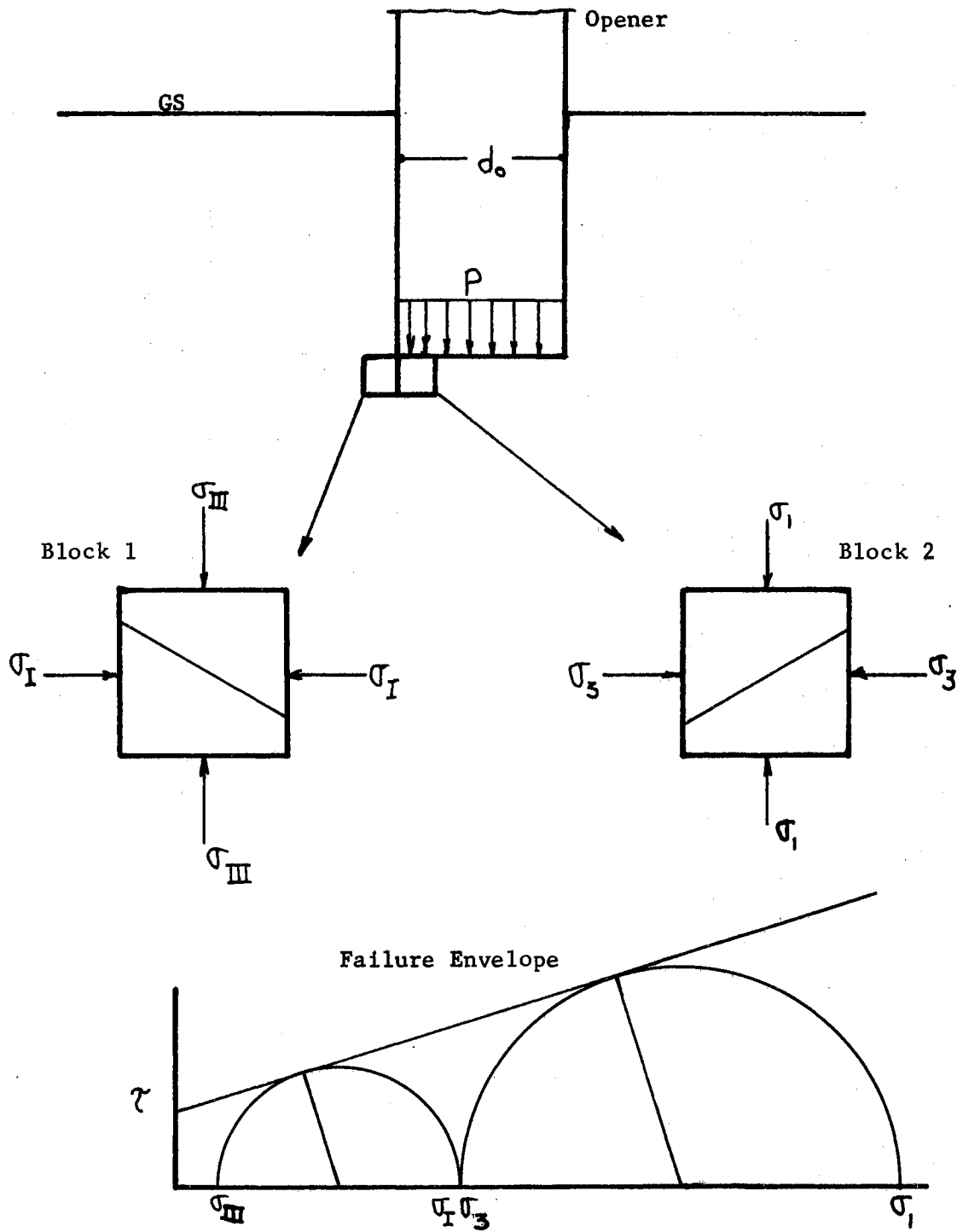


Figure 6. Stress Conditions for Plastic Flow Under a Planter Opener Using Mohr's Circle of Stresses

According to Equation 3.32, the maximum stress that can be applied to a furrow bottom compaction wedge depends on the unit weight of the soil, the depth of the furrow and the shear strength parameters of the soil.

Fracture of Soil Beside Openers

For planter openers, the problem of compacting the furrow bottom is further complicated because the soil immediately beside the opener must be undergoing distortion by either plastic flow or fracture. Thus the material at the lower corner of the opener may not have sufficient vertically applied stress to resist plastic deformation. The mode of action beside the opener may be comparable to the predicted failure of soil which is laterally displaced by a retaining wall. Solution to this problem has been presented by Terzaghi and Peck (1948).

In Figure 7, two principle stresses are acting on each unit cube of soil to the right of the wall. These are the hydrostatic pressure due to the weight of soil above the cube and the pressure applied by the wall. The familiar formula for shear strength of cohesive soils is Equation 3.19.

The failure angle previously found was

$$\alpha = 45 + \phi/2 \quad . \quad (3.33)$$

If the failure angle α' is measured from a horizontal plane, the failure is seen to rise at an angle of

$$\alpha' = 45 - \phi/2 \quad . \quad (3.34)$$

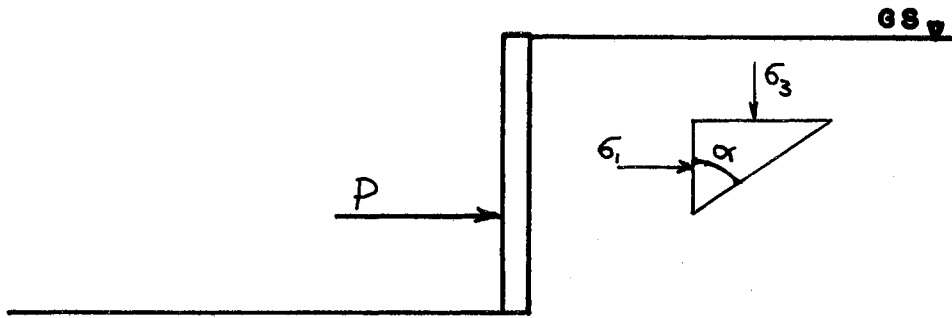


Figure 7 . Loading Condition for the Derivation of the Rankine Passive Earth Pressure Formula

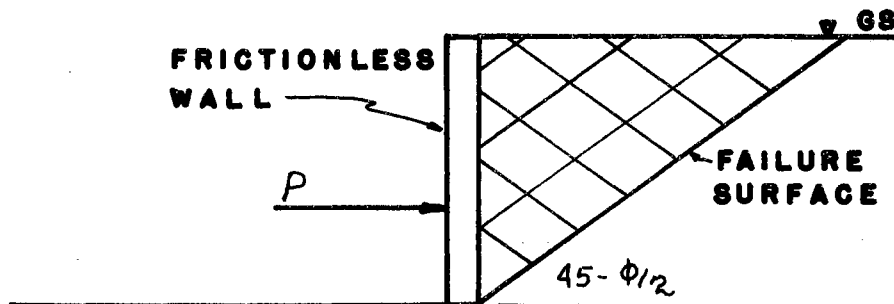


Figure 8 . Failure Block Predicted by the Rankine Theory

The simplest solution to the problem of predicting soil failure pattern is then that the soil block will fracture at an angle of $(45 - \phi/2)$ from the bottom of the opener to the soil surface in the form of a triangular block as shown in Figure 8.

The second approximation of failure results from considering the wall to be rough. In this case, the net force exerted by the wall on the soil face is not horizontal but at an angle resisting movement of soil upward along the face. This condition has been analyzed by Coulomb and is also given by Terzaghi and Peck. The concept is graphically shown in Figure 9. If equilibrium is assumed at the moment of failure, the three vector forces W , F , and P acting on the soil block ABC must sum to zero. The plane of probable failure can be found by successive locations of point C such as C' and C'' . At each point the value of P required to close the vector triangle is computed. The plane on which a minimum P occurs is the assumed plane of failure. Convenient graphical means of solution have been devised and are presented in the above reference and others.

When a rough surfaced retaining wall is forced against a vertical wall of a cut in cohesive soil, failure has been observed to occur in a pattern similar to Figure 10. The block of soil $ABCD$ fails as a mass along the line BCD . The segment CD rises at an angle of $(45 - \phi/2)$ or the Rankine failure line. The line segment BC is usually considered to be a logarithmic spiral with its center at some point E . A series of arbitrary slip surfaces are chosen and the surface resulting in the smallest force required for slip is taken as the answer. The procedure for computing the force P required to cause slip is rigorous but tedious.

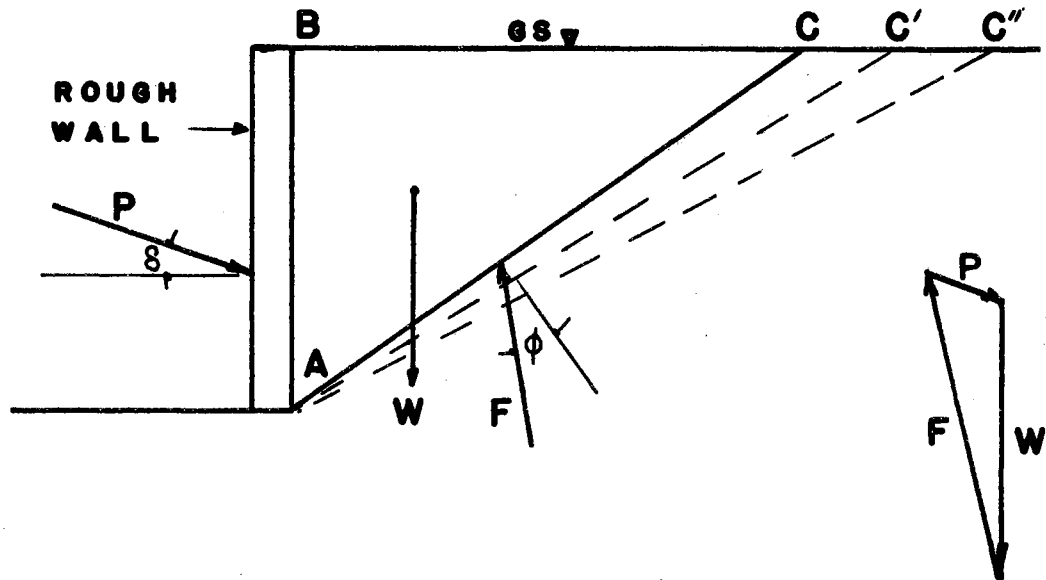


Figure 9. Diagram of the Coulomb Theory of Failure Behind a Rough Faced Retaining Wall

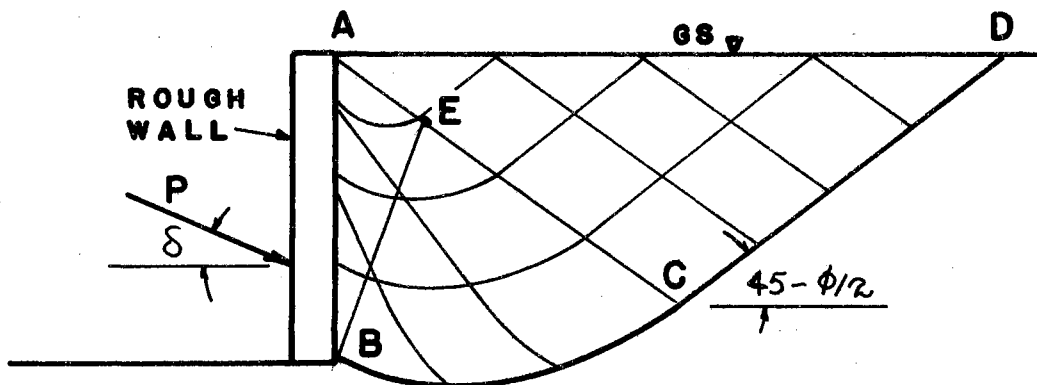


Figure 10. Soil Failure Line Resulting from Pushing a Rough Faced Retaining Wall Against a Cohesive Soil

It does not seem rational that classical retaining wall theory can be applied to soil openers with face angles from the direction of travel in both the horizontal and vertical directions. In Figure 20 are shown the horizontal angles used in the experiment and in Figure 11 is a view of the vertical cross sections of those openers with vertical angles. From these sketches we see that considerable deformation of the soil is necessary before the opener establishes sufficient soil contact to cause a classical retaining wall failure.

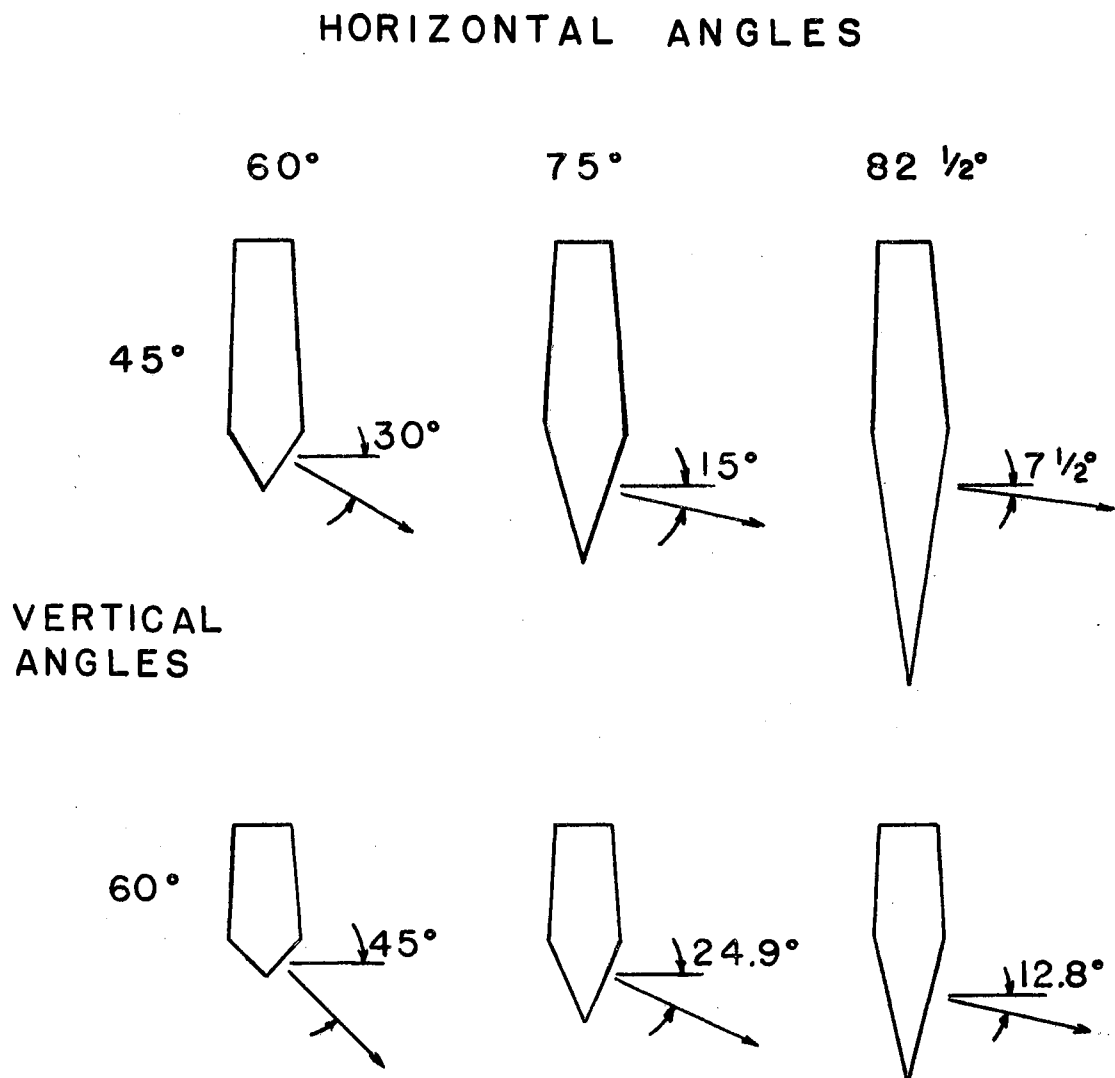


Figure 11. Vertical Cross Sections of Those Openers Having Angularity in the Vertical Plane

CHAPTER IV

METHODS AND PROCEDURES

Apparatus

To evaluate the effect of planter opener shape on the soil density pattern it was first necessary to design laboratory equipment to pull experimental openers through soil samples. An apparatus was designed specifically for this purpose and is shown in Figure 12. It consisted of a three-horsepower electric motor pulling a movable carriage on which the test opener was mounted. The opener was pulled through the soil sample at a speed of five miles per hour and at a depth of two inches. The soil samples were twelve inches wide, eight inches deep, and three feet long. Calculations indicated that the three-horsepower motor would accelerate the cart to full speed in a distance of twelve to eighteen inches. The cart was stopped by disengaging the pulling cable and engaging a set of flexible rubber pads which absorb energy from the cart.

A transducer for measuring forces acting on the planter openers was also designed. It consisted of a pair of parallel cantilever beams to measure drag force. These were connected through hinge points to a simply supported beam which measured lift force. At the center of the simply supported beam was another cantilever beam on which the opener was mounted. A sketch of this transducer is shown in Figure 13. All

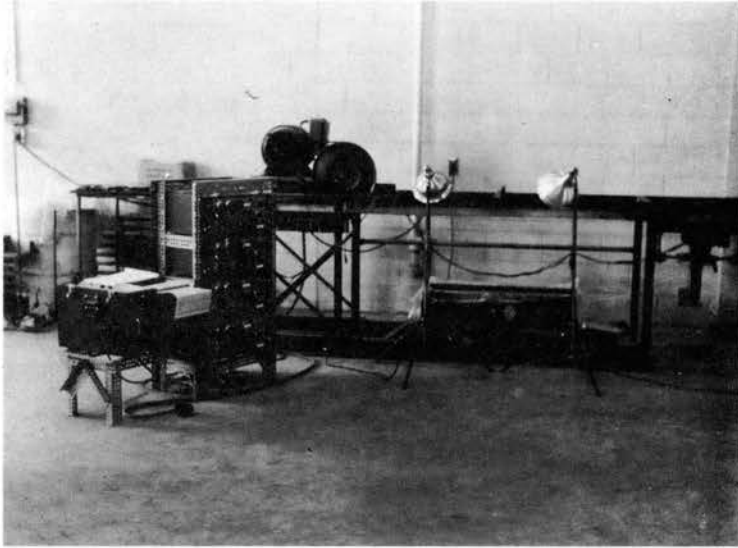


Figure 12. Apparatus Used to Operate Test Furrow Openers Through Soil Samples

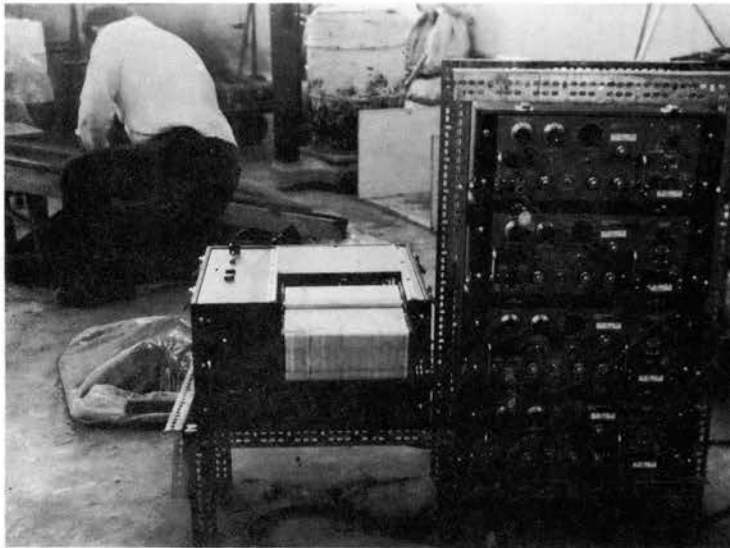


Figure 13. Strain Gage Recorder Used to Determine Forces Acting on Furrow Openers

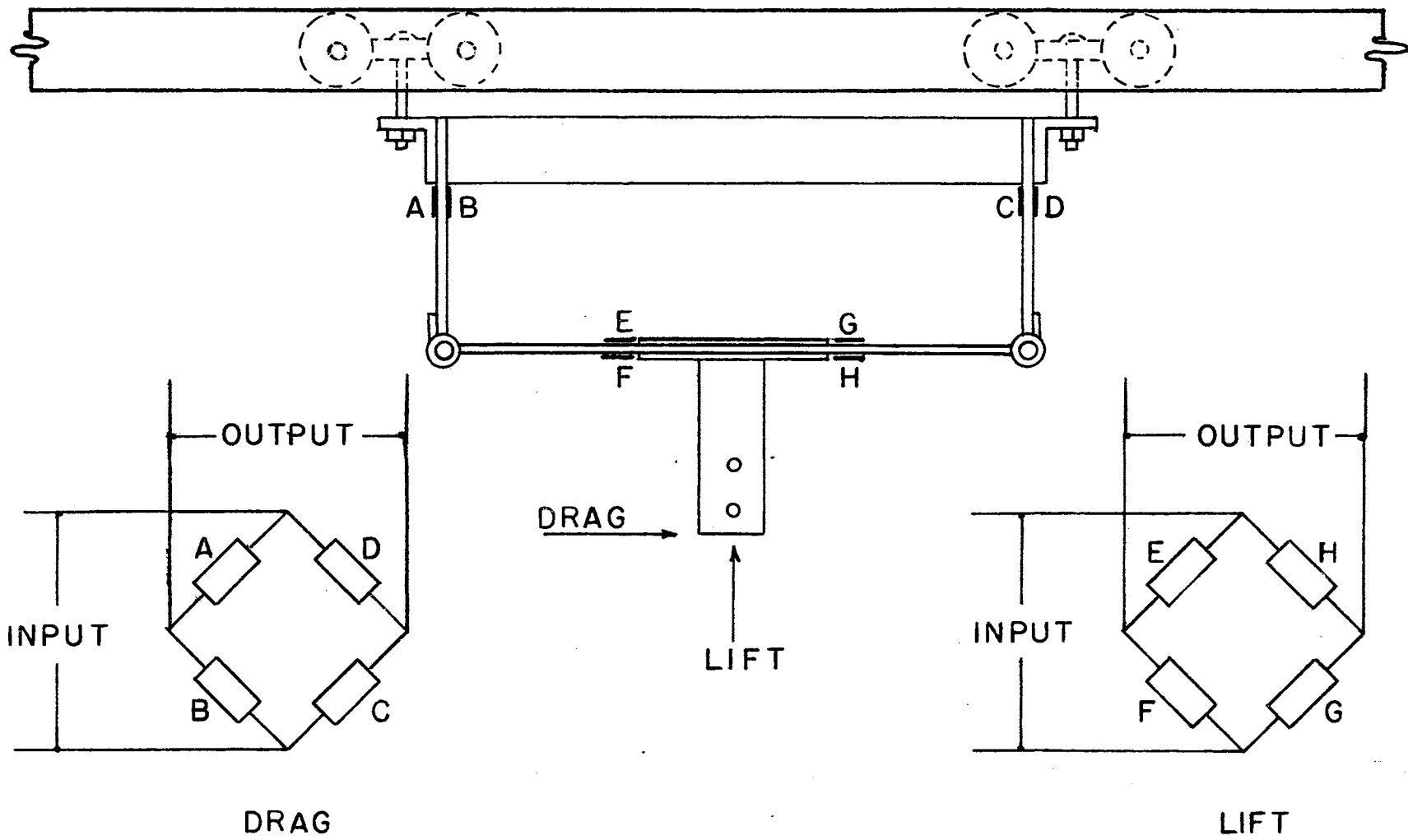


Figure 14. Strain Gage Transducer Used to Measure Drag and Lift Forces Acting on Experimental Openers

of the sensing elements were made of aluminum. The original design of this transducer called for rigid, rather than flexible, hinge points at the ends of the simply supported beam. This arrangement was not satisfactory for a large moment as compared to drag force such as that produced by a rearward angled opener. The moment tended to cause deflection through the rigid corners which produced a negative drag reading. The revised design gave reasonable and consistent force records and was considered to be satisfactory.

All sensing elements on the beams were Baldwin, Lima, Hamilton electrical strain gauges type S-1 paper-backed, 120 ohm resistance with a gauge factor of 2.06 ohms per micro-inch of deflection. All were connected as full Wheatstone bridges. Recording was on a four channel Sanborn recorder at appropriate amplification factors and at a chart speed of 100 millimeters per second. The recorder is shown in Figure 13. A sample recording appears as Figure 15. Calibration was determined by loading the transducer with a ground-fit hydraulic cylinder, pump, and pressure gauge. A picture of the calibration setup is shown in Figure 16. Both calibration curves were second degree with zero intercept. They are shown in Figures 18 and 19.

The soil box consisted of a full-inch by sixteen-inch wide board with steel angles bolted to the ends for handling. Grooves were cut in the board to fit a twelve-inch wide by three-foot long metal shell. The shell had open ends to allow entry and exit of the planter opener. Plywood fillers were used in the ends during sample preparation. A picture of the sample box is Figure 17.

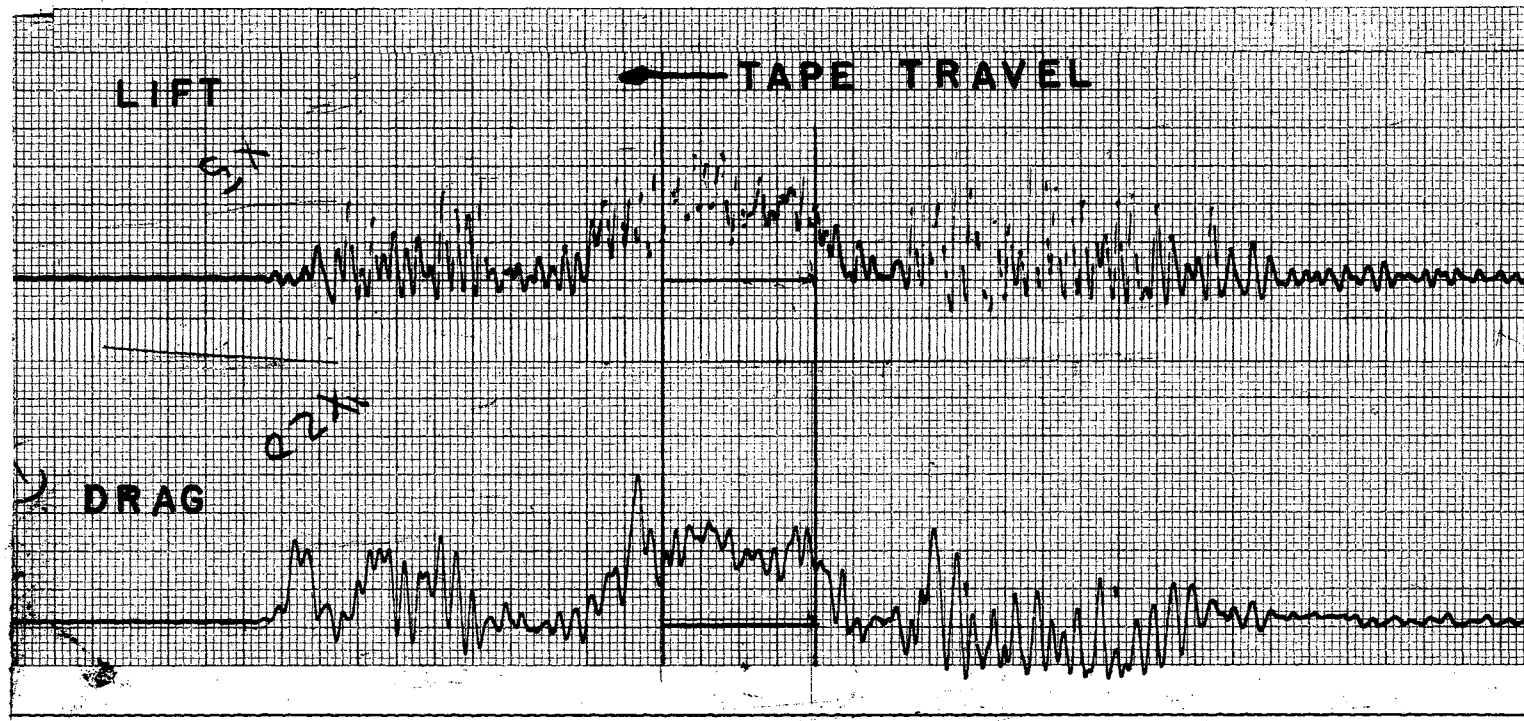


Figure 15. Sample Recording of Drag and Lift Forces Acting on a Planter Opener

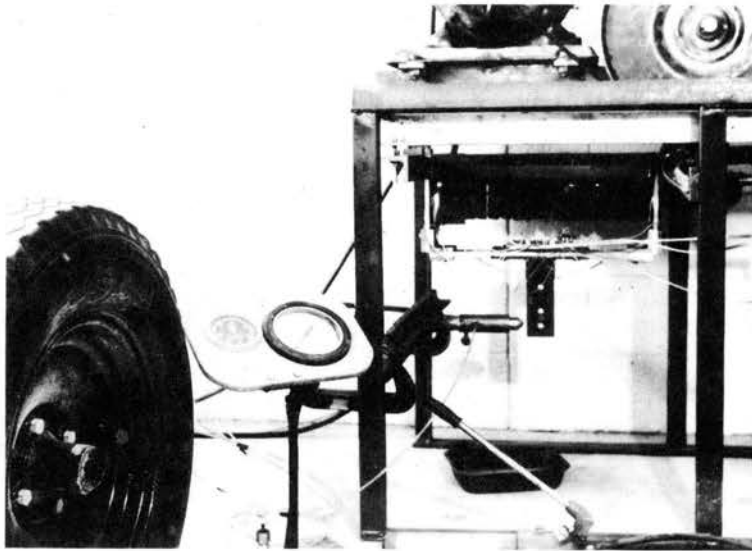


Figure 16. Force Transducer Clamped in Place to Calibrate for Drag Force

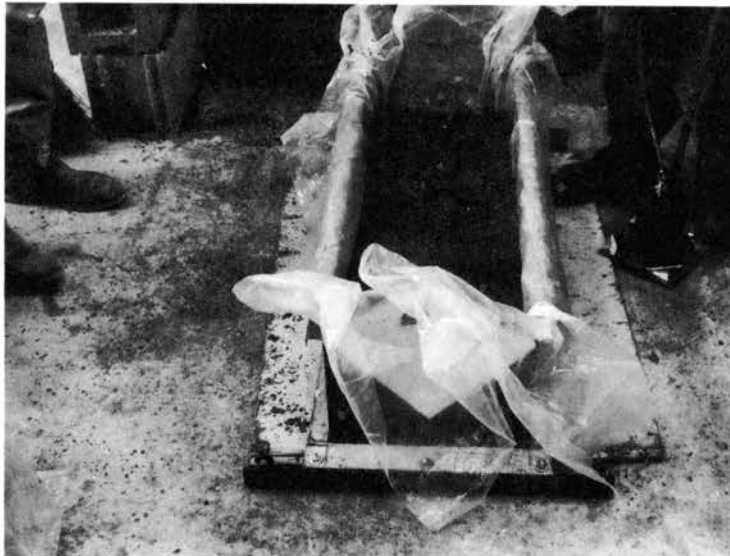


Figure 17. Soil Box Used to Prepare and Hold Test Specimen

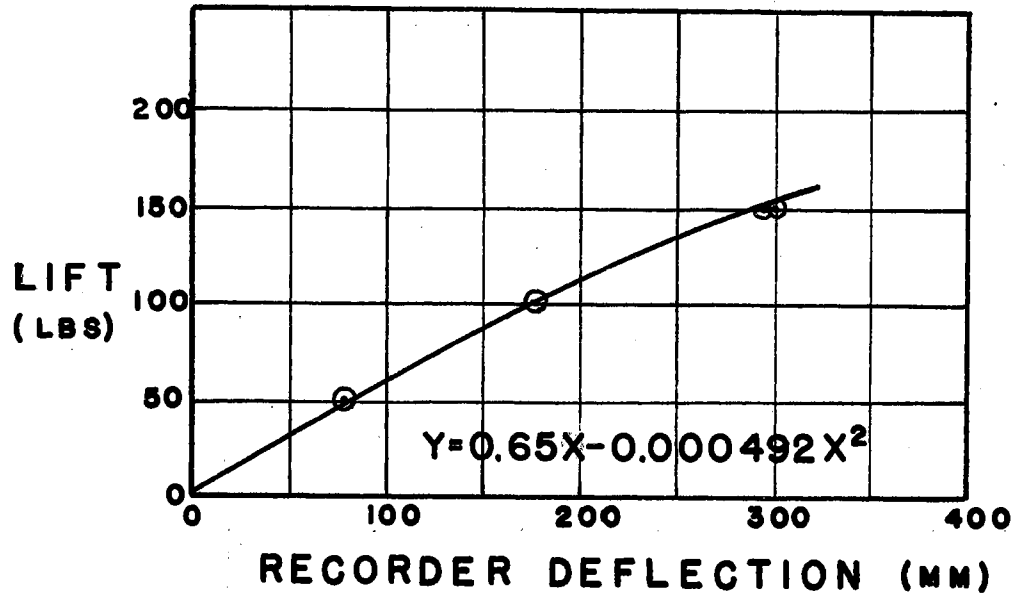


Figure 18. Calibration Curve for Lift Force

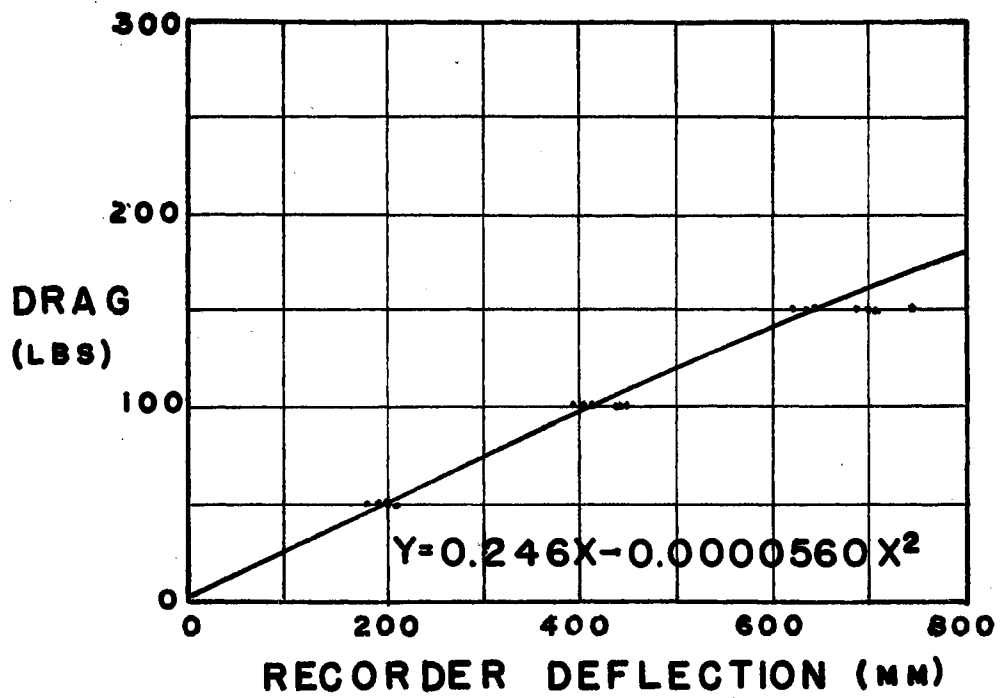


Figure 19. Calibration Curve for Drag Force

Several smaller pieces of apparatus were designed and used in the course of the experiment. These will be explained in conjunction with the procedure for which they were used.

Soil Samples

A supply of clay soil was collected from an area known to be typical of the area. Preparation of natural soil samples consisted of screening through one-quarter inch mesh hardware cloth and placing the soil in the sample box overfilling the top to resemble a planting bed. The samples were soaked overnight with water near the top of the ridge similar to the method of furrow irrigation applied locally. After thorough soaking, the samples were removed from the water and air dried to a reasonable moisture content for planting. This appeared to be about twenty percent moisture on the dry basis. This procedure led to difficulties because there was some montmorillonite in the soil. This caused expansion during the soaking stage and shrinkage of the soil during the drying period. The resulting cracks made these samples quite nonhomogenous and led to erratic results. In the latter days of the experiment, the soils were prepared to the desired moisture content and then placed in the sample containers and compacted to the desired density by a baseplate and drop hammer as will be discussed in the preparation of artificial samples. This method was considerably superior because the sample container was full and the soil could not yield into cracks as it had in the naturally prepared samples. This procedure was consistent with other research on clay soils although the results so obtained are not directly comparable to naturally prepared samples because remolded samples are considerably weaker.

Two artificial soils were chosen for use in this experiment. The most useful of these was called the "artificial fine" soil. The solid phase of this soil consisted of twenty percent Ottawa sand and eighty percent Wyoming bentonite by weight. The liquid phase was SAE-120 transmission oil at the rate of thirty percent on the dry basis. The components were mixed in an ordinary cement mixer. The large aggregates that tended to form were broken up by hand forcing the sample through ordinary screen wire. Small aggregates remained but the soil had the feel of a granulated medium-textured soil. Large aggregates did not reform during the use of the soil. According to previous work on artificial soil, one would expect this one to have a coefficient of internal friction about 20 degrees and cohesion of less than five pounds per square inch. Apparently, the size of aggregates affected the frictional characteristics since test results did not agree with these values. By direct shear test the internal friction angle was 35 degrees and the cohesion was 0.6 psi. The soil-to-metal shear strength was determined by placing a steel plate in the bottom section of the shear box. The soil-to-metal friction angle was 27 degrees and there was no measurable adhesion.

The second artificial soil was called "artificial coarse." In this mixture the solid phase consisted of eighty percent Ottawa sand and twenty percent Wyoming bentonite. Motor oil of grade SAE-10 was then added to give ten percent liquid on the dry weight basis. This soil was very easy to handle since the characteristics approximated those of a pure sand. The bentonite had very little effect on the mixture. Samples tended to be very dense without appreciable compaction. Energy applied through baseplate and drop hammer was not effective in

raising the density. Shear tests indicated no cohesion or adhesion for the soil. The internal friction angle was 39.0 degrees and the soil-to-metal friction angle was 22.0 degrees. The use of this soil was limited in the experiment because it was obvious that the mixture was too sandy for comparison to agricultural soil.

Samples of artificial soil were prepared by filling the eight-inch deep box with one-inch layers of soil and compacting each layer with a baseplate and drop hammer. In the early stages of the experiment, the baseplate was a six-inch square. The weight was dropped 52 inches to compact the soil to approximately the density that was expected in natural soil samples. The application of a six-inch square baseplate to a sample 12 inches wide and three feet long resulted in a questionable pattern of density since the center of the sample, where the opener was to run, was not uniformly compacted due to edge effects of the plate. In later experiments, the baseplate was twelve inches square and the drop was reduced to 26 inches in an effort to produce a more compactable soil. The last layer was overfilled slightly so the sample top could be trimmed to size. As each sample was ready for running, it was weighed to determine the average density.

Opener Shapes

So little information was found about the action of planter openers on soil that it was difficult to logically choose a set of test shapes. Commercial runner-type openers were constructed of thin metal plates welded together to form a "V" in the horizontal plane with the point of the "V" oriented in the direction of travel. A single thickness of plate extends forward in a variety of shapes. Stub runners

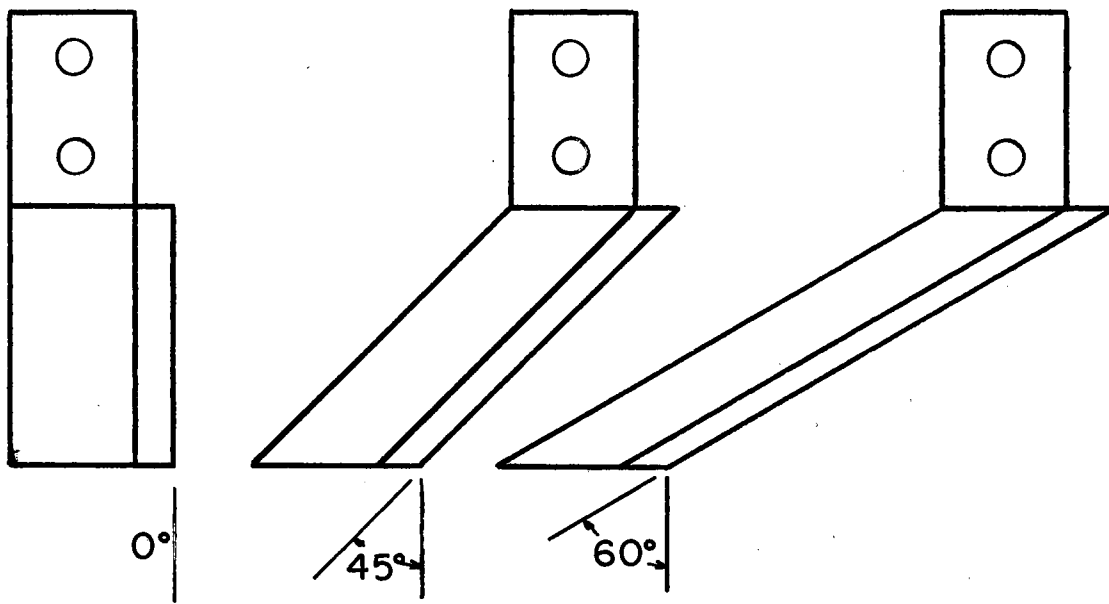
usually have a point near the ground surface and curved runners extend forward with the lower edge curving upward to a point well above the soil surface.

After inspection of typical runner-type openers it was assumed that the thin plate extending forward from the "V" had a minor effect on the action of the opener. Such a blade was not used on experimental openers. It appeared that the angle between the plates forming the "V" would have some effect on furrow shape. Horizontal cross sections of opener shapes chosen for the experiment are shown in Figure 20. Various companies produce openers with different vertical angles along the front of the "V" wedge. Vertical angles chosen for the experiment are also shown in Figure 20. Vertical cross sections have previously appeared in Figure 11. Throughout the remainder of this discourse, vertical and horizontal opener angles will refer to the angle between the plane normal to the direction of travel and the soil engaging faces of the openers. The use of three vertical and three horizontal angles resulted in nine opener shapes.

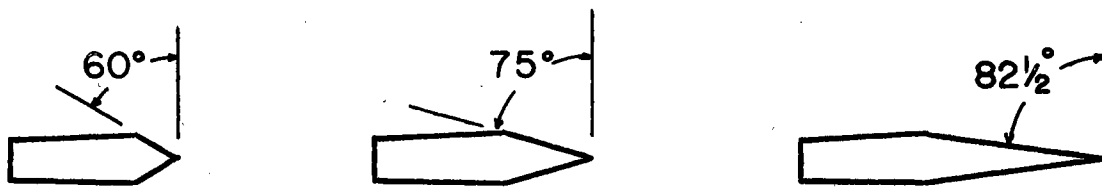
In an attempt to compact soil in the bottom of the furrow, a set of compaction wedges was made as shown in Figure 21. These were used exclusively on the opener with zero vertical angle and eight-two and one-half degrees horizontal angle.

Sampling

As the opener was pulled through the soil sample, the force transducer recorded drag and lift. Slow-motion pictures were taken of the opener as it went through the sample. Some of these will be discussed in the chapter on results. Photographs were taken at a speed of 64 or



VERTICAL ANGLES



HORIZONTAL ANGLES

DIRECTION OF TRAVEL \longrightarrow

Figure 20. Vertical and Horizontal Angles Used to Describe Test Openers

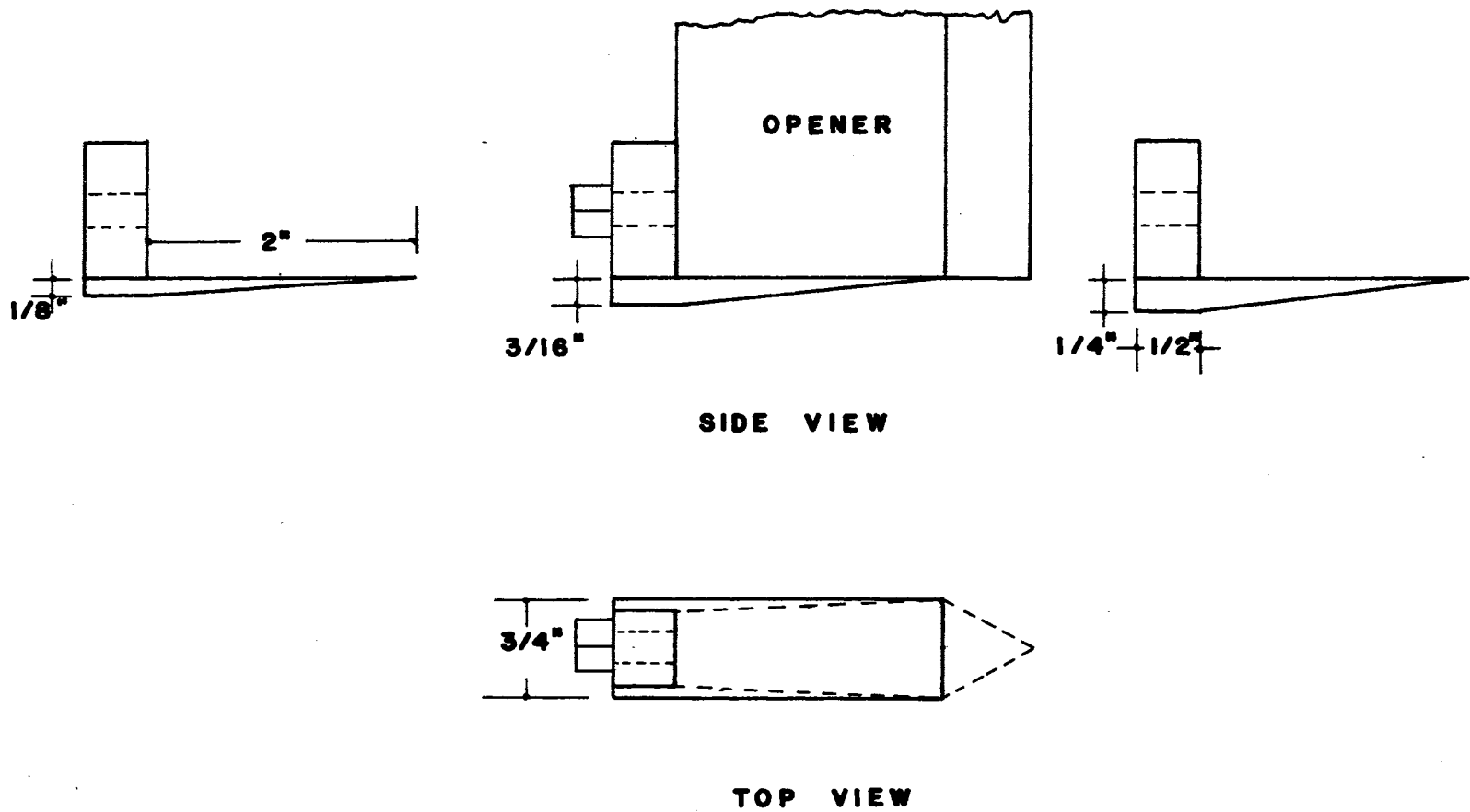


Figure 21. Furrow Bottom Compaction Wedges Used in the Experiment

48 frames per second, depending on which of two cameras were available to take the pictures. Higher speeds would have been desirable, but equipment was not available and considering the expense of such equipment it was not feasible to obtain it for this experiment. After an opener had been pulled through the soil sample, the sample container was removed from the opener operating frame and the sheet metal container around the sample was removed. A sampling guide was placed over the test sample and two three-inch long cross sectional subsamples were taken using sampling boxes like those shown in Figure 22. After the sampling boxes were driven the full depth of the soil, as in Figure 23, sheet metal slides were placed under the boxes and the cross sectional samples were removed for density evaluation. Samples taken from natural soil were wrapped in polyethylene film to reduce moisture losses since density evaluation required considerable time. Wrapping was not necessary for oil moistened artificial soils.

For density evaluation the soil cross section in the sampling box was placed in a jig where it could be sampled at points of known position to determine the density pattern. For test specimens used to evaluate opener shape, density measurements were made on one-half inch increments. In the vertical direction, measurements were made from one-half inch above the original ground surface to four inches below. In the horizontal plane, readings were made between points six and one-half inches on each side of the centerline. For furrow compaction wedge, sample readings were made on one-fourth inch increments. In the vertical direction, readings were taken from one and one-half inches deep to four inches deep and included points for one and one-half inches on both sides of the centerline.

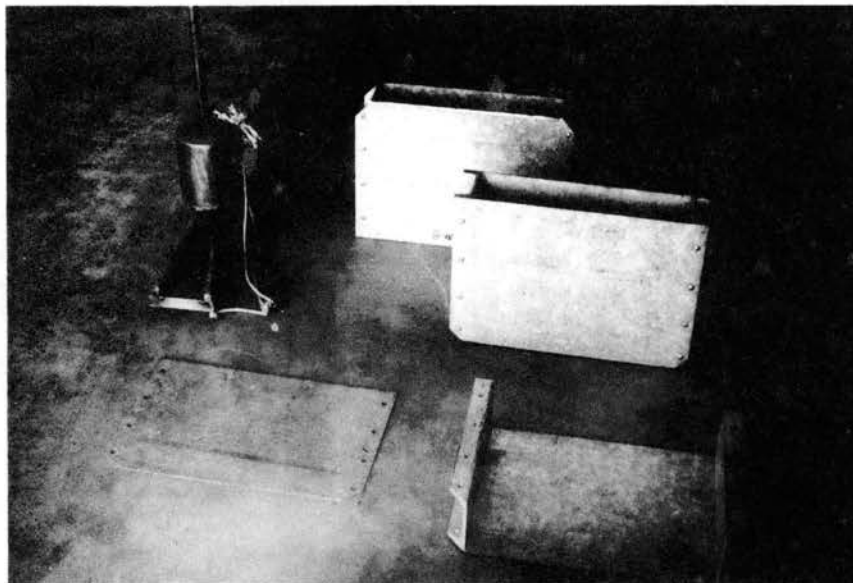


Figure 22. Cross Sectional Sampling Box

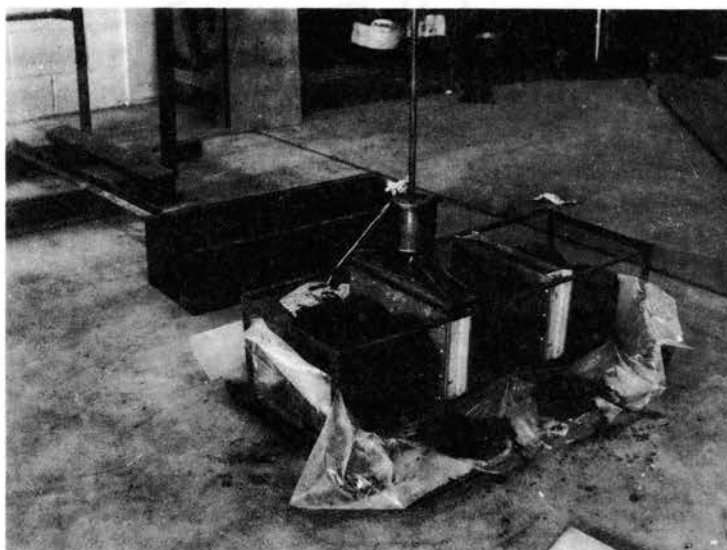


Figure 23. Cross Sectional Samples Being Taken from a Soil Sample After an Opener has Passed Through

Density Measurement

Density was measured in this experiment by the gamma radiation technique. Gamma photons from a radium 226 source rated at 1.95 millicuries were collimated through a one-fourth inch hole in a lead shield. A rigid frame held a shielded Gieger counting tube in position so the photons could only reach the tube through the soil sample and then a one-fourth inch hole that was aligned with the beam from the source. The arrangement of parts is shown schematically in Figure 24. The rigid frame holding the source and counter tube was supported by movable pins for vertical positioning and it could be positioned horizontally by sliding. The jig with a sample in place is shown in Figure 25. In this research, the soil sample was three inches long. Photons were counted using the commercial rate meter shown in Figure 26.

It was necessary to calibrate the density measuring equipment. Small samples three inches long were compacted into a section of four-inch diameter brass pipe in one-inch layers using a modified Procter compaction hammer. These samples were then weighed to determine the average density and a series of readings were taken. During calibration the exact length of soil sample had not been established so the data were compiled using a density factor defined as average bulk density (gms/cc) times the length of sample (cm). Values of density factor were plotted against the decrease in photon count rate due to the beam passing through soil. The point of zero count decrease was determined by reading the count rate with only metal side plates in place. This curve is shown as Figure 27. Due to the limited range of count values it was possible to use a linear relationship without appreciable error.

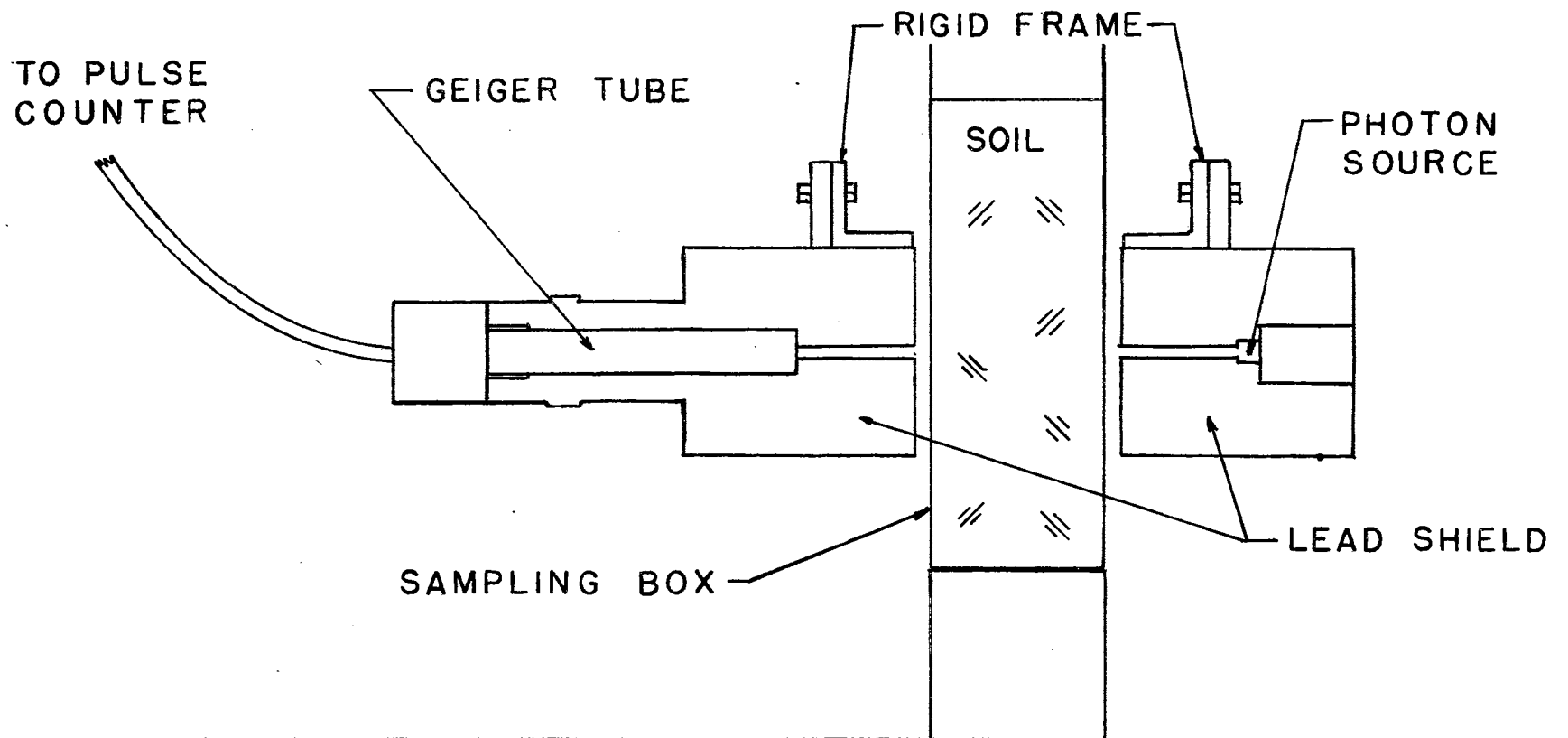


Figure 24. Schematic Diagram of Equipment Used to Determine Soil Density by the Gamma Radiation Technique

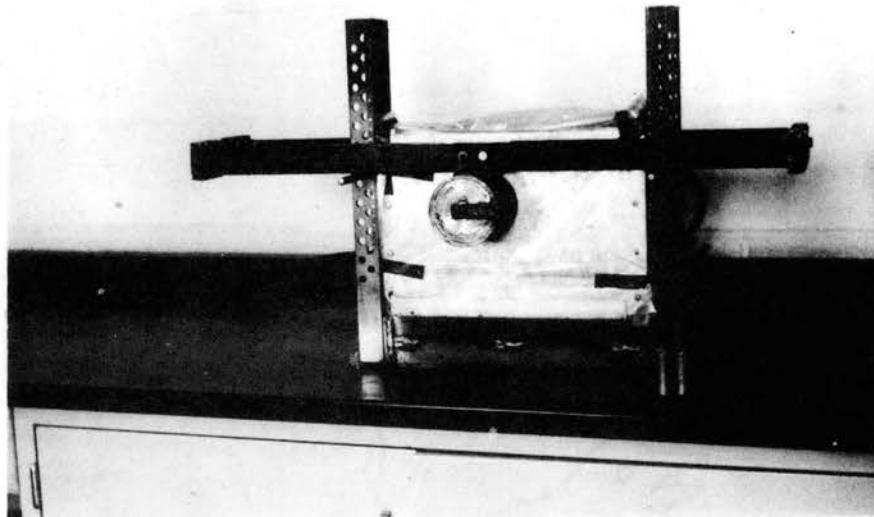


Figure 25. Cross Sectional Sample of Natural Soil in Jig for Gamma Radiation Density Measurement

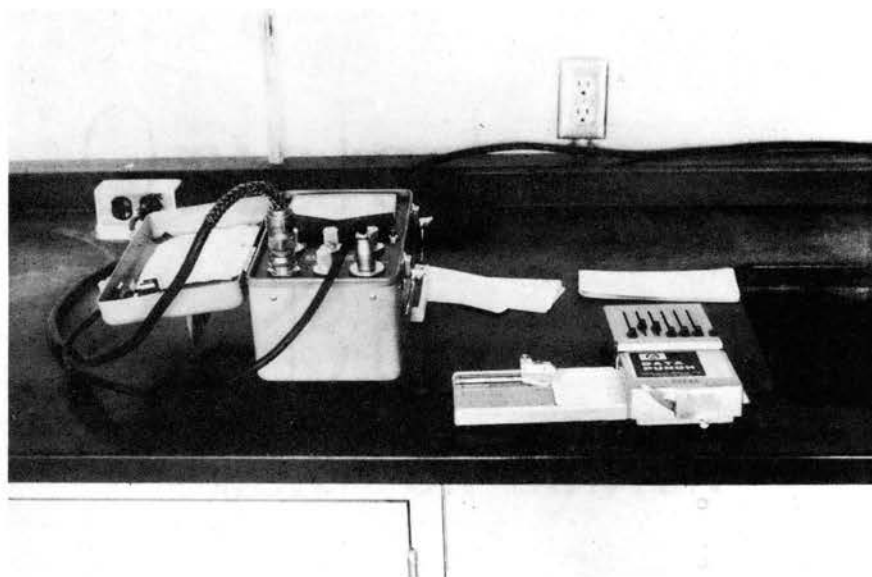


Figure 26. Rate Meter and Hand Card Punch Used to Record Radiation Readings

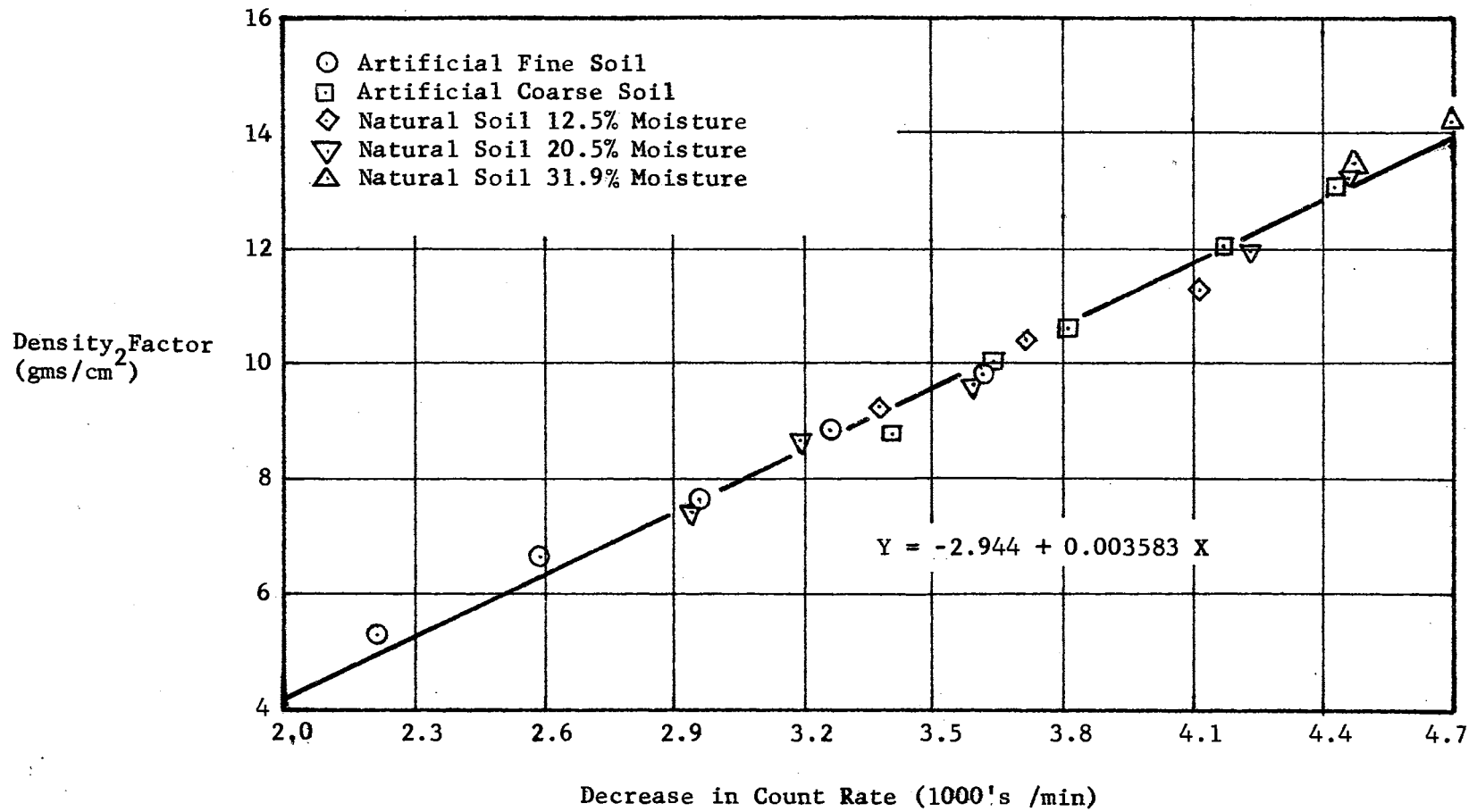


Figure 27. Calibration Curve for Gamma Ray Density Apparatus

Each reading on the rate meter required twenty to thirty seconds. For the opener test samples, four hundred sixty readings were required for each run.

Data Processing

Rate meter readings were punched directly onto computer cards using the small, hand data punch shown in Figure 26. Since a large volume of data had to be collected in this experiment, almost no other method would have been feasible. The raw data were read into the computer in the form of a three-dimensional array. Rows and columns represented vertical and horizontal placement of points on one cross section and the two cross sections were referenced by the third dimension. Density was computed at each point using the calibration curve. Lateral and longitudinal symmetry were assumed. This gave four density values at each point in a one-half cross-section. A sample analysis sheet is shown in Figure 28. The left two columns of numbers represent bulk density measurements on the centerline of the sample. Numbers in these columns are repeated since there was only one reading taken on the centerline. A typical point is enclosed in a box. The top two numbers represent two readings the same distance from the centerline and at the same height on the first cross section. The second row of two numbers represent the corresponding two points on the second cross section. The third pair of numbers from the top is the mean and the five percent confidence interval of the mean in the left and right positions respectively. The bottom numbers are a test for significant differences between pairs of samples in the longitudinal and lateral directions respectively. A zero indicates acceptance of the null

BUSINESS FORMS INC., EL PASO, TEXAS

NEW MEXICO STATE UNIVERSITY

RUN NUMBER 9

.020	-.020	-.016	-.027	-.018	-.018	-.030	.08	-.020	-.006	-.027	.08	-.030	.13	-.020	.01	-.025	.08	-.030	-.030	-.025	-.027	-.030	-.030		
.43	-.43	-.48	-.43	-.34	-.13	-.20	-.06	.13	-.06	.13	-.20	.13	-.25	-.11	-.34	-.22	.36	-.32	-.39	-.29	-.50	-.25	-.43		
.32	.21	-.34	.24	-.21	.15	-.12	.26	-.05	.22	-.07	.32	-.07	.37	-.16	.24	-.19	.30	-.32	.07	-.33	.19	-.32	.13		
0	0	0	0	0	0	0	0	0	0	0	0	0	0	0	0	0	0	1.0	1.0	0	0	0	0		
.45	.45	.64	.64	.76	.76	.78	.83	.81	.83	.78	.83	.78	.78	.92	.78	.92	.83	.78	.55	.76	.31	.55	-.016		
.46	.46	.72	.62	.69	.69	.76	.65	.69	.72	.86	.79	.88	.83	.88	.69	.83	.13	.69	.43	.55	.34	-.01	.08		
.46	.00	.66	.07	.73	.06	.76	.12	.76	.11	.81	.06	.82	.07	.82	.16	.68	.59	.62	.25	.49	.33	.12	.48		
0	0	0	0	0	0	1.0	1.0	1.0	1.0	0	0	0	0	0	0	0	0	1.0	1.0	0	0	0	0		
.90	.90	.88	.81	.88	.92	.90	.92	.88	.92	.92	.99	.97	.92	1.02	.99	1.02	1.02	.97	.95	.90	.78	.88	.69		
.79	.79	.69	.74	.74	.74	.69	.72	.76	.83	.93	.93	.90	1.02	.95	.93	.93	.90	.98	.93	.93	.95	.46	.93		
.84	.10	.78	.13	.82	.15	.81	.19	.85	.11	.94	.05	.96	.08	.97	.07	.97	.10	.96	.03	.89	.12	.74	.34		
0	0	0	0	0	0	1.0	1.0	1.0	1.0	1.0	1.0	1.0	1.0	1.0	1.0	1.0	0	0	0	0	0	0	0		
.83	.83	.92	.92	.83	.90	.88	.88	.88	.92	1.02	1.02	1.02	.97	1.02	.99	.99	.97	.99	.97	.99	.92	.92	.92		
.74	.74	.88	.72	.83	.81	.83	.83	.98	.88	.98	.98	.93	1.02	1.02	1.02	.98	1.07	.98	1.02	.95	.93	.92	.90		
.79	.08	.86	.16	.84	.06	.86	.04	.91	.07	.97	.06	.99	.07	1.01	.02	1.00	.07	.99	.04	.95	.05	.89	.09		
0	0	0	0	0	0	0	0	0	0	1.0	1.0	0	0	0	0	0	0	1.0	1.0	0	0	0	0		
.81	.81	.92	.90	.90	.90	.92	1.02	1.02	1.07	1.02	1.07	1.04	1.07	1.02	1.02	1.04	1.02	1.07	1.11	1.14	1.09	1.07	1.16	1.07	1.11
.83	.83	.88	.88	.83	.88	.95	.88	.95	1.07	1.02	1.02	1.02	1.07	1.07	1.07	1.00	1.07	1.02	1.02	1.02	.93	.93	.88	.88	
.82	.02	.90	.03	.88	.05	.94	.09	1.03	.09	1.03	.04	1.05	.03	1.05	.04	1.06	.07	1.07	.09	1.04	.15	1.00	.17	.17	
0	0	0	0	0	0	0	0	0	0	0	0	0	0	0	0	0	0	0	0	0	0	0	0	0	
.78	.78	.88	.88	.88	1.04	1.02	1.07	1.07	1.07	1.11	1.04	1.07	1.07	1.07	1.04	1.14	1.14	1.07	1.07	1.11	1.04	1.02	1.04	1.04	
.83	.83	.81	.83	.93	1.02	1.05	.98	1.07	1.02	1.09	1.05	1.02	.98	.98	1.07	1.02	1.02	1.07	1.00	1.05	.95	1.00	.93	.93	
.81	.05	.85	.05	.97	.12	1.03	.06	1.06	.04	1.07	.06	1.03	.07	1.04	.07	1.08	.10	1.05	.05	1.04	.11	1.00	.08	.08	
0	0	1.0	1.0	0	0	1.0	1.0	1.0	1.0	0	0	0	0	0	0	0	0	0	0	1.0	1.0	0	0	0	
1.07	1.07	1.02	1.04	.99	1.11	1.07	1.04	1.11	1.11	1.11	1.04	1.07	1.09	1.07	1.11	1.14	1.16	1.11	1.11	1.16	1.16	1.09	1.11	1.11	
1.07	1.07	1.07	1.02	1.05	1.07	1.00	1.05	1.02	1.02	1.02	1.07	1.12	.98	1.02	.98	1.05	1.02	1.14	.95	1.02	1.07	1.02	.93	.93	
1.07	.00	1.04	.04	1.06	.08	1.04	.04	1.07	.08	1.06	.06	1.06	.10	1.04	.09	1.09	.11	1.08	.14	1.10	.11	1.04	.13	.13	
0	0	0	0	1.0	1.0	0	0	1.0	1.0	1.0	1.0	0	0	0	0	0	0	1.0	1.0	0	0	0	0	0	
1.11	1.11	1.02	1.07	1.04	1.11	1.07	1.09	1.07	1.11	.99	1.11	1.04	1.02	1.11	1.07	1.04	1.07	1.11	1.11	1.09	1.07	.41	1.02	1.02	
1.07	1.07	1.07	.95	1.05	1.05	1.14	1.07	1.14	1.05	1.09	1.05	1.16	1.07	1.05	1.07	.98	1.02	1.07	1.07	1.05	1.02	.93	1.05	1.05	
1.09	.04	1.03	.09	1.06	.05	1.09	.05	1.09	.07	1.06	.08	1.07	.10	1.07	.04	1.03	.06	1.09	.04	1.06	.05	.85	.48	.48	
0	0	0	0	0	0	0	0	0	0	0	0	1.0	1.0	0	0	0	0	0	0	1.0	1.0	1.0	1.0	1.0	
.97	.97	.92	.97	1.04	1.04	1.07	1.07	1.02	1.07	1.04	1.07	1.02	1.07	1.04	1.02	1.02	1.16	1.04	1.14	1.02	1.02	.92	.90	.90	
1.05	1.05	1.02	1.00	.98	1.07	1.07	1.07	1.07	1.02	.98	1.02	1.02	.98	1.02	.95	1.02	1.14	1.09	1.14	1.07	1.12	.93	1.07	1.07	
1.01	.07	.98	.07	1.03	.06	1.07	.00	1.04	.04	1.03	.06	1.02	.06	1.01	.06	1.08	.12	1.10	.07	1.06	.07	.96	.12	.12	
0	0	0	0	0	0	0	0	1.0	1.0	0	0	0	0	0	0	0	0	0	0	1.0	1.0	0	0	0	
1.07	1.07	1.07	1.02	1.07	1.04	1.04	1.04	1.07	1.09	1.02	1.02	1.02	.99	1.11	1.07	1.02	1.02	1.04	.99	1.11	.97	.92	.64	.64	
1.07	1.07	1.07	1.02	1.05	.98	1.05	1.02	1.07	1.02	1.05	1.05	1.12	1.05	1.05	1.05	1.05	1.12	1.05	1.12	1.05	1.16	1.00	1.07	1.07	
1.07	.00	1.04	.04	1.03	.06	1.04	.02	1.06	.04	1.03	.02	1.04	.08	1.07	.05	1.04	.06	1.05	.08	1.07	.13	.91	.30	.30	
0	0	1.0	1.0	0	0	0	0	0	0	0	0	1.0	1.0	0	0	0	0	0	0	0	0	0	0	0	

Figure 28. Sample Data Sheet Showing Point Readings and Averages for a Section

hypothesis and a one indicates rejection. With such a small sample, the analysis of variance almost never showed a significant difference except by random chance when the error was near zero. The test was valuable in detecting errors in data punching and so it was retained throughout the experiment.

After the average density was computed at each point, a linear interpolation subroutine was used to find contours of equal density. These were plotted using a computer plotting routine and several of these are included in Appendix A. For the "artificial fine" soil it was possible to choose a certain density contour to outline a zone of decreased density caused by the action of the planter opener. For this soil the 0.9 grams per cubic centimeter contour was chosen for two reasons. First, it represented a ten percent reduction in bulk density compared to an undisturbed sample. The sampling procedure would be expected to do some averaging near the boundary between dense and loose material. Secondly, the 0.9 grams per cubic centimeter contour terminated at the centerline of the cross section very near the bottom of the opener.

For natural soil samples, the initial average sample density was not as constant as it was for the artificial soils. For this reason, a new contour was chosen at ninety percent of the average wet density. There was a natural gradient in the moisture content with lower moistures near the surface. The zone of decreased density would then be slightly erroneous near the surface; however, the difference in moisture between one-half inch deep and four inches was only about two percentage points which is within the experimental error of this research.

It is not possible to state that any particular contour represents the lines of shear failure, but the use of one density contour will permit comparison of furrow shape and size between samples. The shape of the contours suggested the use of an exponential curve of the form

$$y = A + Bx + Ce^{-Dx} \quad (4.1)$$

where

y = depth to the decreased density line,

x = distance from centerline, and

A , B , C , and D = constants.

The method of least mean squares was used to fit a curve of the form

$$z = A + Bx + Cy^r \quad (4.2)$$

where the transformations

$$y^r = e^{-Dx}$$

and

$$z = y$$

gave the final form of Equation 4.1.

A sample of six curves were fitted using values of D between one and ten. For those six the average standard deviation from the curves was a minimum using a value of D equal to four. That constant was used throughout the remainder of the curve fitting. After curves were fitted the depth, width, and area were computed using the fitted equation. After depth, width, and area had been computed they were related to

opener face angles by appropriate statistical models as explained in the results chapter.

No such convenient method of analysis was found for the research on compaction at the bottom of the seed furrow. Wedge sample density cross-sections will be discussed in the chapter on results.

CHAPTER V

RESULTS

The results of this experiment will be discussed in the following paragraphs. Cross sectional density patterns will be discussed for the various soils used in the experiment, followed by an analysis of the effect of furrow opener shape on density of the "artificial fine" soil. Results will be compared to theoretical models and slow motion films will be discussed. Statistical models were fitted to furrow characteristics and these have been included to allow prediction of results for openers within the range of angles tested. Last will be a discussion of the compaction wedge trials on three different soil samples.

Density Patterns for the Various Soils

Cross sectional density patterns for the various soils and opener shapes are presented in Appendix A. Duplicates of some density pattern figures have been included in the text of this chapter to simplify reading. These plotted patterns include the original soil surface, an approximation of the final soil surface and the boundary of a zone of reduced soil density. In these figures the left edge of the graph represents the center line of the opener. Distance beside the opener and depth were plotted in inches. The curves were plotted using the line printer on the computer and the plotted symbols were keyed to the density in grams per cubic centimeter. For instance, 0.8 gm/cc was plotted

using the figure 8 and 1.0 grams was plotted using the 0. Since these were plotted on the printer it is possible for the letters to be displaced slightly from their true locations since they could be plotted only to the nearest print position. In the horizontal direction, the maximum plotting error was 0.05 inches and in the vertical direction it was 0.0833 inches.

Appendices A-I through A-X are the plots of density patterns in the "artificial fine" soil caused by the various furrow openers. Each of these plots represents the average of two replications. Using the compaction method explained in the procedure chapter of this report, the average density of the "artificial fine" soil was 1.05 grams per cubic centimeter.

Figure 29 shows the density pattern in an undisturbed sample of "artificial fine" soil. In this plot the density decreased near the soil surface across the entire sample. Coming downward from the soil surface at the opener center line the density increased rapidly reaching a value of one gm/cc at about one-half inch deep. This lower density may have been due to some edge effect in the reading instrument, but more probably was due to surface irregularities in the soil samples. The plastic liner that was used to prevent adherence in the soil samples box made accurate surface trimming difficult. Also, it would be expected that the density would decrease near the surface since there was no confining pressure to hold it a high density. There is a more serious decrease in density down the right side of the sample. This was near the side of the box and was attributed to failure of the base-plate to compact soil in this region. Most of the runs in this experiment showed a zone of decreased density extending about three inches to

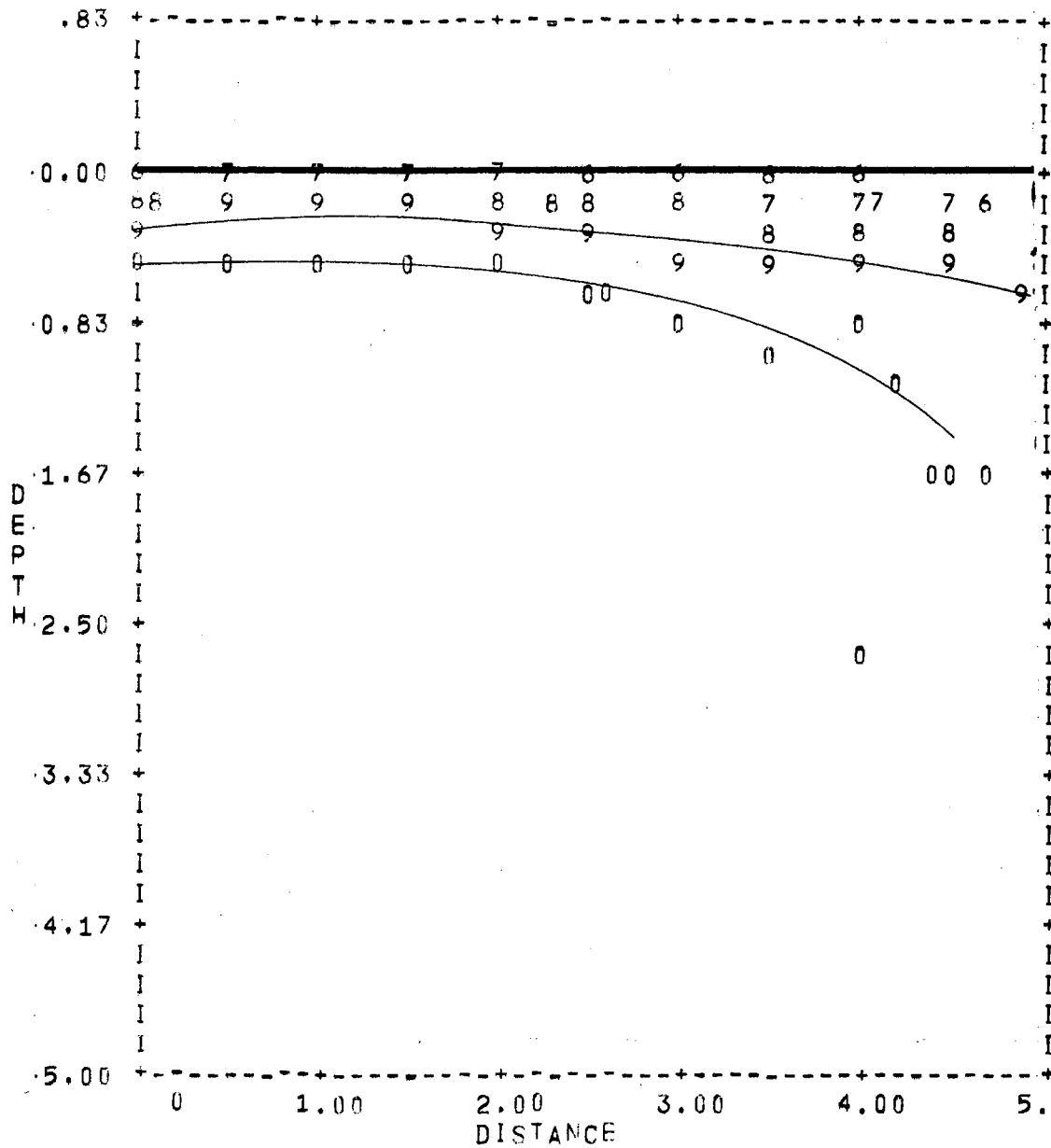


FIGURE 29. DENSITY PATTERN IN AN UNDISTURBED SAMPLE OF ARTIFICIAL FINE SOIL, TWO REPLICATIONS

the side of the opener. The decreased density at the boundary should not have affected the results, but for future research a wider sample box would be recommended.

Figure 30 is a typical density pattern for "artificial fine" soil. Final soil surface was poorly correlated to any particular density contour. The surface line was determined by measuring down from the top of the cross section box to an estimated final surface. Typically, large loose aggregates were present on the surface making the measurement a gross approximation. In granular form the "artificial fine" soil could be loose-filled in a sample container at a density of about 0.6 gm/cc. The density measuring equipment averaged the density across the length of the three-inch long cross section so large individual aggregates on the soil surface were probably not detected by the density measuring equipment.

The zone of decreased soil density for the "artificial fine" soil was taken to be bounded by the 0.9 gm/cc density contour. On the plotted cross sections this contour is seen to intersect the center line of the opener (left edge of the figure) and then curve upward into a straight line until it intersects the original 0.9 contour. Near this intersection a slight rounding or blending of the curves may be seen in some samples. This may have been related to the original fracture line or caused by soil movement over the area after failure. This minor effect was ignored in the analysis of the results. In fitting the chosen statistical model to the boundary of the zone of decreased density, it was necessary to use some judgment in selecting the number of points to be included in the calculations. In general, when the points along the contour began to deviate badly from a visual straight line, the

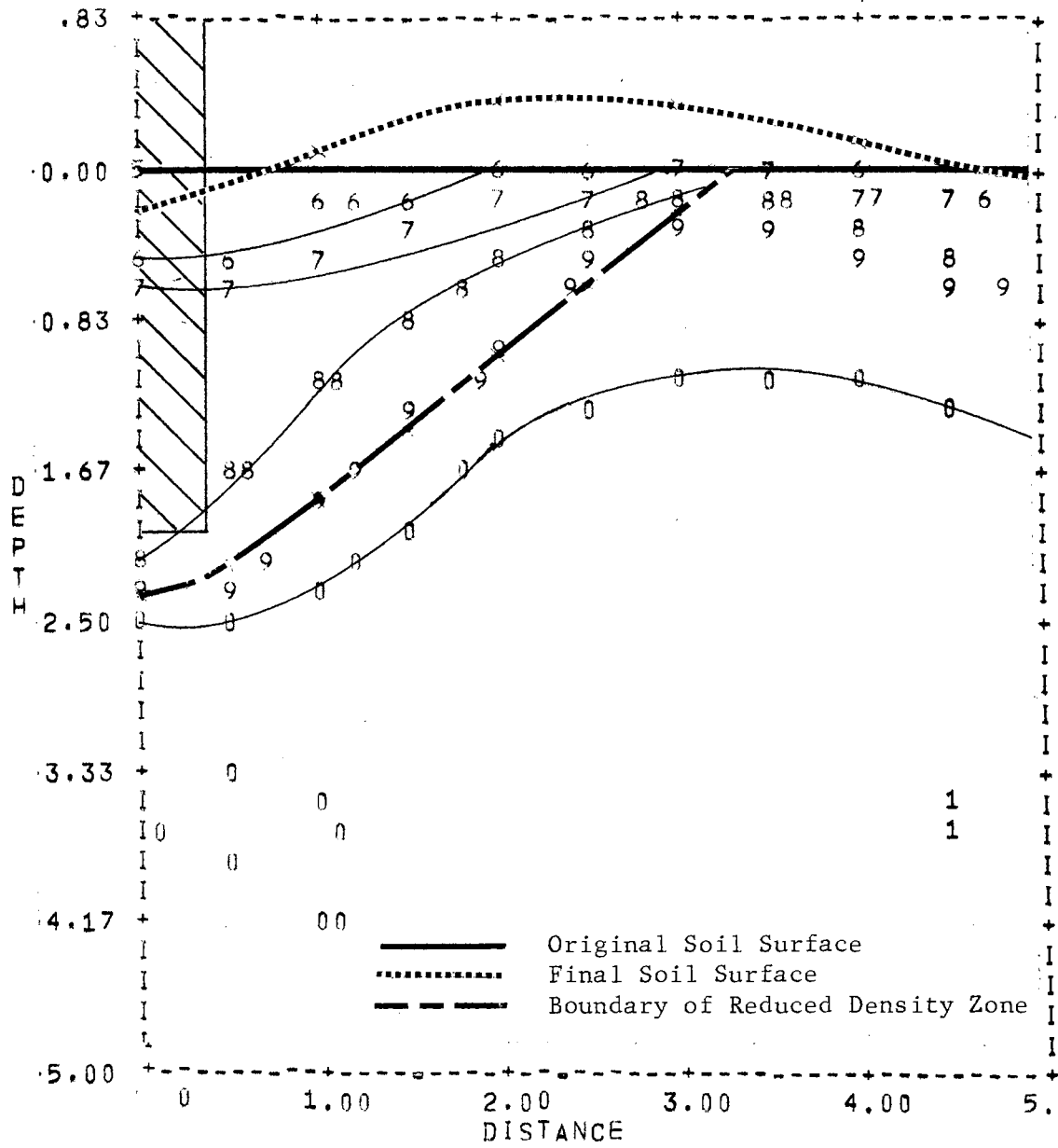


FIGURE 30. DENSITY PATTERN FOR OPENER 0-82 1/2 IN ARTIFICIAL FINE SOIL, TWO REPLICATIONS

remainder of the contour points were ignored. Only the width beyond which points were ignored was chosen arbitrarily. No points before or after the chosen width were selected for inclusion or deletion except where linear interpolation had produced two points of essentially the same coordinates.

Some of the other contours may be of interest. The 1.0 gm/cc contour (plotted as 0) is seen to wander about in most of the plots. This contour was very near the average density of the sample and normal variation of the reading technique and of the soil density causing the density surface to undulate. The 0.8 gm/cc contour generally follows the 0.9 contour although for some samples it was much nearer the surface.

Some sample runs on natural soil are presented in Appendices A-XVI through A-XXIII. The soaking and drying time was so long that only a few samples of the natural soil were run. Also, the lack of homogeneity of the samples was quite apparent and the results were correspondingly erratic. In natural soil samples, wet densities of ten percent less than the average sample density were considered to define the boundary of the area of reduced soil density. This contour was plotted with the letter X.

Average moisture contents of the samples near the bottom of the furrow ranged from 14.6 to 22.0 percent on the dry basis. The dryer samples caused the most difficulties due to shrinkage. Figure 31 shows the density pattern of a sample dried to the point that large soil blocks tended to be pushed apart within the sample container. The density pattern reflected this effect. The zone of decreased density was quite small and there were some areas of loose soil below the opener path. The curves defining the boundary of the decreased soil density

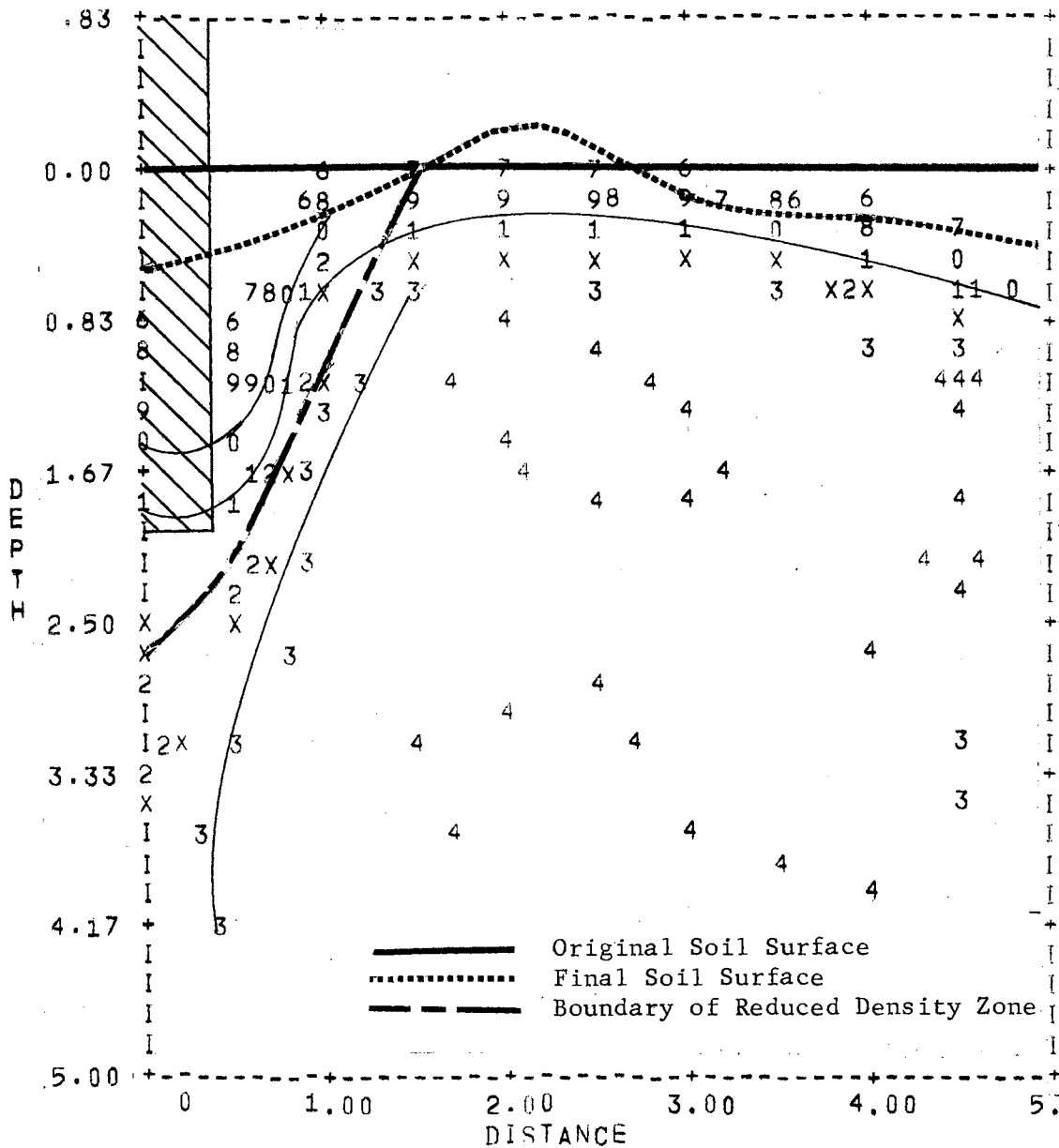


FIGURE 31. DENSITY PATTERN OF OPENER 45-75 IN NATURAL MEDIUM SOIL

zone for other samples had the same form as the boundary curves for the "artificial fine" soil.

Density patterns for certain openers on the "artificial coarse" soil appear as Appendices A-XI through A-XV. An undisturbed sample and several test runs have been included. The 1.4 gm/cc contour was chosen as the boundary of the decreased density zone. This contour consistently intersected the center line near the bottom of the opener. The shape of the contour was consistent with that found for the "artificial fine" soil.

Results on "Artificial Fine" Soil

After the statistical model curve was fitted to the boundary of the zone of decreased soil density for each run, width, depth, and area of the zone were computed using the fitted equation. The slope of the linear portion of the curve was also computed.

The results of these observations have been grouped into Table I. Comparison of factor values between replications shows good agreement in most cases. The most variation existed among runs of the 60 degree vertical angled openers. Lift and drag force measurements appear in Table II.

The data of Tables I and II were subjected to statistical analyses as factorial experiments. Factor one was vertical face angle and factor two was horizontal face angle. The data have been presented first as a set of curves representing individual observations and subsequently as two bar graphs under which the Duncan's Multiple Range Test has been indicated with letters. Two bars underscored by the same letters are not significantly different at the five percent significance level.

TABLE I
SUMMARY OF DECREASED DENSITY ZONE CHARACTERISTICS
FOR OPENER FACE ANGLES ON
ARTIFICIAL FINE SOIL

Vertical Angles, degrees.....0	0	0	45	45	45	60	60	60		
Horizontal Angles, degrees....60	75	82.5	60	75	82.5	60	75	82.5		
Factor	Replication									
Center line Depth (inches)	1	2.45	2.30	2.33	2.46	2.37	2.37	2.72	2.45	2.57
	2	2.42	2.44	2.34	2.45	2.44	2.36	2.53	2.32	2.44
	Average	2.43	2.37	2.33	2.46	2.40	2.36	2.63	2.39	2.48
Width (inches)	1	6.59	6.38	6.60	8.02	8.23	6.29	6.14	6.49	5.96
	2	6.95	6.63	6.62	8.04	7.46	7.25	6.44	7.50	7.38
	Average	6.77	6.51	6.61	8.03	7.84	6.77	6.29	6.99	6.67
Area (square inches)	1	9.17	7.57	8.64	10.13	10.52	8.46	9.93	8.74	8.01
	2	9.91	8.95	8.44	10.78	10.09	9.46	9.33	9.94	9.15
	Average	9.54	8.26	8.54	10.45	10.31	8.96	9.63	9.34	8.58
Side Slope (degrees from vertical)	1	49.2	53.2	51.0	57.7	57.9	49.8	42.6	49.8	47.5
	2	49.9	50.4	52.0	56.0	53.6	53.8	47.4	54.2	56.0
	Average	49.6	51.8	51.5	56.8	55.8	51.3	45.0	52.0	51.8

TABLE II

DRAG AND LIFT FORCES FOR VARIOUS OPENER FACE
ANGLES ON ARTIFICIAL FINE SOIL

Vertical Angles, degrees.....0		0	0	45	45	45	60	60	60	
Horizontal Angles, degrees....60		75	82.5	60	75	82.5	60	75	82.5	
Factor	Replication									
Drag Force (pounds)	1	35.3	45.4	31.5	48.2	45.4	43.0*	63.5	40.6	51.5
	2	24.3	44.4	36.5	69.8	46.6	51.2	84.5	65.6	54.8
	Average	29.8	44.9	34.0	59.0	46.0	47.12	74.0	53.1	53.1
Lift Force (pounds)	1	11.6	4.9	7.3	31.6	21.7	17.0	52.9	27.4	26.3
	2	10.7	6.8	4.3	39.5	15.8	12.3	72.2	43.4	28.7
	Average	11.1	5.8	5.8	35.5	18.8	14.7	62.5	35.4	27.5

* Estimated Missing Value

Figure 32 shows the effect of face angle on furrow depth. The openers with 60 degree horizontal face angles decreased the density to a greater depth than openers with 75 or 82.5 degree horizontal angles at all vertical face angles. In the factorial analysis, depth of disturbance is seen to increase with vertical face angle although only the 0 and 60 degree angled openers gave results that were significantly different. Horizontal angles of 75 and 82.5 degrees produced disturbed zones significantly shallower than those of the 60 degree horizontal angled openers. The interaction between horizontal and vertical angles was nonsignificant.

Figure 33 depicts the slope of the linear portion of the boundary of the decreased density zone. Angles were measured from the vertical so large angles correspond to large areas for equal furrow depths. The 60 degree horizontal angled openers produced steeper sides than the other openers with vertical angles of 0 and 60 degrees and the least steep sides with a 45 degree vertical angle. The same pattern is seen in the statistical analysis of vertical angles. Horizontal face angles had a non-significant effect on boundary slope.

Width of the decreased density zone is shown in Figure 34. The most dramatic effect seen in the graph of individual values is that openers with 60 and 75 degree horizontal angles and 45 degree vertical angles produced decreased density zones wider than all the other openers. In the factorial analysis, the 45 degree vertical angled openers produced reduced soil density zones that were significantly wider than either the 0 or 60 degree vertical-angled openers. There were no significant differences in the width of the disturbed soil zone for openers with different horizontal face angles.

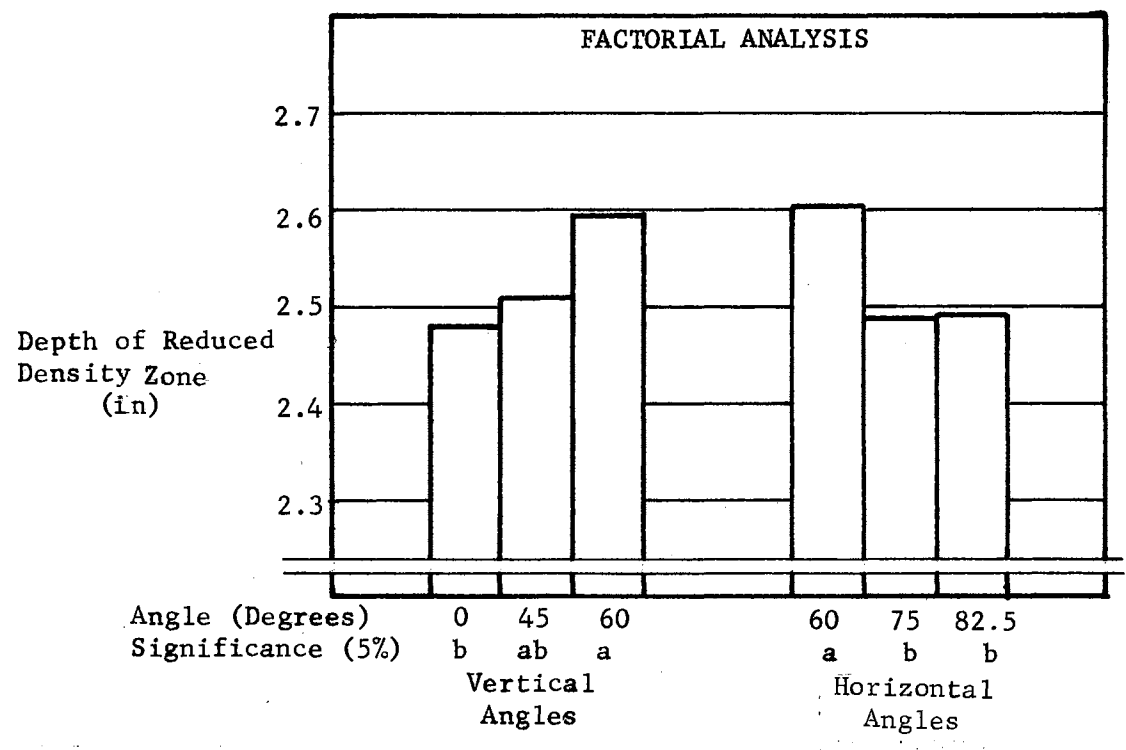
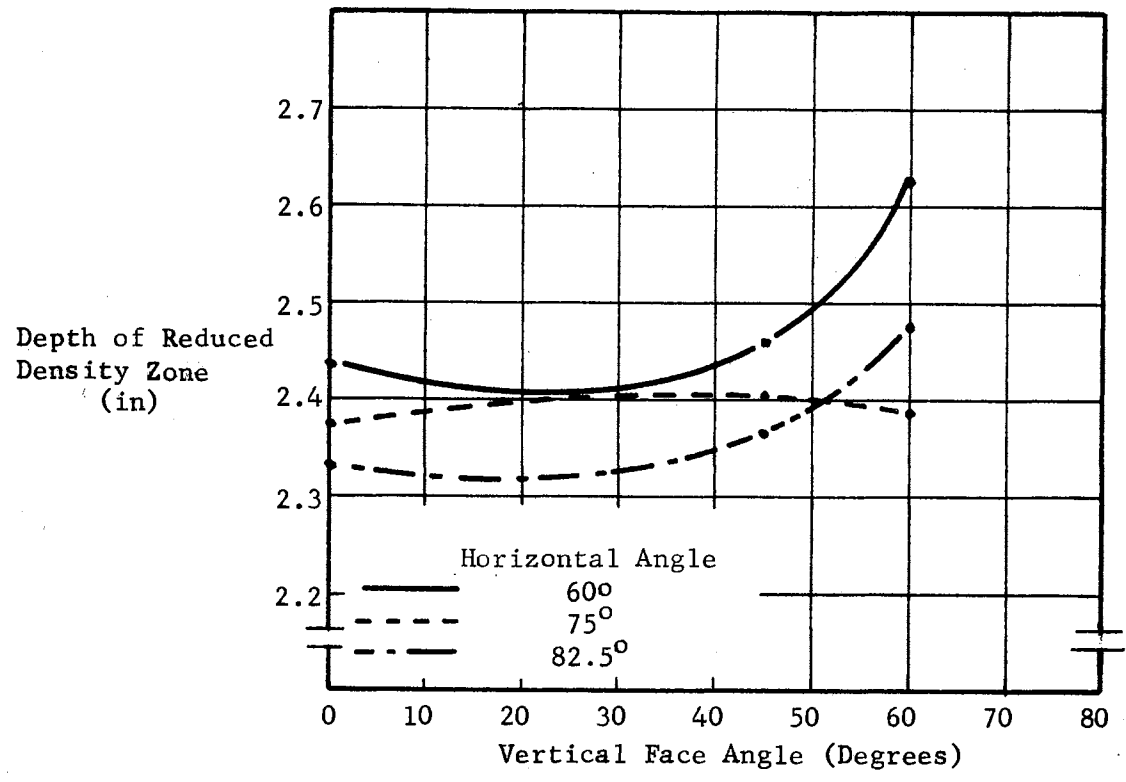


Figure 32. Effect of Opener Face Angle on Depth of the Reduced Soil Density Zone

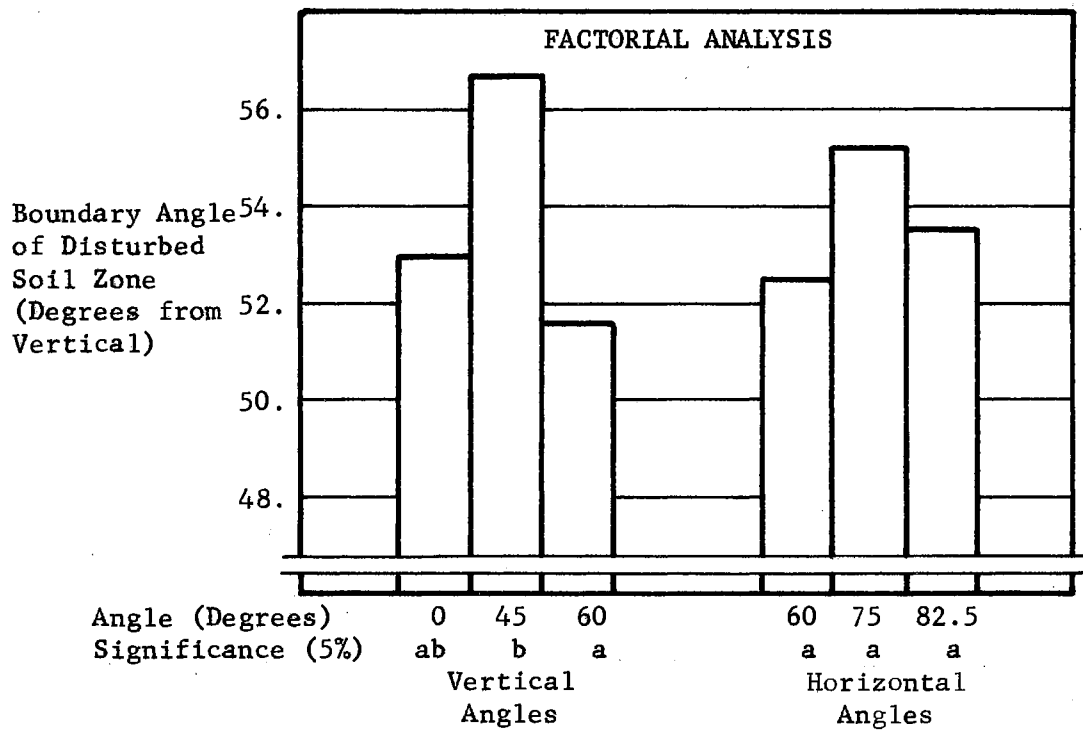
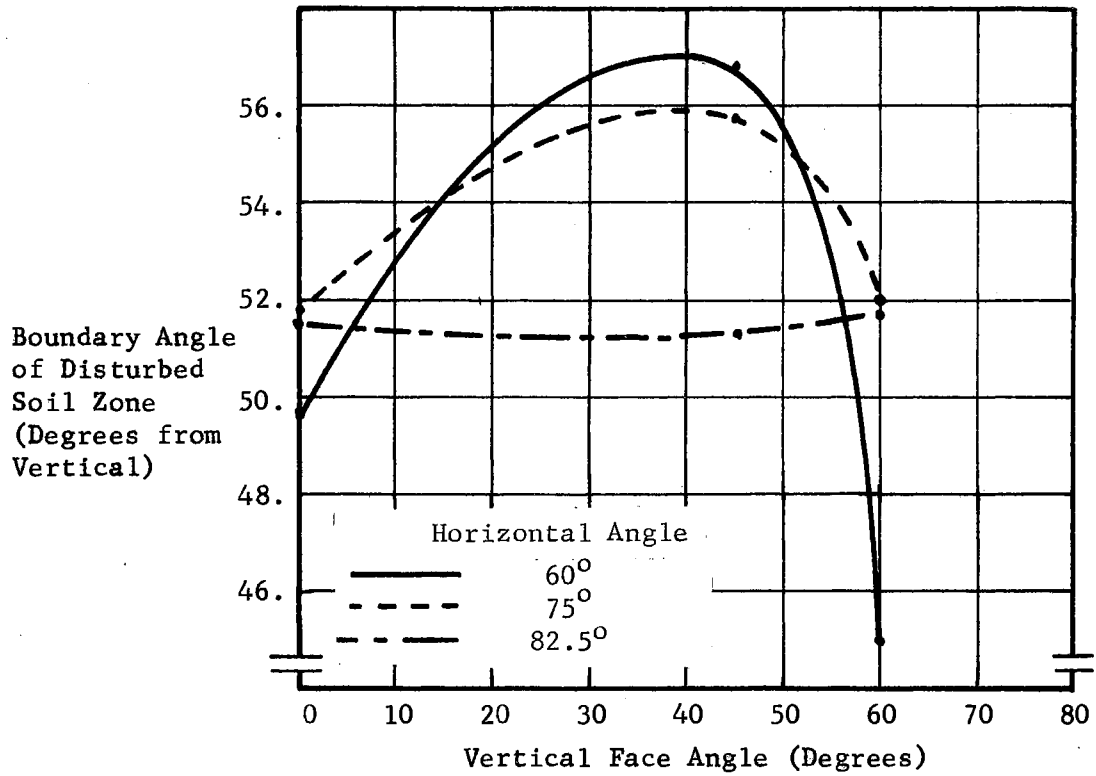


Figure 33. Effect of Opener Face Angles on Side Slope of the Reduced Soil Density Zone

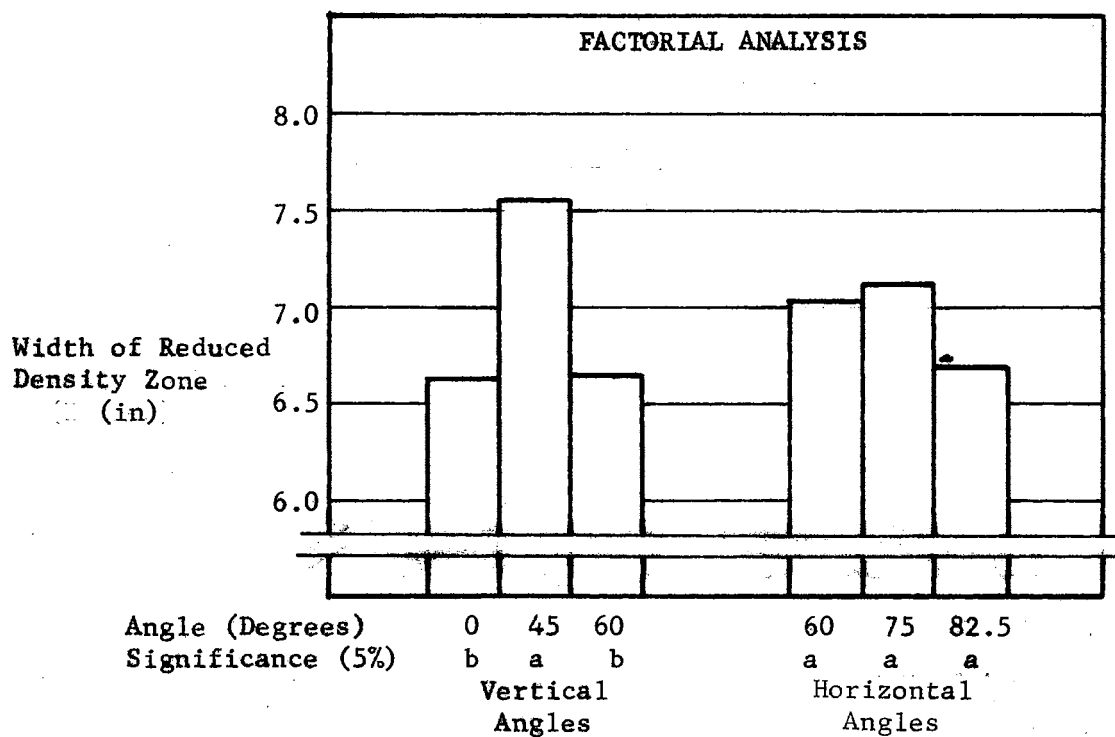
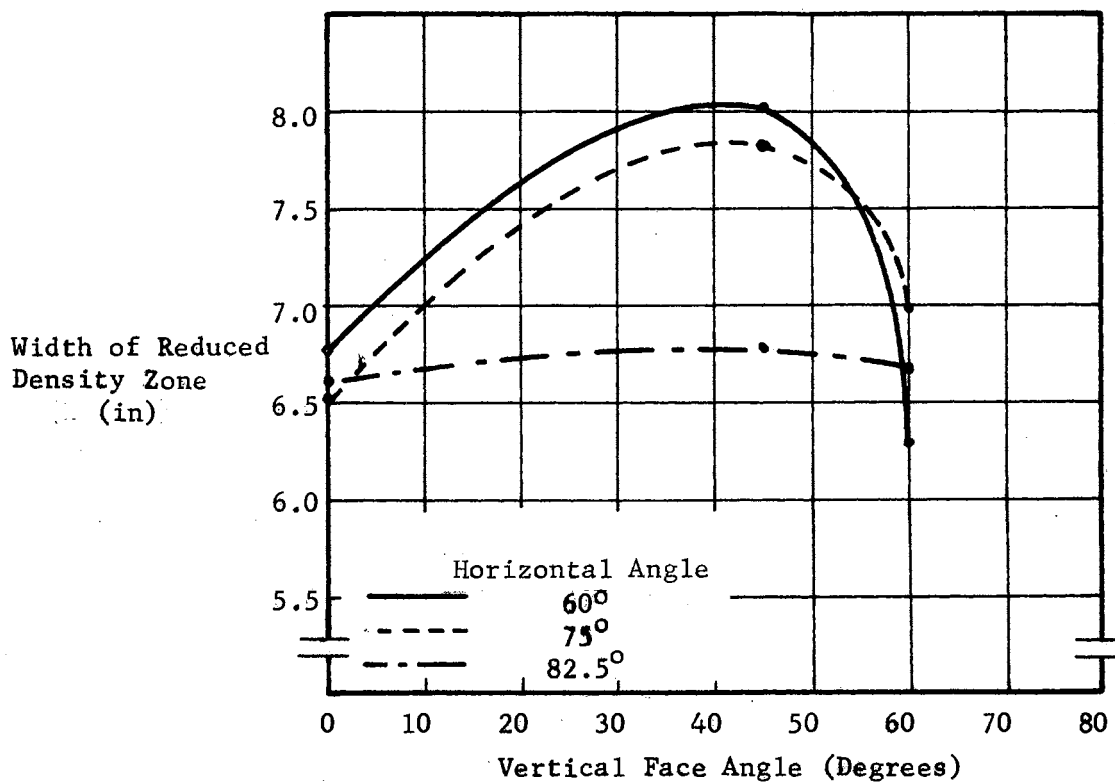


Figure 34. Effect of Opener Face Angles on the Width of the Reduced Soil Density Zone

The area of reduced soil density produced by the openers is shown in Figure 35. Area includes effects of both depth and width of disturbed soil. The curves indicate a more consistent pattern of results for area than did either depth or width. Sixty degree horizontal angled openers produced larger areas of lowered soil density than either 75 or 82.5 degree openers at all vertical face angles. The 82.5 degree horizontal angled openers disturbed smaller areas than all other openers except at 0 degrees vertical angle where the 75 degree horizontal angled opener disturbed less soil. The bar graphs show 45 degrees vertical angled openers to produce significantly larger areas of disturbed soil than either 0 or 60 vertical angled openers. The area of reduced soil density decreased as horizontal angle increased. Areas of disturbed soil from the 82.5 degree horizontal angled openers were significantly lower than those from the 60 degree horizontal angled openers.

Drag and lift forces were related to vertical and horizontal face angles and the results appear in Figures 36 and 37. Drag force is seen to have increased with increasing vertical face angle for all values of horizontal face angle. However, there was a reversal in this data. For small vertical angles the 75 degree horizontal angled opener showed the greatest drag force, but at higher vertical angles the 60 degree horizontal opener had the largest drag force. The factorial analysis showed drag to increase with increased vertical angle and decrease with increased horizontal angle. The effect of vertical angles was significant between zero and both inclined openers. The effect of horizontal angle on drag was not significant.

For lift force the effect of face angle was quite pronounced. All vertical face angles resulted in lift forces that were significantly

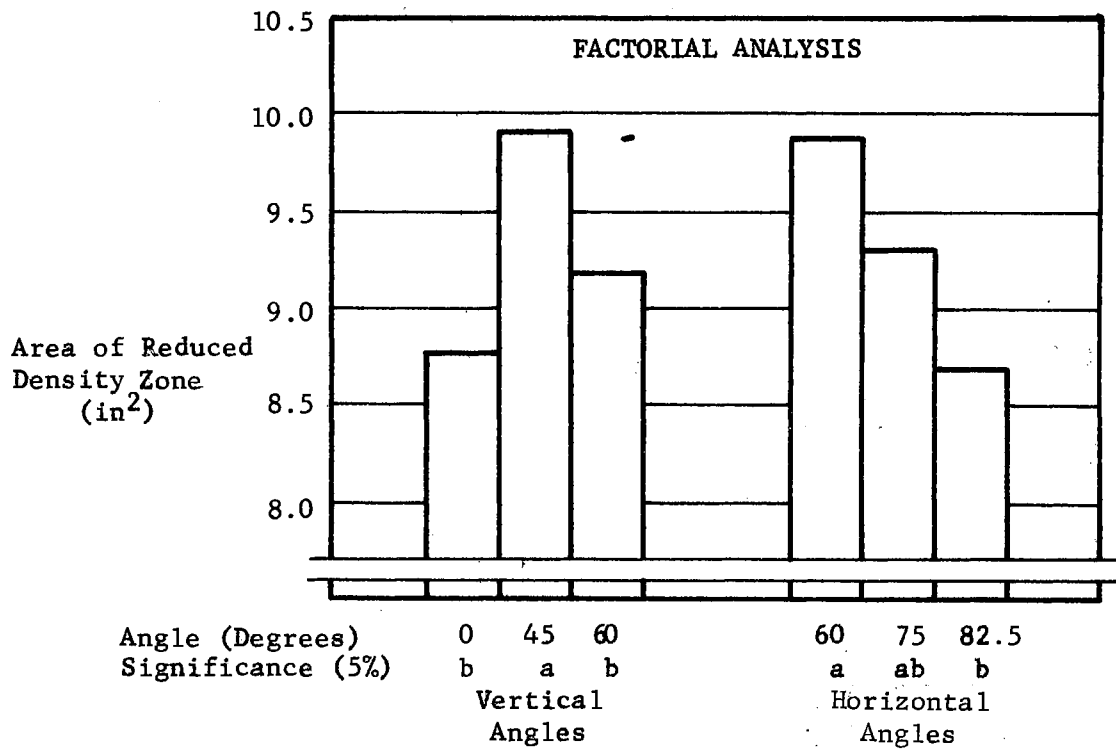
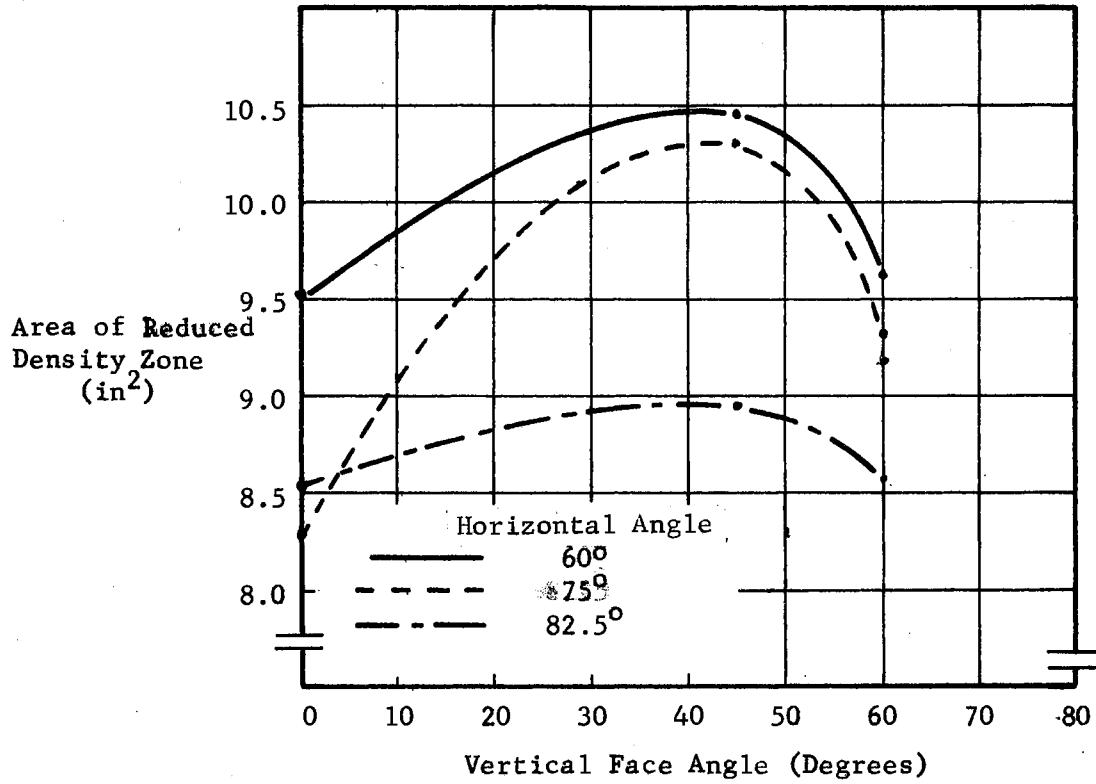


Figure 35. Effect of Opener Face Angle on Area of the Reduced Soil Density Zone

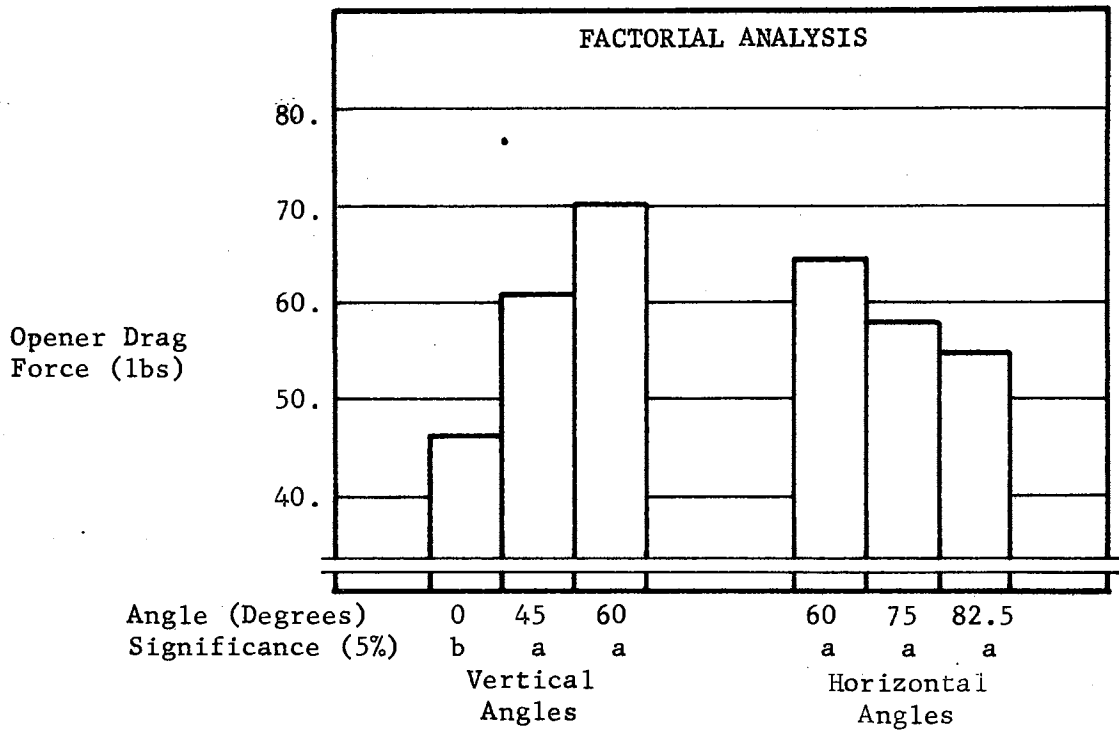
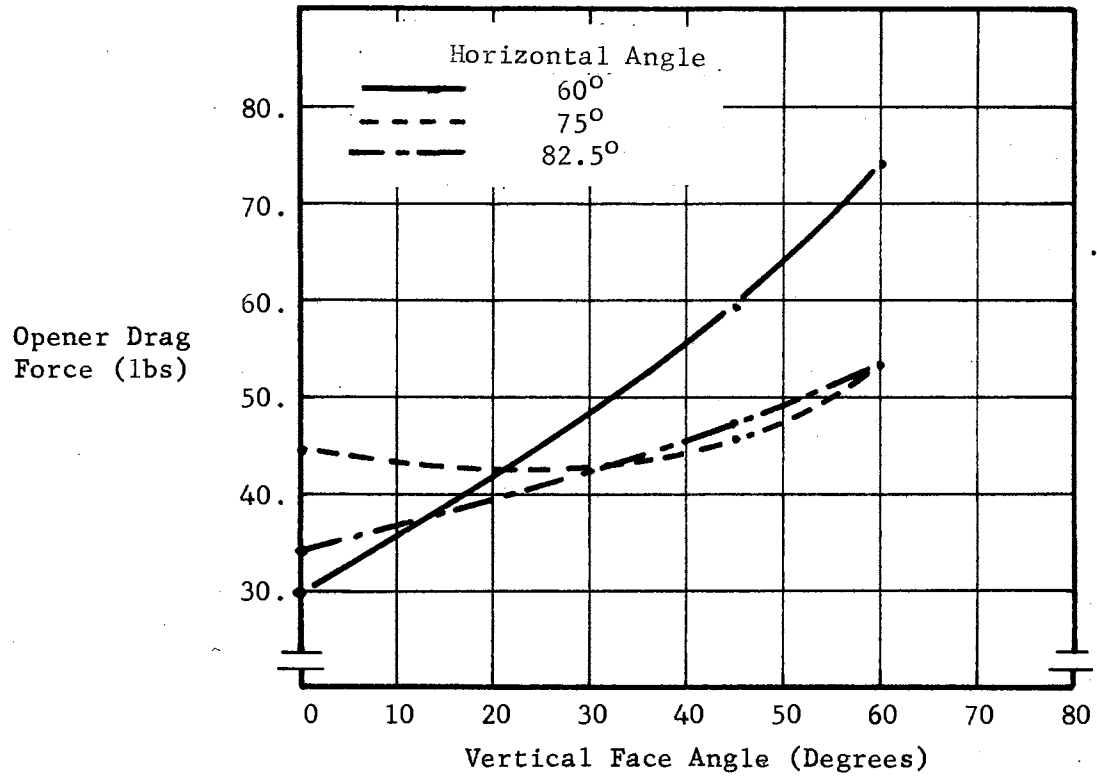


Figure 36. Effect of Opener Face Angles on Opener Drag Force

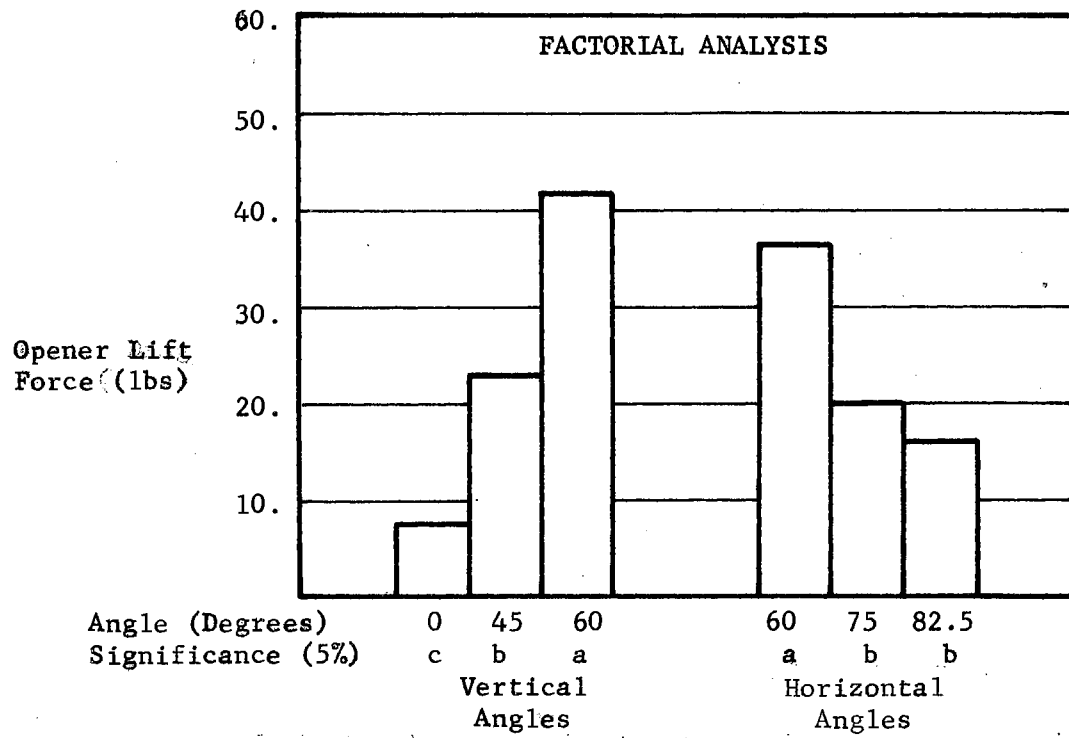
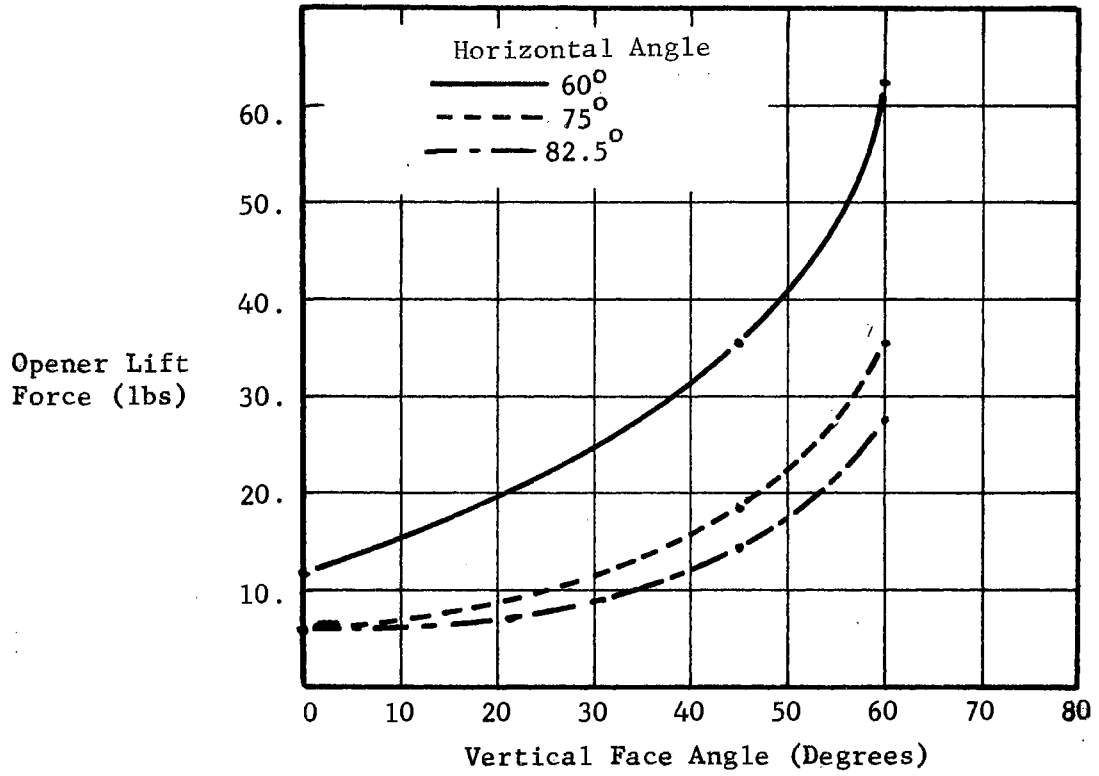


Figure 37. Effect of Opener Face Angle on Lift Force

different than those of the other vertical face angles. Increased vertical angles caused increased lift force. Openers with horizontal angles of 60 degrees had higher lift forces than openers with other horizontal angles. There was no significant difference in lift between openers with 75 and 82.5 degree horizontal angles.

Comparison to Theoretical Models

No combination of soil and planter opener shape tested in this experiment resulted in measurable soil compaction. For this reason, the model suggested for soil compaction beside a planter opener was not tested. This experiment demonstrated that it does not apply to a granular soil with low cohesion where there is no confinement of the soil. The model may have application to cohesive soils where some stress may be exerted on the soil mass when the minor principle stress (confining pressure) is zero. A confining mechanism, such as a flat plate, might aid compaction. It would impose another frictional force on the assumed soil element further restricting horizontal movement. This force could be included in the derivation.

Fracture beside planter openers was predicted to occur by any one of three modes. The first was the Rankine failure plane. As determined by direct shear test, the angle of internal friction, ϕ , of the soil was 35 degrees. The Rankine failure plane would then be $45 + \phi/2$ or 62.5 degrees measured from the vertical. Failure plane angles measured from the vertical in the plane normal to the direction for the various openers appears in the column entitled "Normal Failure Angle" in Table III. The average failure angle in the plane normal to travel was 51.7 which is quite different than the predicted value. If the

Rankine failure occurred in some direction forward of the normal plane, as illustrated in Figure 38, there would be some average curve along the block such as line AB. Two dimensional density sampling would define such average value. Rankine failure at an angle of β would make a furrow whose side slopes appeared greater than the failure angle when cross-sectioned at right angles to opener travel. The β angles required to adjust the observed angles in the normal plane to the expected Rankine failure angle appear in Table III in the column entitled "Forward Angle for Rankine Failure." The angle β was computed using the relationship

$$\beta = \cos^{-1} \left(\frac{\cot(45 + \phi/2)}{\cot\alpha} \right) \quad (5.1)$$

where α was the observed failure angle in the plane normal to travel. The average β for all openers was 47.0 degrees, but the variation was greater among β angles than among angles observed in the normal plane. The most variation in β angles appears among the 60 degree horizontal angled openers. There was almost no variation among β angles for openers with 82.5 degree horizontal face angles.

One might expect the β angle to be related to the horizontal opener face angle and the coefficient of friction between soil and steel. For this soil and steel the adhesion was zero and the friction angle, ϕ' , was 27 degrees. It seems reasonable that β should be directed forward of a line normal to the planter opener face by an angle of ϕ' in the horizontal plane. The differences between β 's calculated in this manner and those calculated from the observed data are in the column entitled "Deviation from Normal Plus Friction Angle" of Table III. Reasonable agreement was found for openers with horizontal angles of

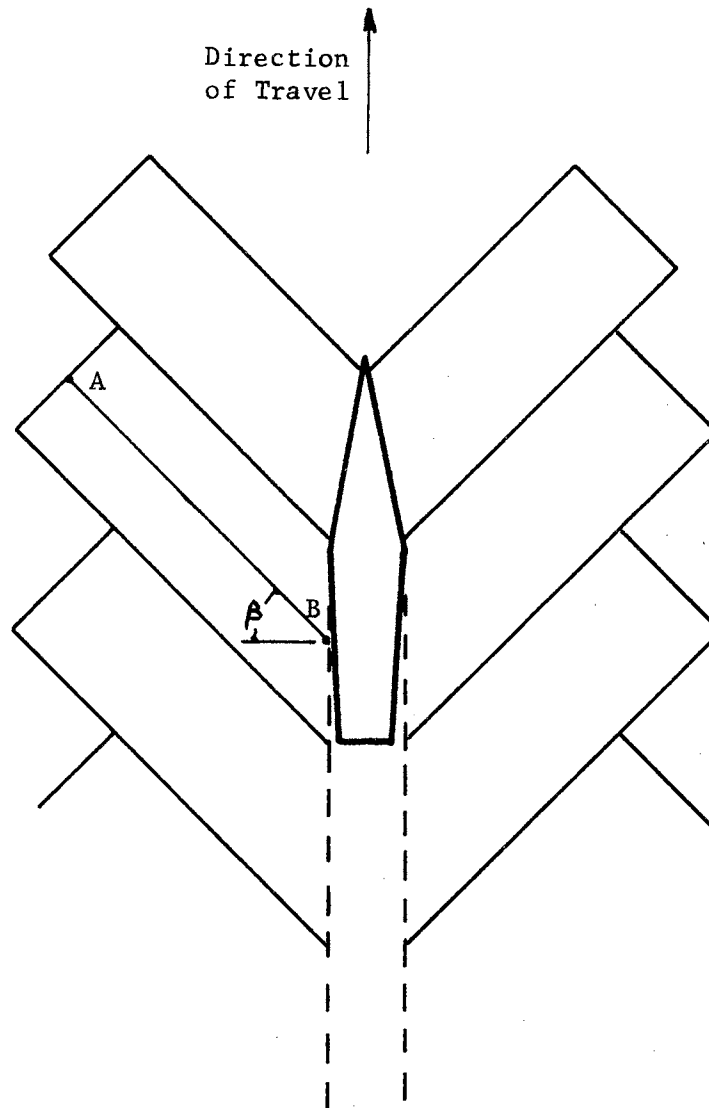


Figure 38. Top View of Failure Block Orientation Necessary to Justify Rankine Solution of Furrow Wall Fracture

TABLE III
 COMPARISON OF PREDICTED AND
 OBSERVED FAILURE ANGLES

OPENER FACE ANGLES		Observed Failure Angle Normal to Travel (degrees)	Forward Angle for Rankine Failure (degrees)	Deviation from Normal Plus Friction Angle (degrees)
Vertical (degrees)	Horizontal (degrees)			
0	60	49.6	52.2	- 4.8
0	75	51.8	48.6	6.6
0	82.5	51.5	49.0	14.5
45	60	56.8	37.9	-19.1
45	75	55.8	40.0	- 2.0
45	82.5	51.3	49.5	15.0
60	60	45.0	58.6	1.6
60	75	52.0	48.1	6.1
60	82.5	51.8	48.5	14.0

60 and 75 degrees except for the 45-60 opener. For it the error was 19.1 degrees. For 82.5 degree angled openers the error was consistently near 15 degrees. For 82.5 degree horizontal angled openers the Rankine failure surface would appear to be angled $1.5 \phi'$ in front of a line normal to the opener face. The existence of a set of factors relating Rankine failure direction to the soil friction angle on the opener face would have to be verified by the use of soils with various soil to opener friction angles.

The second failure model considered wall friction and a soil block. The Coulomb theory for rough faced retaining walls was evaluated for an opener and the "artificial fine" soil using the Culmann technique (Jumikis, 1964). The predicted failure angle was 77.5 degrees from the vertical which was unreasonable, compared to observed values.

The third model proposed was the observed failure shape for cohesive soils behind retaining walls presented by Terzaghi and Peck (1948). They state that the exponential portion of the failure surface does not exist for cohesionless soils. Since the soil used in this experiment had very little cohesion, the exponential portion of the curve should be small and it was for most openers. The curvature could have been caused by the distance the soil was moved laterally by the opener rather having been a portion of the original failure surface. Since the linear portion of the failure surface predicted by this method rises at the Rankine angle, all of the comparisons previously made apply to this model.

None of the modes of action predicted that soil would be disturbed below the planter opener. An experiment involving soil pressure distribution and flow lines around soil tools would be required to evaluate

the reason for this effect. From the data presented here, we can only state that openers with large vertical angles from the direction of travel applied a vertical force to the soil mass. A portion of this force was apparently transmitted to the soil immediately below the tool causing disturbance, perhaps by plastic flow.

The applicability of soil failure theories from the static analyses of soil mechanics to the failure patterns around planter openers appears doubtful. Data from this study cannot be used to determine the mechanics of soil flow around openers. Such a study would have to evaluate soil pressure distributions as the opener passes a point, or use observation of soil flow patterns, perhaps with Plexiglas openers and high speed motion picture equipment. Until those data become available, studies such as this can provide useful information of an empirical nature and perhaps stimulate further work toward a theoretical solution.

Evaluation of Slow Motion Films

Review of slow motion films made during test runs indicated movement of individual soil particles rather than soil failure in a series of blocks. In artificial soils the individual grains appear to flow. In the natural soil samples which had greater shear strength than the artificial soils, fracture beside openers resulted in larger aggregates. For all samples, some material was given enough energy to be separated from the surface of the soil. This effect was greater for openers with small angles from the plane normal to travel. Increased horizontal angle appeared to decrease the effect more effectively than did increased vertical angle.

The maximum filming rate used in this experiment was 64 frames per second which was not sufficient to stop action in every frame for an opener moving at five miles per hour. For this reason particle paths could only be observed generally rather than being traced frame by frame. Particles that were separated from the soil surface were observed to have velocity components in the lateral, longitudinal, and vertical directions, but no quantitative relationships to opener face angle were attempted. To do so, one would require two sets of pictures: one from directly above the sample surface and the other from the side of the opener.

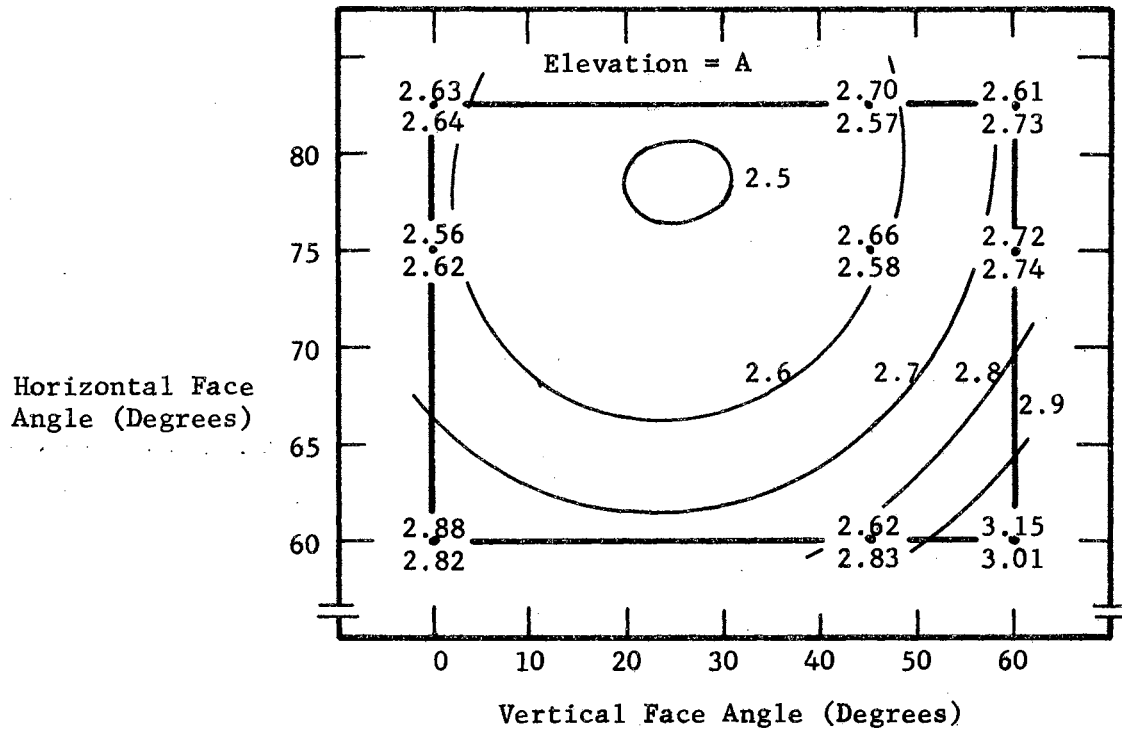
After test runs had been completed, two test samples were prepared and openers were pulled through by hand at a very slow rate. The two openers used had face angles of 0 and 60 degrees in the vertical plane and both had 82.5 degree horizontal angles. The zero degree vertical angled opener produced soil cracks at right angles to the direction of travel at irregular intervals of one to two inches and for a distance of about three inches beside the opener. The cracks began to appear about one-half inch behind the leading edge of the opener. There was some rearrangement of the soil particles before the cracks appeared. The rearwardly inclined (60 degree vertical angle) opener made surface crack in a direction rearward from the opener at an angle of about 30 degrees and extending laterally to about three inches. For this opener the cracks were irregularly spaced. These cracks could not be detected in the full speed test runs. Comparison of slow speed runs to the five miles per hour samples indicated that different modes of failure may occur at different speeds. The analysis of soil failure

around tillage tools has often been based on failure patterns for slow speed runs. This procedure does not seem to be justified.

Prediction Equations

The first attempt to form a set of prediction equations for the characteristics of the zone of decreased density consisted of a set of statistical models for the three constants in the assumed equation of the boundary. The results of this method appears in Figures 39, 40, and 41. For factors A and B the prediction is perhaps acceptable, but for the C the standard deviation is too high. The variation is probably due to the interaction of the three constants. In the least mean squares fitted curves, a low intercept might be canceled by a high exponential term. Generally, the three constants did not show as logical a response as did depth, width, boundary slope, and area. Notwithstanding the shortcomings of this method, the A and B terms uniquely describe the straight line portion of the reduced density zone boundary. The straight line portion comprises the larger part of the curve. For many of the samples the straight line portion, extended upward from the lower, outer corner of the tool represented a fair approximation of the reduced density zone.

In the equation for the reduced density zone boundary, the constant A is the intercept of the straight portion at the center line of the opener. The model in Figure 39 shows A to be a minimum for openers with large horizontal angles and with vertical angle between 20 and 30 degrees. Since the minimum occurred some distance away from an observed point, it should be verified by future research. The maximum value of the intercept (increased depth) occurred at 60 degree horizontal and



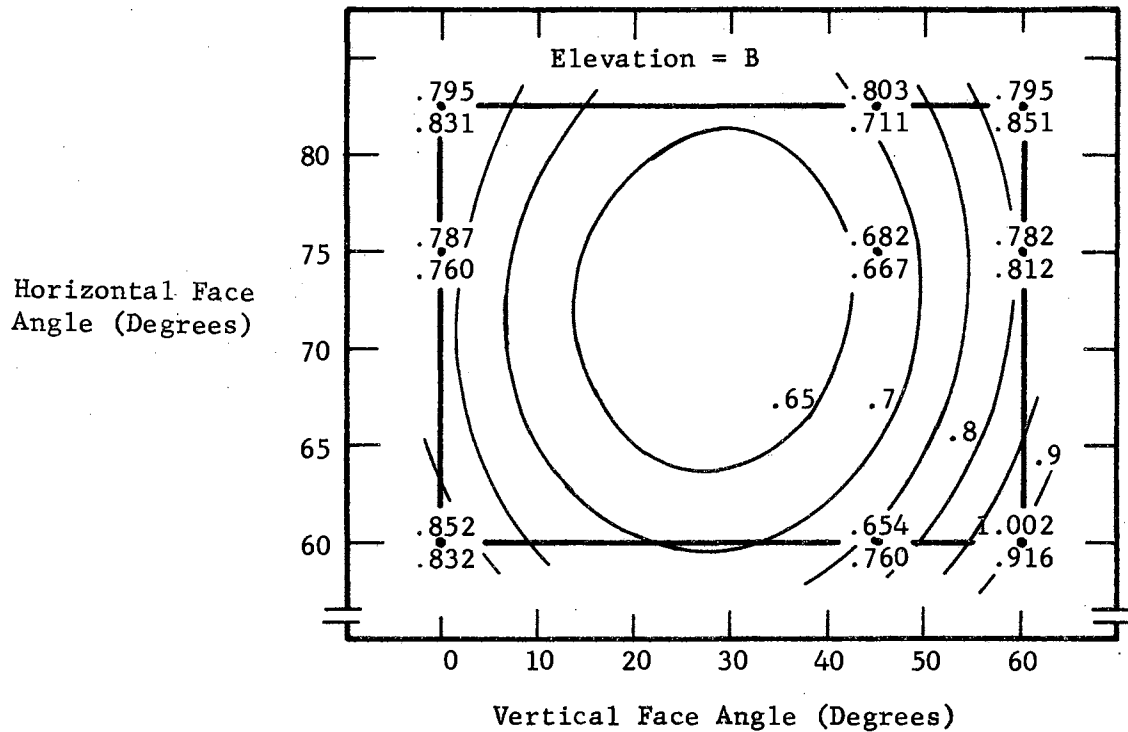
STATISTICAL MODEL

$$Z = 6.631 - 0.004037 X + 0.0001910 X^2 - 0.1038 Y + 0.0006716 Y^2 - 0.00007165 XY$$

Standard Deviation (Absolute) = 0.1887

Standard Deviation (Percent of Mean) = 6.92

Figure 39. Effect of Opener Face Angles on Constant A of the Reduced Density Zone Boundary Equation. Numbers Above Points were Observed, Those Below were Calculated.



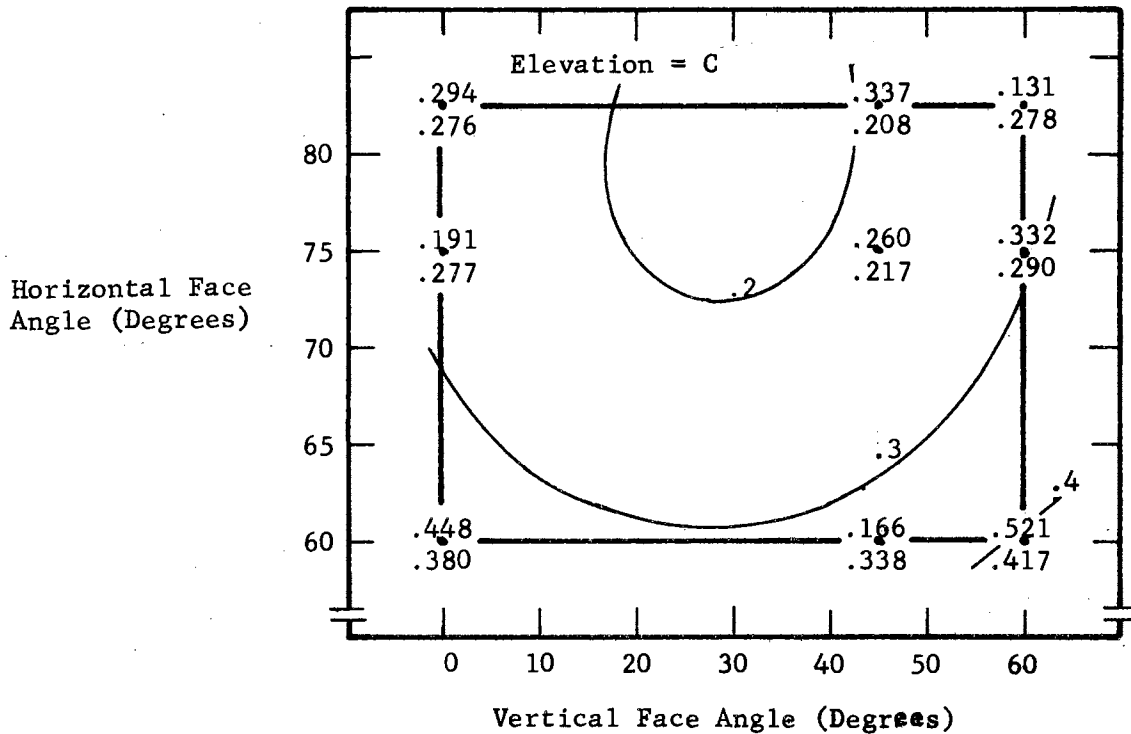
STATISTICAL MODEL

$$Z = 3.480 - 0.007721 X + 0.0001994 X^2 - 0.07619 Y + 0.0005343 Y^2 - 0.00004740 XY$$

Standard Deviation (Absolute) = 0.8048

Standard Deviation (Percent of Mean) = 13.10

Figure 40. Effect of Opener Face Angles on Constant B of the Reduced Density Zone Boundary Equation. Numbers Above Points were Observed, Those Below were Calculated.



STATISTICAL MODEL

$$Z = 2.172 - 0.003978 X + 0.0001028 X^2 - 0.04823 Y + 0.0003026 Y^2 - 0.00002632 XY$$

Standard Deviation (Absolute) = 0.1775

Standard Deviation (Percent of Mean) = 59.60

Figure 41. Effect of Opener Face Angles on Constant C of the Reduced Density Zone Boundary Equation. Numbers Above Points were Observed Those Below were Calculated.

vertical angles. The maximum did occur at an observed point and with high probability represented a maximum for the range of opener shapes observed.

Constant B is the slope of the straight portion of the reduced density zone boundary. In Figure 40, the model shows a large flat area for openers with medium vertical and horizontal angles. A maximum slope occurred for openers with 60 degree horizontal and vertical angles.

Constant C determined the magnitude of the exponential factor. The model in Figure 41 shows that the minimum exponential factor occurred at medium vertical angles and at a maximum horizontal face angle.

Since the various constants of the fitted equations interact, a more consistent relationship may exist between opener angle and the gross effects such as width, depth, and area of the reduced density zone. A set of statistical models relating opener face angles to depth, side slope, width area, drag force, and lift force were computed. Each factor was fitted to a second degree response surface with opener vertical and horizontal face angles being the X - Y values.

To generalize the results the dimensions were reduced using some characteristics of the openers. Depth values were divided by the operating depth of the tool, d_o . The values plotted were then numbers of tool depths. Width was divided by the sum of tool width and depth since both contribute to the total furrow width. Area was divided by the product of tool width and depth. The boundary slope was left in degrees measured from the vertical. Drag and lift forces were converted to unit draft and unit lift by dividing force values by the projected area of the tool in the direction of travel. Thus generalized,

the prediction equations should be applicable to tools of different size but similar geometry. Chisels and other tools are usually classified by their width over depth ratio. This ratio was 0.375 for the openers included in the study. Prediction equations would not be valid for tools with different width to depth ratios or different speeds.

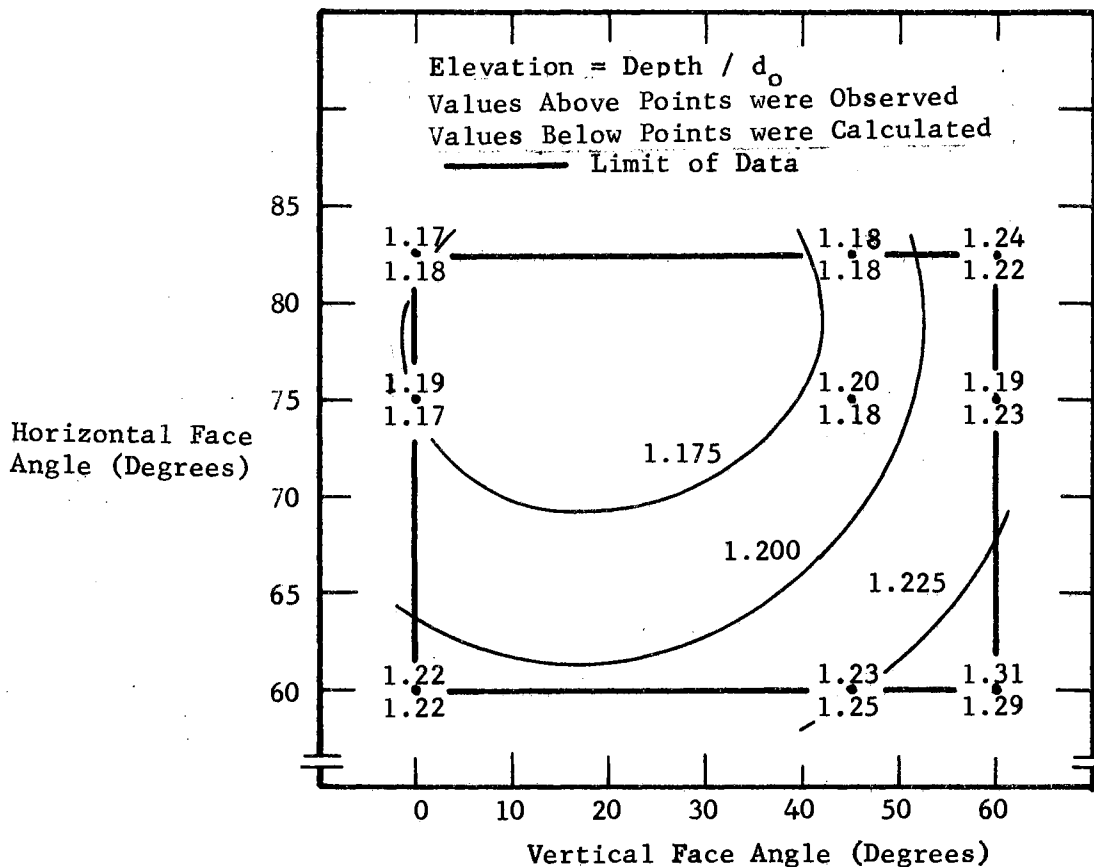
Figure 42 shows the second degree model for depth of the reduced density zone as a function of horizontal and vertical opener face angles. The maximum furrow depth would be produced by openers with small horizontal angles and large vertical angles.

Figure 43 is the model for side slope of the reduced density zone. A maximum occurred in the model at medium horizontal and vertical opener face angles, but it should be viewed with some skepticism since no data was collected in this vicinity. The minimum slope would occur using openers with small horizontal angles and large vertical angles.

To some extent the width model in Figure 44 reflects the effect of boundary slope although depth and the value of the exponential term in the boundary equation also affect width. A maximum width was predicted for openers with medium vertical angles and small horizontal angles.

The area model of Figure 45 was affected by all the previous factors. The minimum cross sectional area of reduced soil density was predicted for openers with large horizontal angles and either large or small vertical angles. A maximum was predicted at medium vertical angles and small horizontal angles.

Prediction of the unit draft acting on an opener is possible using the model of Figure 46. The minimum unit draft occurred with openers having small vertical and horizontal angles. A clear maximum occurred at horizontal and vertical face angles of 60 degrees.



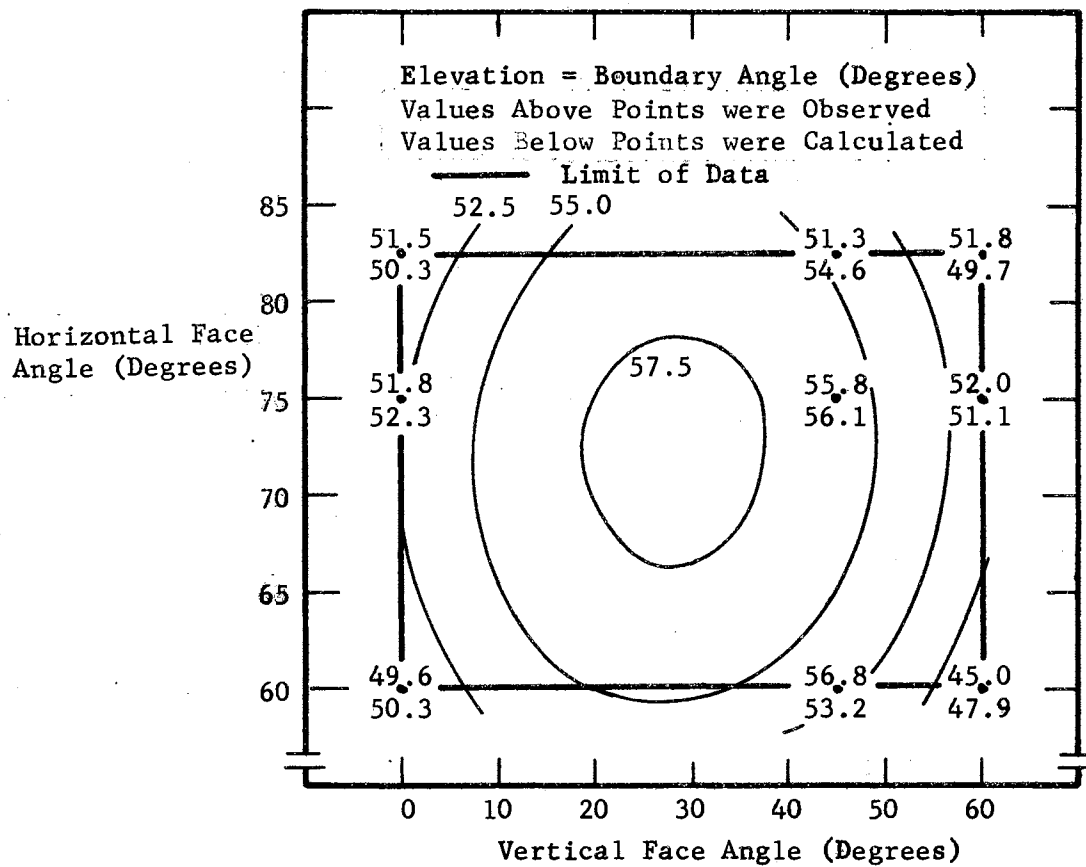
STATISTICAL MODEL

$$Z = 2.244 - 0.000007428 X + 0.00004395 X^2 - 0.02822 Y + 0.0001857 Y^2 - 0.00002278 XY$$

Standard Deviation (Absolute) = 0.0297

Standard Deviation (Percent of Mean) = 2.45

Figure 42. Effect of Opener Face Angle on the Depth of the Reduced Soil Density Zone



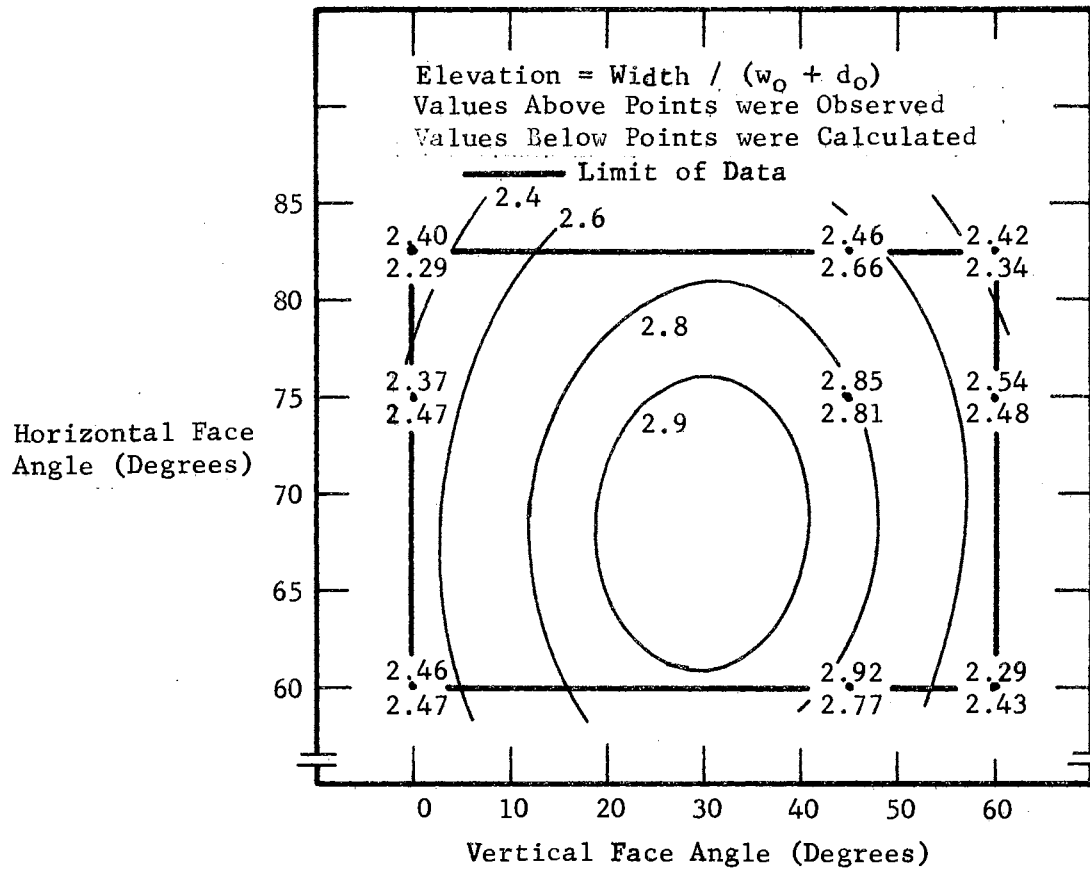
STATISTICAL MODEL

$$Z = - 38.55 + 0.3018 X - 0.006975 X^2 + 2.556 Y - 0.01793 Y^2 + 0.001295 XY$$

Standard Deviation (Absolute) = 3.637

Standard Deviation (Percent of Mean) = 7.03

Figure 43. Effect of Opener Face Angles on the Boundary Slope of the Reduced Soil Density Zone



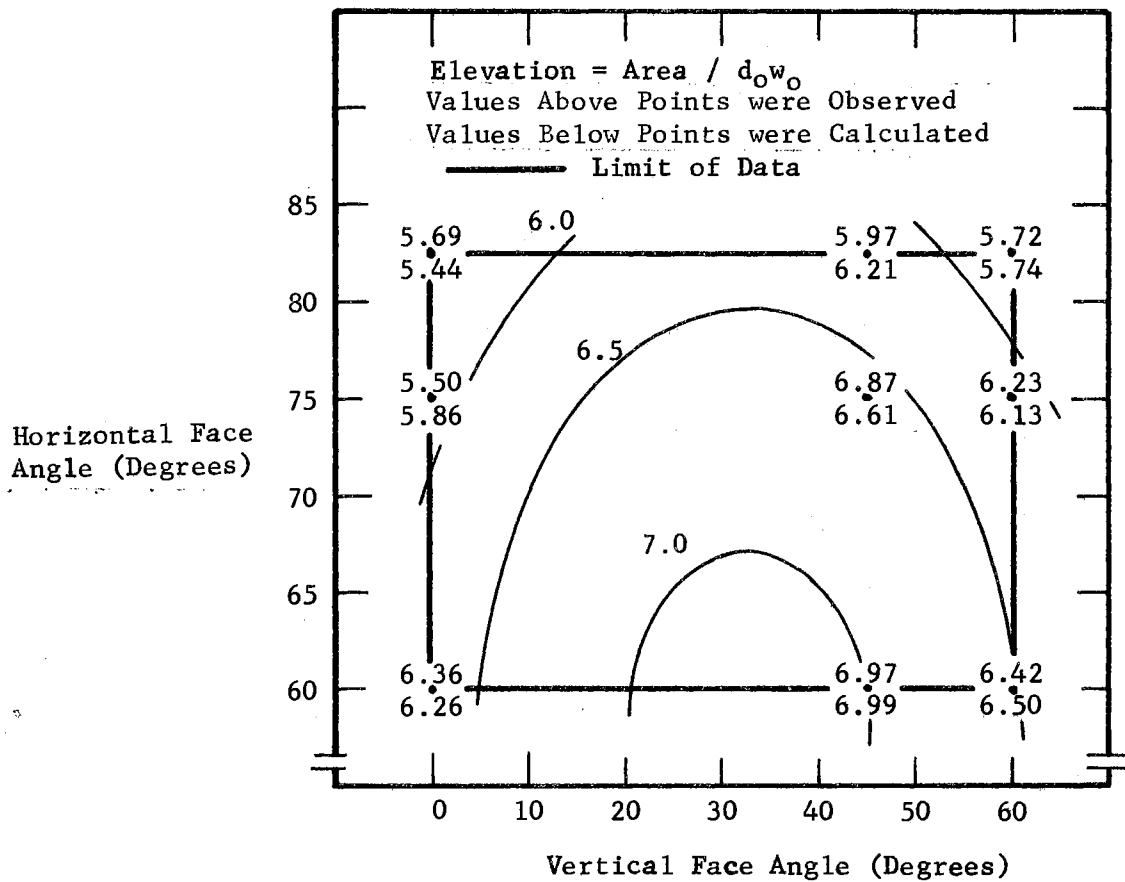
STATISTICAL MODEL

$$Z = - 2.123 + 0.02486 X - 0.0004864 X^2 + 0.1379 Y - 0.001022 Y^2 + 0.00006151 XY$$

Standard Deviation (Absolute) = 0.1964

Standard Deviation (Percent of Mean) = 7.78

Figure 44. Effect of Opener Face Angles on the Width of the Zone of Reduced Soil Density



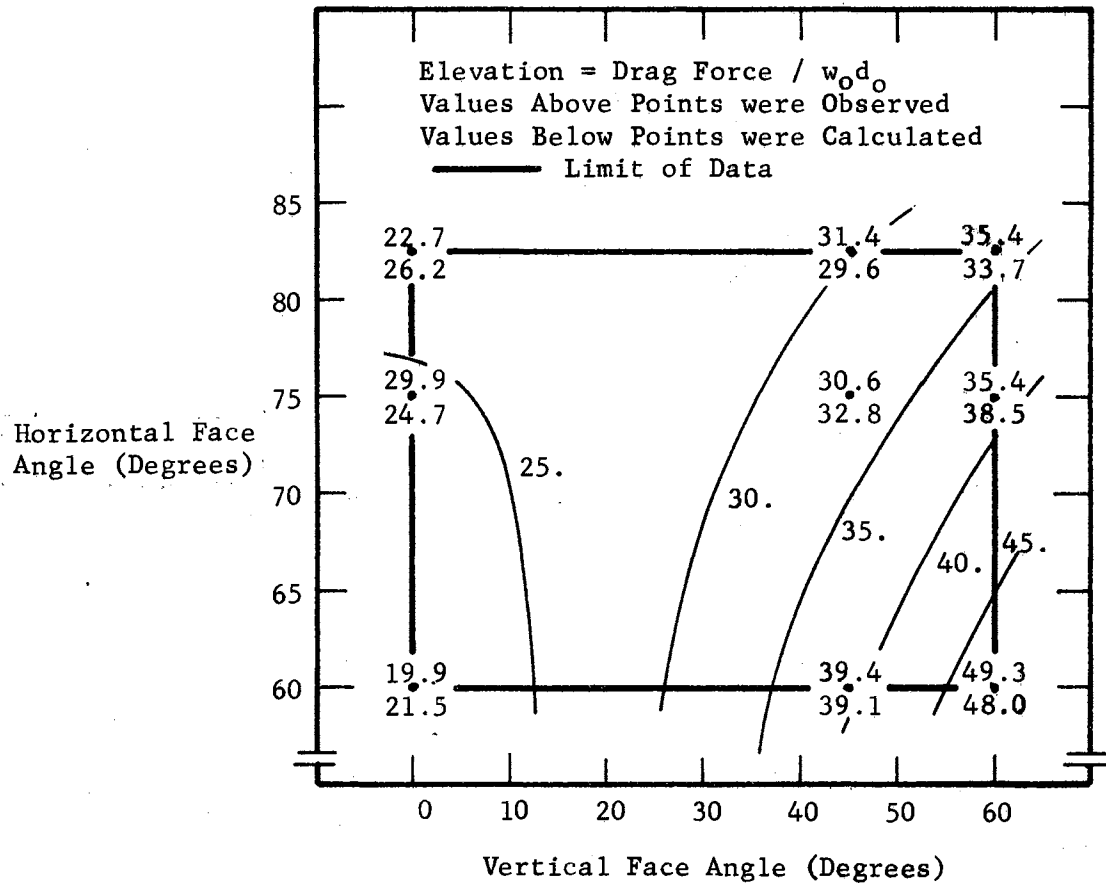
STATISTICAL MODEL

$$Z = 2.179 + 0.05059 X - 0.0008144 X^2 + 0.1439 Y - 0.001264 Y^2 + 0.00003827 XY$$

Standard Deviation (Absolute) = 0.3348

Standard Deviation (Percent of Mean) = 5.41

Figure 45. Effect of Opener Face Angles on Cross Sectional Area of the Reduced Soil Density Zone



STATISTICAL MODEL

$$Z = 6.660 + 1.086 X + 0.003367 X^2 + 0.2732 Y - 0.0004346 Y^2 - 0.01410 XY$$

Standard Deviation (Absolute) = 4.656

Standard Deviation (Percent of Mean) = 14.25

Figure 46. Effect of Opener Face Angle on Drag Force

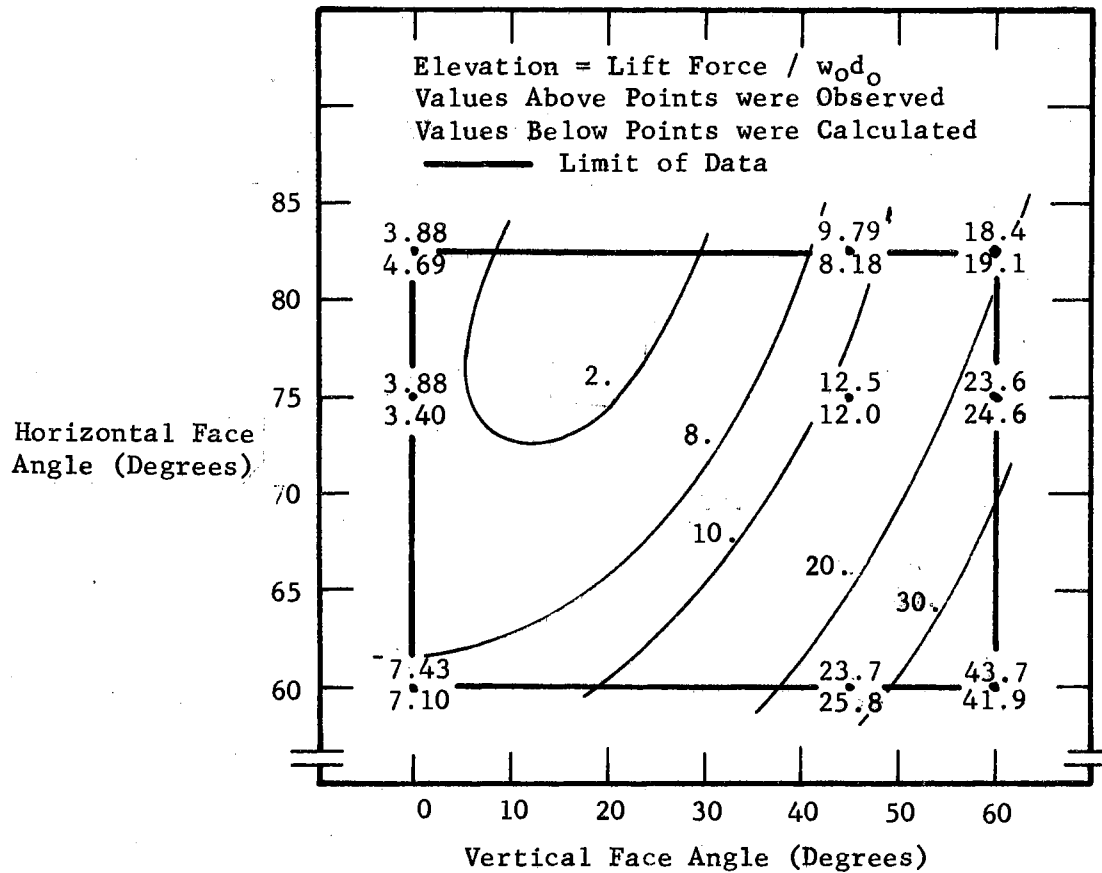
Unit lift force appears as Figure 47. A minimum was predicted for openers with small vertical angles and large horizontal angles. A definite maximum occurred at horizontal and vertical angles of 60 degrees.

The above prediction models should be useful in computing the expected operating forces and furrow characteristics that will result from a specific opener shape. The models are subject to certain limitations. They are based on only two replications which is a relatively small sample. The horizontal and vertical angles chosen for the study were not uniformly spaced within data range. Some large gaps resulted and the models should be used with caution in these areas. The models should be useful in choosing a reduced range of treatments for future research. Models apply for a speed of five miles per hour only.

Effect of Furrow Compaction Wedges

Three furrow bottom compaction wedges were made for use with the zero degree vertical and 82.5 degree horizontal angled furrow opener. These wedges were made with plane surfaces to displace soil downward. Displacements of one-eighth, three-sixteenths, and one-fourth inch were used. These wedges were run on three different kinds of soil samples. These patterns were plotted at a scale of 2:1. Density readings were made on one-fourth inch spacings. On natural soil samples and on artificial soil samples the density pattern was read twice on each cross section box. This resulted in considerable refinement of the density readings.

The effect of compaction wedges on "artificial fine" soil samples may be seen in Figures 48, 49, and 50. These samples were prepared to the same average density as those utilized in determining the effect of



STATISTICAL MODEL

$$Z = 105.4 + 0.8293 X + 0.01088 X^2 - 2.753 Y + 0.01857 Y^2 - 0.01505 XY$$

Standard Deviation (Absolute) = 2.116

Standard Deviation (Percent of Mean) = 12.98

Figure 47. Effect of Opener Face Angle on Lift Force

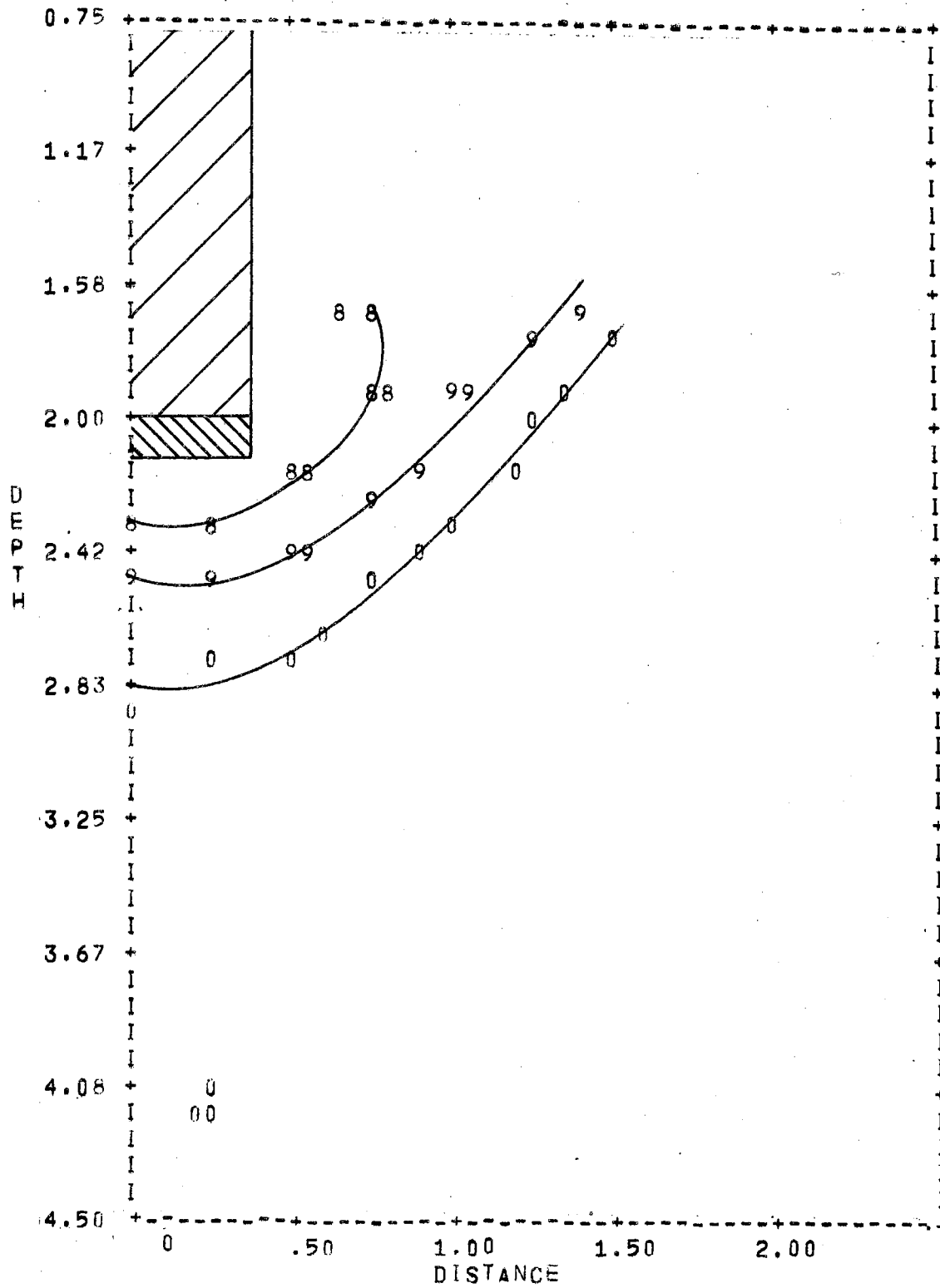


FIGURE 48. DENSITY PATTERN FOR COMPACTION WEDGE OF 1/8 INCH IN ARTIFICIAL SOIL

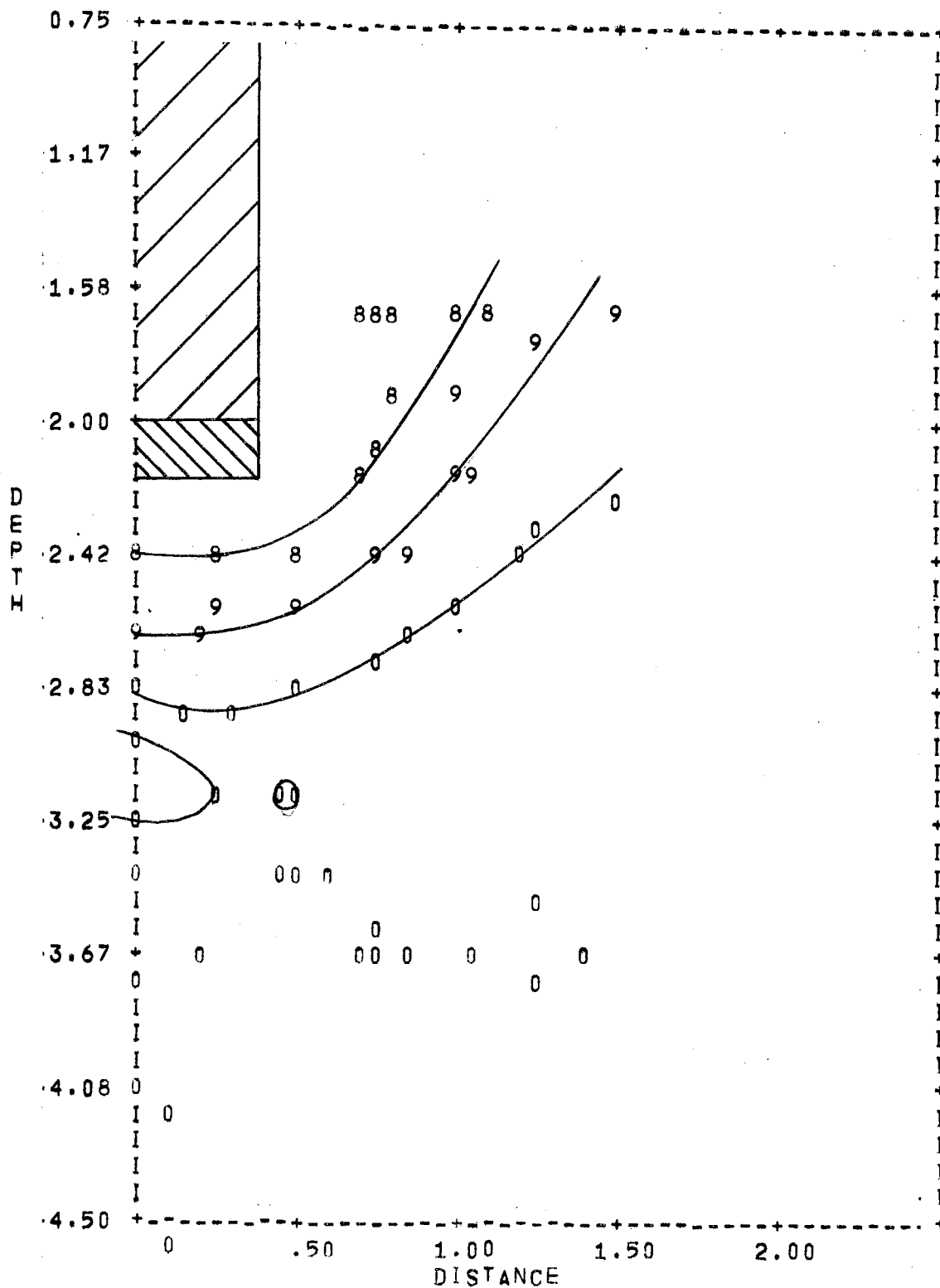


FIGURE 49. DENSITY PATTERN FOR COMPACTION WEDGE OF 3/16 INCH IN ARTIFICIAL SOIL

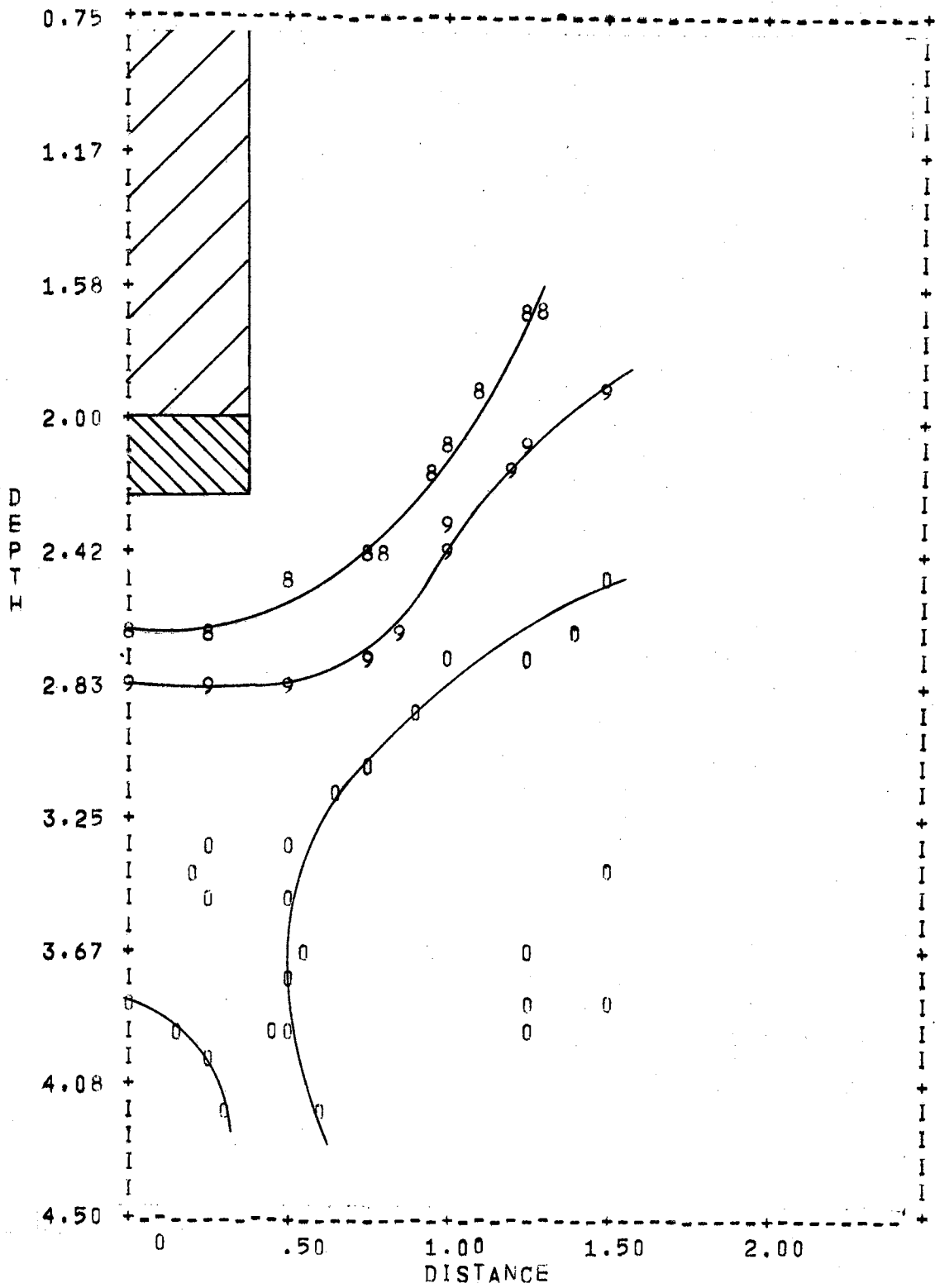


FIGURE 50. DENSITY PATTERN FOR COMPACTION WEDGE OF 1/4 INCH IN ARTIFICIAL SOIL

opener face angle. The soil density patterns were similar to those in the face angle test. The 0.9 gm/cc contour intersected the opener center line well below the compaction wedge. As an analysis of these samples, a curve of the same form used in the face angle test was fitted to the 0.9 gm/cc contour. The results are shown in Table IV. The column representing zero inches displacement was taken from the previous test, so the results are not directly comparable since density was measured on a different pattern in the face angle test. Depth of the reduced density zone is seen to increase with wedge displacement more than the actual downward displacement of the wedge. At one-eighth inch wedge displacement the decreased density zone was 0.40 inches below the wedge bottom, and for the one-fourth inch compaction wedge it was 0.55 inches below the wedge. Slope of the boundary also increased with increased wedge displacement. Width of the zone increased with increased displacement, discounting the zero displacement sample. Since all of the above factors increased, area of disturbed soil also increased with greater downward displacements. Drag force showed only a slight response to increased wedge displacement. Lift force increased four fold between zero and one-fourth inch wedge displacement. There was no evidence that soil was in fact compacted using plane faced wedges in the bottom of the seed furrow. Density patterns would indicate that the soil was disturbed below the compaction wedge, perhaps by granular flow.

The maximum pressure that could be exerted in a furrow bottom without causing plastic flow of the "artificial fine" soil was computed using Equation 3.32. These values are shown in the last column of Table V. The maximum pressure was computed for the lowest point of each compaction wedge. Opener lift forces appear in the second column.

TABLE IV
EFFECT OF WEDGE DISPLACEMENT
ON FURROW CHARACTERISTICS

Factor	Wedge Displacement (inches)			
	0*	1/8	3/16	1/4
Depth (Inches)	2.33	2.52	2.62	2.80
Slope (Y/X)	0.895	0.940	.975	1.034
Width (Inches)	6.61	6.22	6.34	6.64
Area (Inches ²)	8.54	8.89	9.56	11.08
Drag	34.0	35.3	34.1	46.1
Lift	5.82	13.1	22.0	23.9

* Taken from the Face Angle Test.

TABLE V
 COMPARISON OF OBSERVED AND CALCULATED
 MAXIMUM PRESSURES UNDER FURROW
 COMPACTION WEDGES

Soil	Wedge Displacement (inches)	Observed* Lift Force (pounds)	Pressure for Uniform Distribution (psi)	Maximum Pressure for Triangular Distribution (psi)	Calculated Pressure for Plastic Flow (psi)
Artificial Fine	1/8	7.3	4.87	9.74	10.83
	3/16	16.2	10.80	21.60	11.96
	1/4	18.1	12.07	24.14	11.99

* Observed lift force minus the lift force on the opener without a compaction wedge attached.

These have been corrected by subtracting the lift force that was exerted on the opener when there was no compaction wedge attached. The next column shows the vertical pressures that would be exerted by the wedges if the lift forces were uniformly distributed over the vertically projected wedge areas. For the three-sixteenth and one-fourth inch wedges, excellent agreement was obtained between calculated maximum values and the observed values. In the fourth column of Table V the lift forces have been assumed to result in triangular pressure distributions under the wedges. The maximum pressure would be assumed to occur at the point of maximum displacement. The one-eighth inch wedge gave the only maximum pressure that agreed with the calculated maximums.

Since the three-sixteenth and one-fourth inch wedges had nearly equal observed lift forces and the pressures calculated from these forces agreed with calculated maximum pressures, we can conclude that plastic flow occurred. Such flow would cause all disturbed material to undergo a decrease in density due to the dilatant nature of the artificial soil. Plastic flow would also be consistent with the increase in boundary side slope. Opener face angles had already caused disturbance of the material beside the opener. Plastic flow from underneath the wedge would probably not cause extensive side slope failures but it would disturb soil near the bottom of the furrow producing a deep disturbed zone with steep side slopes.

The effect of compaction wedges on natural soil samples appear as Figures 51, 52, and 53. Densities were plotted on the wet basis. The same difficulties that were experienced in the face angle test were found in this test. No consistent density contour intersected the opener center lines near the bottom of the compaction wedge.

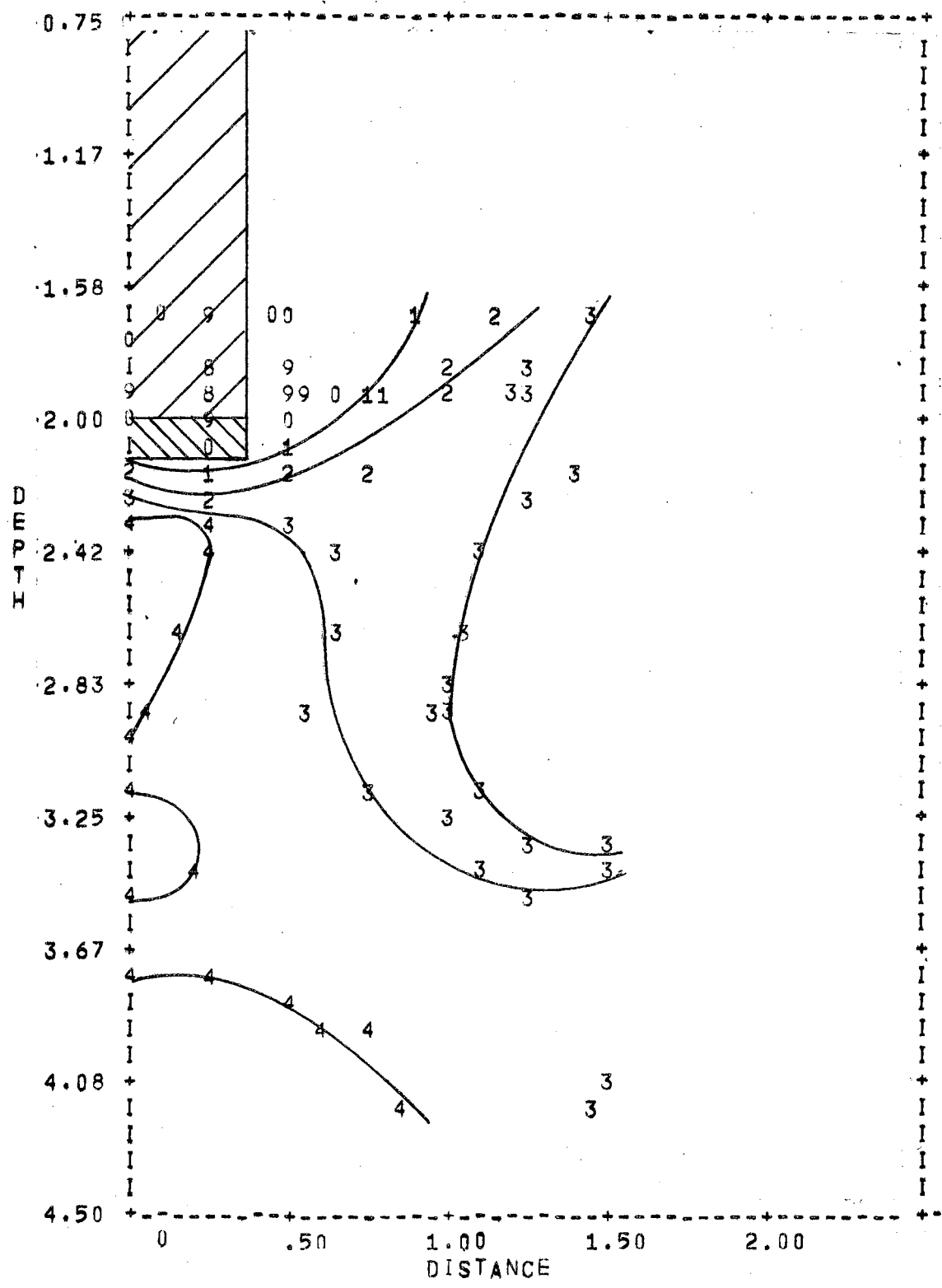


FIGURE 51. DENSITY PATTERN FOR COMPACTION WEDGE OF 1/8 INCH IN NATURAL SOIL

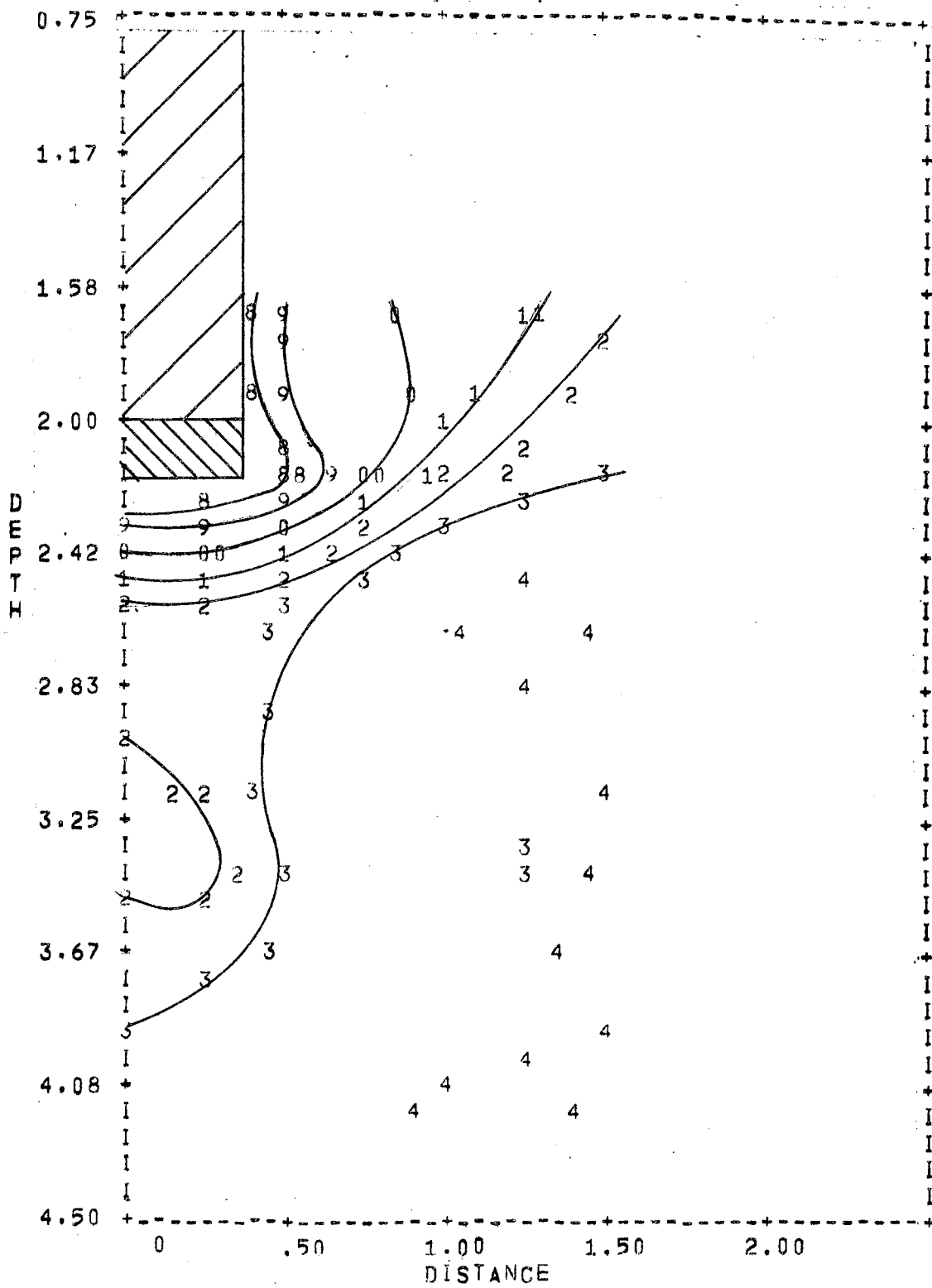


FIGURE 52. DENSITY PATTERN FOR COMPACTION WEDGE OF 3/16 INCH IN NATURAL SOIL

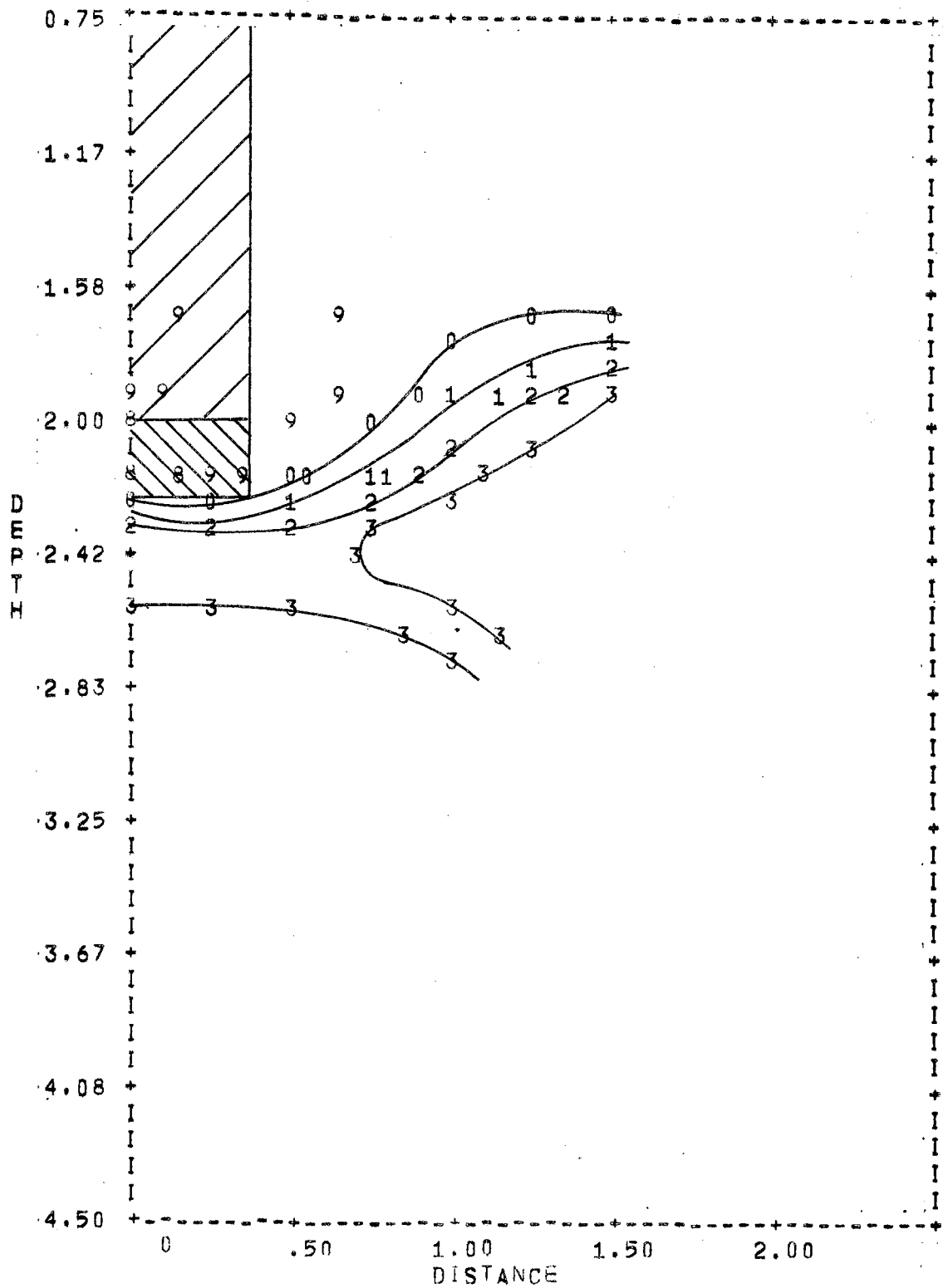


FIGURE 53. DENSITY PATTERN FOR COMPACTION WEDGE OF 1/4 INCH IN NATURAL SOIL.

Higher densities were found at the bottom of the one-eighth and one-fourth inch wedges than at the bottom of the three-sixteenth inch wedge.

To overcome the shrinkage problem of natural soil samples, a set of runs were made using remolded natural soil. It was difficult to moisten the soil to the desired moisture content without producing aggregates. Large aggregates were broken by screening through hardware cloth but considerable aggregation remained. The moisture content of the one-eighth and one-fourth inch displacement samples was about twenty percent. The three-sixteenth displacement sample had about sixteen percent moisture. All samples were initially compacted with the baseplate and drop hammer to an average density of 1.28 gm/cc. The wet density plots of these samples were plotted as Figures 54, 55, and 56.

In no case were densities found to be significantly higher than the sample average. In all samples a bulb of soil greater than 1.3 gm/cc appeared under the compaction wedge, but there was no logical pattern. The 1.1 gm/cc contour passed immediately beneath the compaction wedge for all samples. The 1.2 gm/cc contour stays close to the 1.1 contour except for the one-fourth inch compaction wedge in which case it is well below it. This was interpreted to indicate some plastic flow of the material under the one-fourth inch wedge.

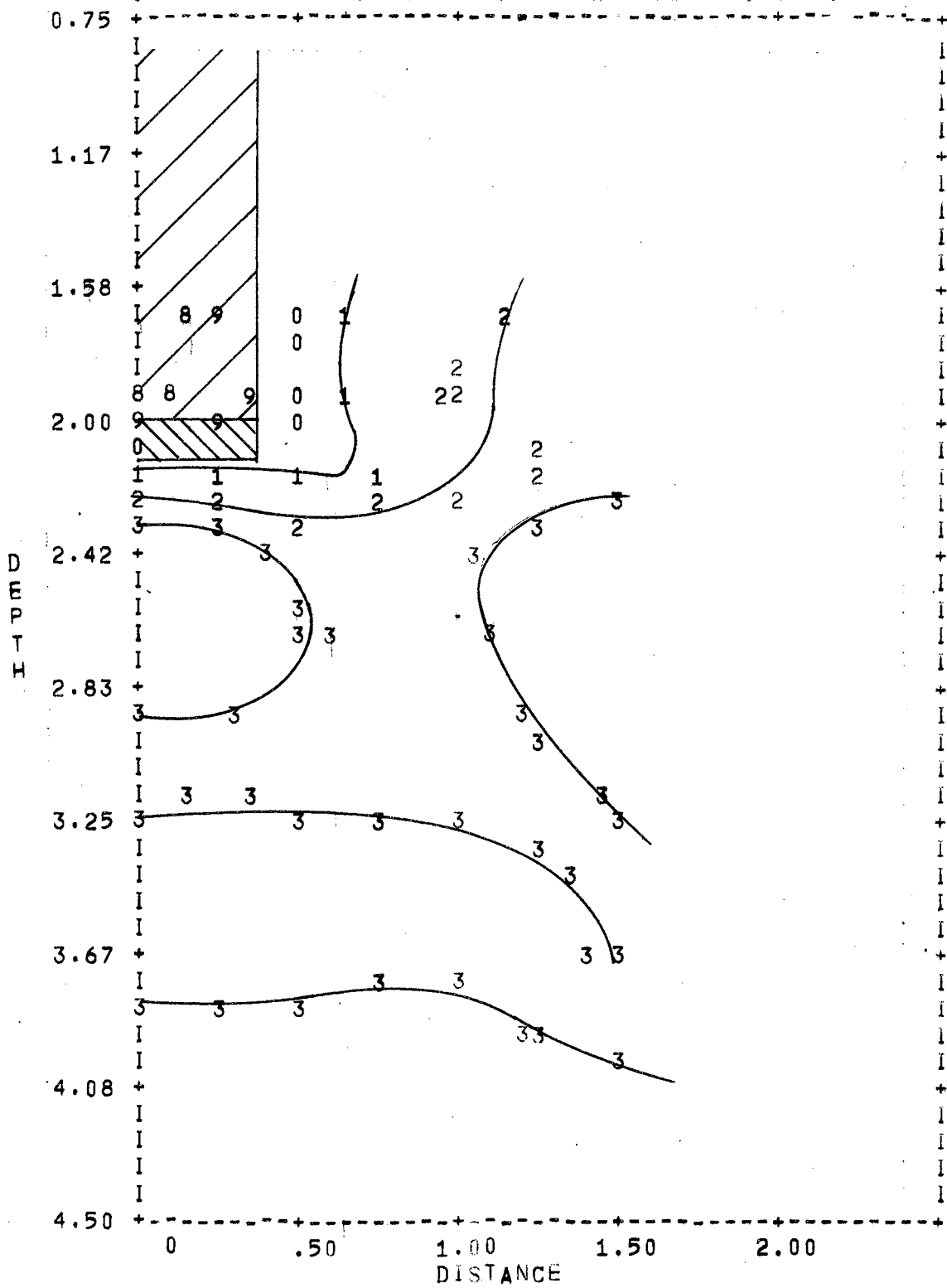


FIGURE 54. DENSITY PATTERN FOR COMPACTION WEDGE OF 1/8 INCH IN REMOLDED NATURAL SOIL

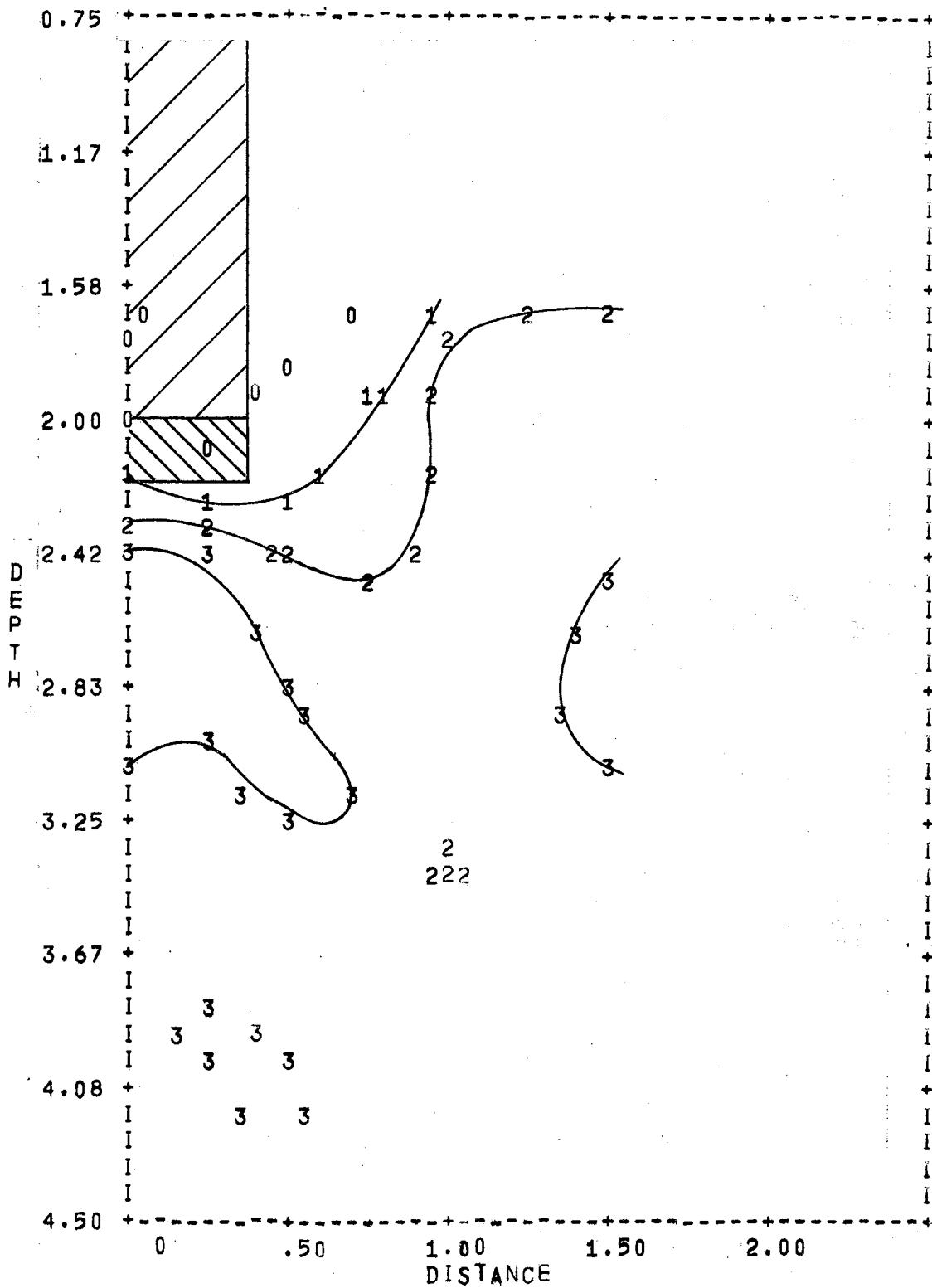


FIGURE 55. DENSITY PATTERN FOR COMPACTION WEDGE OF 3/16 INCH IN REMOLDED NATURAL SOIL

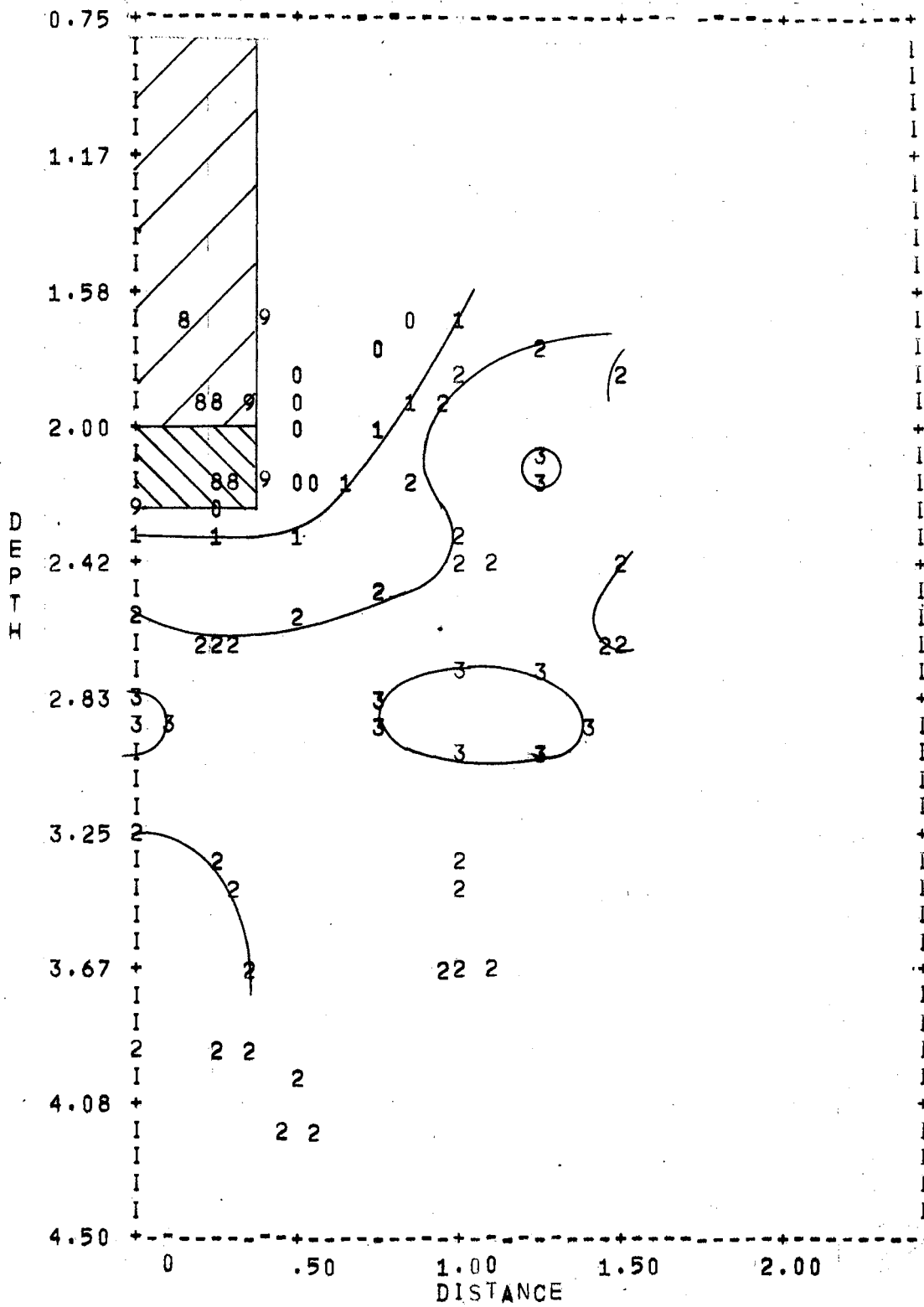


FIGURE 56. DENSITY PATTERN FOR COMPACTION WEDGE OF 1/4 INCH IN REMOLDED NATURAL SOIL

CHAPTER VI

SUMMARY AND CONCLUSIONS

The original purpose of this research was to determine the effect of planter furrow opener shape on seed bed soil density. In retrospect, this was a rather ambitious goal since a recognized method of measuring density in seed bed cross sections was not available. Considerable time was spent in the beginning of the project trying various methods of density measurement. An apparatus was designed to use gamma ray decay rate for this purpose. The method proved quite satisfactory and has been described in detail in Chapter IV. Essentially, it consisted of a gamma ray beam passing through a sample soil cross section to a counting device. The amount of decrease in count rate due to the presence of soil was found to be proportional to the soil density for equal sample lengths.

The gamma radiation technique was used to measure the effect of opener shape on seed bed soil density using an artificial soil. On the granular artificial material, no opener shape tested produced measurable soil compaction. Considerable disruption of the soil in the immediate vicinity of the opener could be observed during the test runs and on the slow motion films of the runs. This disruption caused a large area of soil beside the opener to have lower density than the initial density of the sample. The zone of reduced soil density was found to have a shape similar to that expected behind a retaining wall,

but the depth and the angle of the side slopes were both functions of opener face angle. Drag and lift forces acting on the planter opener were also found to vary with horizontal and vertical face angles, but they were not well correlated with the area of disturbed soil.

Nine furrow openers with horizontal angles of 60 to 82.5 degrees and vertical angles from 0 to 60 degrees were tested in the face angle test. Statistical models were fitted to the test data to obtain a set of equations to predict furrow depth, side slope, width, and area for openers with face angles within the range of the data and of similar geometry. Lift and drag forces were also fitted to statistical models. A possible criteria for planter openers is that they disturb the least amount of soil. If the area of the reduced soil density zone is used as a basis of comparison, openers with large horizontal angles were superior to other openers tested in this experiment. For that set of openers, the fitted model shows those with vertical angles of zero and 60 degrees to be better than the one with a 45 degree vertical angle. Drag and lift forces were a minimum for openers with large horizontal face angles and zero degrees vertical face angle. Among the opener shapes tested, the zero degree vertical and 82.5 degree horizontal angled opener seems a logical best.

The action of the tested openers on soil may be comparable to chisels. Chisels are expected to loosen the largest possible amount of soil. The largest disturbed soil zones were made by openers with 45 degree vertical and 60 or 75 degree horizontal angles. They had medium values for lift and drag forces as compared to other openers in the test.

Density evaluations in natural soil showed the same type of density pattern that was observed with the artificial soil. The difficulty of obtaining homogeneous natural soil samples in the laboratory convinces one that meaningful research on natural soil can only be conducted in the field despite the other advantages of laboratory research. A large number of cross sectional samples could be collected to obtain the average density pattern although excessive density reading time would be a serious limitation. Another problem for field evaluation would be placement of the cross sectional sampling box so the exact location of the opener path could be determined. The extension of the methods used in this experiment to field evaluation of density patterns would comprise a whole new experiment.

Compacting soil in the furrow bottom using a plane surfaced sliding wedge does not appear to be easily accomplished. For the granular materials tested, "artificial fine" soil, density was not increased by a sliding wedge. In the artificial soil, larger wedge displacements caused reduced density to a deeper depth of soil than did the opener without a wedge. This was shown to be caused by plastic flow from beneath the wedge. It is possible that soils with high cohesion could be compacted using sliding wedges. Since planter openers operate near the surface, internal soil friction contributes little to the resistance of soil to plastic flow. The weight of soil above the point of pressure application is very small. Soils with high cohesion should be tested by the procedure used here for a granular material. The artificial soil used in this experiment could possibly be compacted by the combination of a planter opener, compaction wedge, and a flat surface shoe which would resist plastic expulsion of material beside the opener.

The conclusions of this research can be summarized as follows:

1. Cross sectional density patterns can be accurately evaluated using the gamma radiation technique.
2. Soils with little cohesion cannot be compacted by sliding wedge-type furrow openers without some method of confining the soil.
3. For soils with little cohesion, the passive pressure equation accurately predicted the maximum vertical pressure that could be applied to the furrow bottom.
4. The shape of the furrows made by angular-faced openers resembled the failure surface of a passive retaining wall failure, but the side slope was steeper.
5. Furrow side slope was least for openers with medium vertical and horizontal angles. The greatest furrow side slope was for the opener with smallest horizontal angle and the largest vertical angle.
6. Planter openers reduced soil density to a depth greater than the depth of the opener.
7. Furrow depth was greater for openers with large vertical and small horizontal face angles.
8. The area of decreased soil density tended to be least for openers with small vertical angles and large horizontal angles. The largest areas of decreased density occurred for openers with medium vertical angles and small horizontal angles.

9. The lift and drag forces acting on furrow openers increased with increasing vertical face angle and decreased with increasing horizontal face angle.

Suggestions for Future Work

The gamma radiation technique, as used in this experiment, was a highly successful method of measuring seed bed soil density patterns. The procedure would be recommended for use in future research of this nature. The density measuring apparatus was calibrated at the beginning of the research using known density soil samples. For future use of the technique, a set of at least three permanent calibration samples that cover the range of expected soil densities should be constructed. Intermittent checking with these permanent standards would insure that instrument responses, at various times during the research period, will be comparable.

Failure of furrow openers and compaction wedges to compact unconfined soil suggests that a set of test runs should be made on granular soil using some confining devices. The most convenient device would be flat, sliding gauge shoes on the soil surface. For compaction of the furrow bottom, a wider compaction wedge might have increased the compactive effect. The distance that soil had to flow would be increased and friction along the bottom of the opener would resist lateral movement. Compaction devices, such as wheels with various surface shapes, should be included in future research. Perhaps a vertically vibrating wedge would be more effective in compacting soil in the furrow.

Additional research is needed on the effect of planter openers and compaction devices on soils with high cohesion. Such soils are

difficult to handle and a suitable artificial material does not seem to be available. Finer granulation of the mixture used in this experiment might result in slightly higher cohesion but not as high as water-moistened clay soils.

From the data collected in this experiment, it was not possible to define the mechanics of soil failure and flow around planter openers. Several approaches to the problem are available. Soil pressure distributions could be measured with recording equipment and correlated with opener position. If pressure distributions were accurately known, perhaps the failure pattern could be predicted. Another approach to the problem is quantitative observation of particle movements. Surface particles could be photographed with high speed movies. A framing rate of at least 500 frames per second appears to be required. Particles whose original position were on the center line of the opener could be observed in their movement over the opener surface by using a transparent one-half opener running against one side of a transparent soil box.

Several projects have been recommended for future research. One of the important contributions of the experiment herein reported was to narrow the range of treatments needed for future study. All openers with 60 degree horizontal angles and those with 60 degree vertical angles should be eliminated. These openers had large lift and drag forces so they would be expected to wear rapidly in the field. They did not make more desirable furrows than other openers. Openers with vertical angles forward of the plane, normal to travel, should be tested. Curved surfaces for both horizontal and vertical faces offer an endless variety of shapes for testing.

LIST OF REFERENCES

- Abernathy, G. H. "Machine Components for Planting Cotton." New Mexico Agricultural Experiment Station, Bulletin No. 477, November, 1963.
- Anderson, P. "Calculation of Bearing Capacities of Footings by Circular Arcs." Engineering News Vol. 136 (May, 1946) 866-8.
- Anonymous. "Planting in the Mechanization of Cotton Production." Southern Cooperative Series, Bulletin No. 49, February, 1957.
- Bailey, A. C. and J. A. Weber. "Comparison of Methods of Measuring Shear Strength Using Artificial Soils." American Society of Agricultural Engineers, Paper No. 64-113 Presented at Ft. Collins, Colorado, June, 1964.
- Bailey, K. P. "Influence of Soil Strength on Growth of Roots." Soil Science Vol. 96 (September, 1963) 175-80.
- Beacher, B. F. and E. Strickling. "Effect of Puddling on Water Stability and Bulk Density of Aggregates of Certain Maryland Soils." Soil Science Vol. 80 (November, 1955) 363-73.
- Bekker, M. G. "Mechanical Properties of Soil and Problems of Compaction." Transactions of American Society of Agricultural Engineers, Vol. 24, No. 2 (1961) 231-234.
- Bouyoucos, G. "Simple and Rapid Method for Measuring the Stickiness of Soils." Soil Science Vol. 34 (November, 1932) 393-401.
- Bowen, H. D. "Some Physical Impedance and Aeration Effects on Planted Seeds." American Society of Agricultural Engineers Paper Number 60-626, presented at Memphis, Tennessee, December, 1960.
- Buehrer, T. F. and M. S. Rose. "Studies in Soil Structure; Bound Water in Normal and Puddled Soils." Arizona Agricultural Experiment Station Technical Bulletin No. 100, 1943.
- Carnes, A. "Soil Crusts." Agricultural Engineering Vol. 15 No. 5 (May, 1934) 167-9.
- Cohron, G. T. "Model Testing of Earthmoving Equipment." American Society of Agricultural Engineers, Paper Number 61-113, presented at Ames, Iowa, June, 1961.

- Davisson, C. M. and R. D. Evans. "Gamma Absorption Coefficients." Review of Modern Physics Vol. 24 (April, 1952) 79-107.
- Day, P. R. and G. G. Holmgren. "Microscopic Changes in Soil Structure During Compression." Soil Science Society of America, Proceedings Vol. 16 (January, 1952) 73-7.
- Garner, T. H. and H. D. Bowen. "Plant and Soil Mechanics in Seedling Emergence." American Society of Agricultural Engineers, Paper No. 63-148, presented at Miami Beach, Florida, June, 1963.
- Gill, W. R. and R. D. Miller. "Method for Study of the Influence of Mechanical Impedance and Aeration on the Growth of Seedling Roots." Soil Science Society of America, Proceedings. Vol. 20
- Glasstone, S. and A. Sesonski. Nuclear Reactor Engineering. D. Van Nostrand, Princeton, New Jersey, 1963.
- Hendrick, J. G. and G. E. Vandenberg. "Strength and Energy Relations of a Dynamically Loaded Clay Soil." Transactions of The American Society of Agricultural Engineers, Vol. 4, No. 1 (1961) 31-2.
- Holekamp, E. R., E. B. Hudspeth, R. F. Colwick, and L. L. Ray. "Planting Equipment and Practices for Cotton on the High Plains." Texas Agricultural Experiment Station Bulletin No. 992, 1962.
- Jamison, V. C. and H. A. Weaver. "Soil Hardness Measurements in Relation to Soil Moisture Content and Porosity." Soil Science Society of America, Proceedings Vol. 16 (1952) 13-15.
- Johnson, W. H. and J. E. Henry. "Influence of Simulated Row Compaction on Emergence and Soil Drying Rates." American Society of Agricultural Engineers Paper No. 62-147, Miami Beach, Florida, June, 1962.
- Jumikis, A. R. Mechanics of Soils. D. Van Nostrand Co., Princeton, New Jersey, 1964.
- Kondner, R. L. "Hyperbolic Stress-Strain Response." American Society of Civil Engineers, Proceedings Vol. 89 (February, 1963) 115-43.
- Korayem, A. Y. and C. A. Reaves. "Artificial Soils - Frictional Properties and Chisel Tests." American Society of Agricultural Engineers, Paper No. 61-652, presented at Chicago, Illinois, December, 1961.
- Matthes, R. K. and H. D. Bowen. "Transfer of Water Vapor by Thermal Gradients." American Society of Agricultural Engineers, Paper No. 62-141, presented at Washington, D. C., June, 1962.

- Mink, A. E., W. H. Carter, and M. M. Mayeux. "Effects of an Air Slide on Soil Engaging Tools." American Society of Agricultural Engineers, Paper No. 64-105, presented at Fort Collins, Colorado, June, 1964.
- Morton, C. T. and W. F. Buchele. "Basic Factors Affecting the Emergence Energy of Seedlings." American Society of Agricultural Engineers, Paper No. 59-104, presented at Ithaca, New York, June, 1959.
- Nichols, M. L. "The Dynamic Properties of Soil, I, II." Agricultural Engineering Vol. 12 (1931) 259-164, 321-4.
- Nichols, M. L. "The Dynamic Properties of Soil, III." Agricultural Engineering Vol. 13 (1932) 201-4.
- Nichols, M. L. and L. D. Baver. "Interpretation of the Physical Properties of Soil Affecting Tillage Implement Design by Means of the Atterburg Consistence Constants." International Congress of Soil Science, Proceedings Vol. 6 (1932) 175-88.
- Nichols, M. L. and C. A. Reaves. "Soil Reaction to Subsoiling Equipment." Agricultural Engineering Vol. 39 (June, 1958) 340-3.
- Payne, P. C. J. "The Relationship Between the Mechanical Properties of Soil and the Performance of Simple Cultivation Implements." Journal of Agricultural Engineering Research Vol. 1 (1956) 23-50.
- Payne, P. C. J. and D. W. Tanner. "The Relationship Between Rake Angle and the Performance of Simple Cultivation Implements." Journal of Agricultural Engineering Research, Vol. 4 (1959) 312-25.
- Phillips, R. E. and D. Kirkham. "Mechanical Impedance and Corn Seedling Root Growth." Soil Science Society of America, Proceedings Vol. 26 (1962) 319-22.
- Reaves, C. A. and M. L. Nichols. "Surface Soil Reaction to Pressure." Agricultural Engineering Vol. 36 (December, 1955) 813-16.
- Rowe, R. J. and K. K. Barnes. "Influence of Speed on Elements of Draft of a Tillage Tool." Transactions of the American Society of Agricultural Engineers Vol. 4 (1961) 55-57.
- Selig, E. T. and R. D. Rowe. "A Study of Artificial Soils." Armour Research Foundation of Illinois Institute of Technology, November, 1960.
- Siemans, J. C., J. A. Weber, and T. H. Thornburn. "Mechanics of Soil Under the Influence of Model Tillage Tools." American Society of Agricultural Engineers, Paper No. 64-104 presented at Fort Collins, Colorado, June, 1964.




- Smith, R. E. and E. H. Dickson. "Absorption Characteristics of Soils for Cobalt 60 Gamma Rays." American Society of Agricultural Engineers, Transactions, Vol. 6, No. 3 (1963) 209-12.
- Soehne, W. "Fundamentals of Pressure Distribution and Soil Compaction Under Tractor Tires." Agricultural Engineering Vol. 39 (May, 1958) 276-81.
- Sowers, G. B. and G. F. Sowers. Introductory Soil Mechanics and Foundations. The Macmillan Company, New York, N. Y., 1958.
- Stout, B. A. "Effect of Soil Compaction on Moisture Absorption by Sugar Beet Seeds." Michigan Agricultural Experiment Station Quarterly Bulletin Vol. 42 (February, 1960) 548-5.
- Tanner, D. W. "Further Work on the Relationship Between Rake Angle and the Performance of Simple Cultivation Implements." Journal of Agricultural Engineering Research Vol. 5 (1960) 307-15.
- Taylor, H. M. and H. R. Gardner. "Penetration of Cotton Seedling Taproots as Influenced by Bulk Density, Moisture Content and Strength of Soil." Soil Science Vol. 96 (September, 1963) 153-6.
- Taylor, H. M. and H. R. Gardner. "Relative Penetrating Ability of Different Plant Roots." Agronomy Journal Vol. 52 (October, 1960) 579-81.
- Terzaghi, K. and R. B. Peck. Soil Mechanics in Engineering Practice. John Wiley and Sons, New York, N. Y., 1948.
- Triplett, G. B., Jr. and M. B. Tesar. "Effects of Compaction, Depth of Planting and Soil Moisture Tension on Seedling Emergence of Alfalfa." Agronomy Journal Vol. 52 (December, 1960) 681-4.
- Veihmeyer, F. J. and A. H. Hendrickson. "Soil Density and Root Penetration." Soil Science Vol. 65 (June, 1948) 487-93.
- Vomocil, J. A. "In Situ Measurement of Soil Bulk Density." Agricultural Engineering Vol. 35 (1954) 651-654.
- Wheeting, I. C. "Static Friction Measurements in the Study of Soil Moisture Relationships." Soil Science Vol. 41 (January, 1936) 1-11.

APPENDIX A

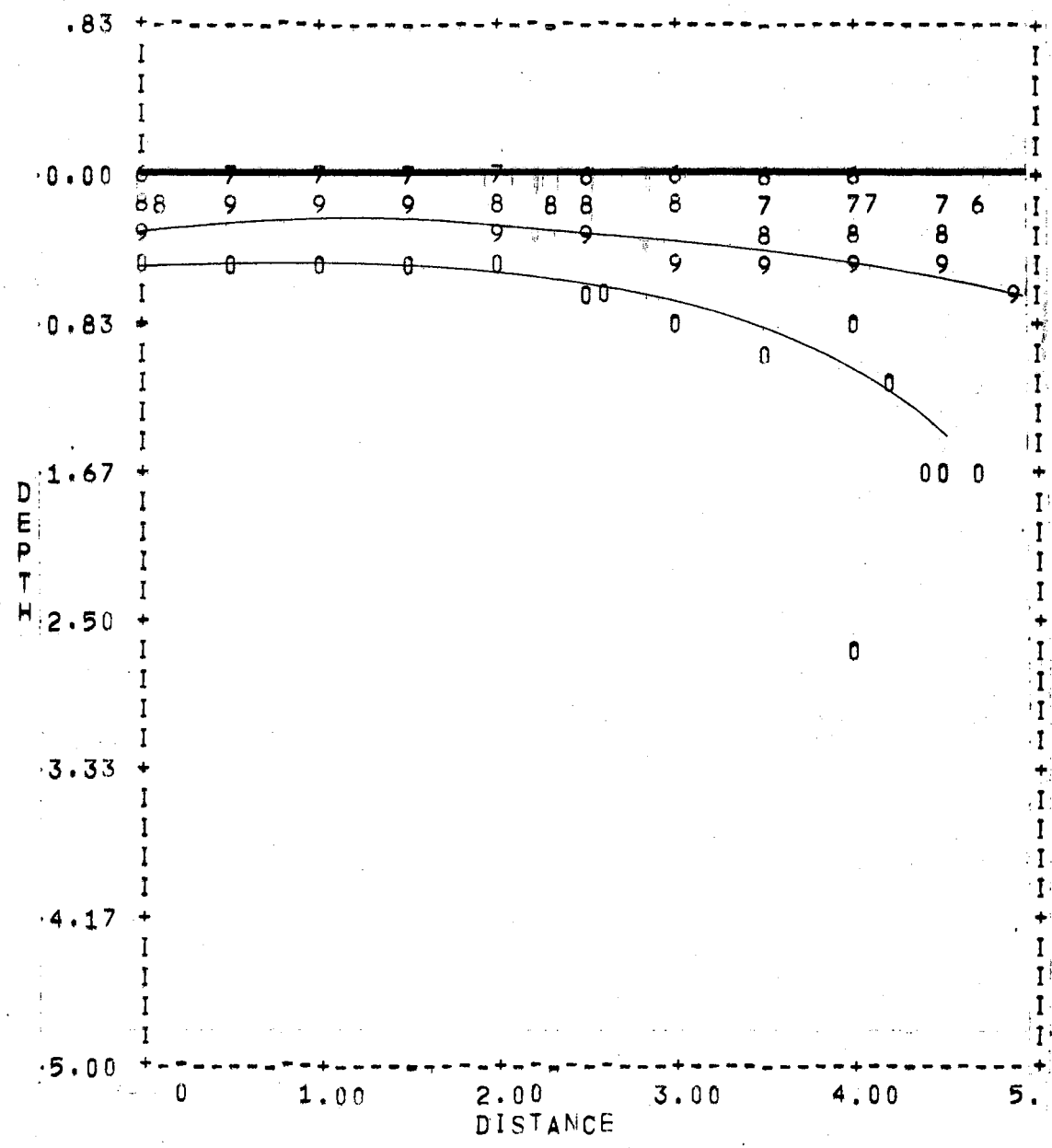
Appendix A includes all density distribution plots for the various runs made during this research. The left edge of each plot represents the center line of the opener and the point of zero depth was the original soil surface. Depth and width were measured in inches and were plotted at a scale of 1:1 except compaction wedge samples which were plotted at a scale of 2:1. Points on the contour lines were keyed to the soil density according to the following list where the first number is the observed density in grams per cubic centimeter and the second number is the plotted symbol.

0.6 = 6	1.1 = 1
0.7 = 7	1.2 = 2
0.8 = 8	1.3 = 3
0.9 = 9	1.4 = 4
1.0 = 0	1.5 = 5

The cross hatched area is the region that was swept out by the planter opener. Other lines on the plots are:

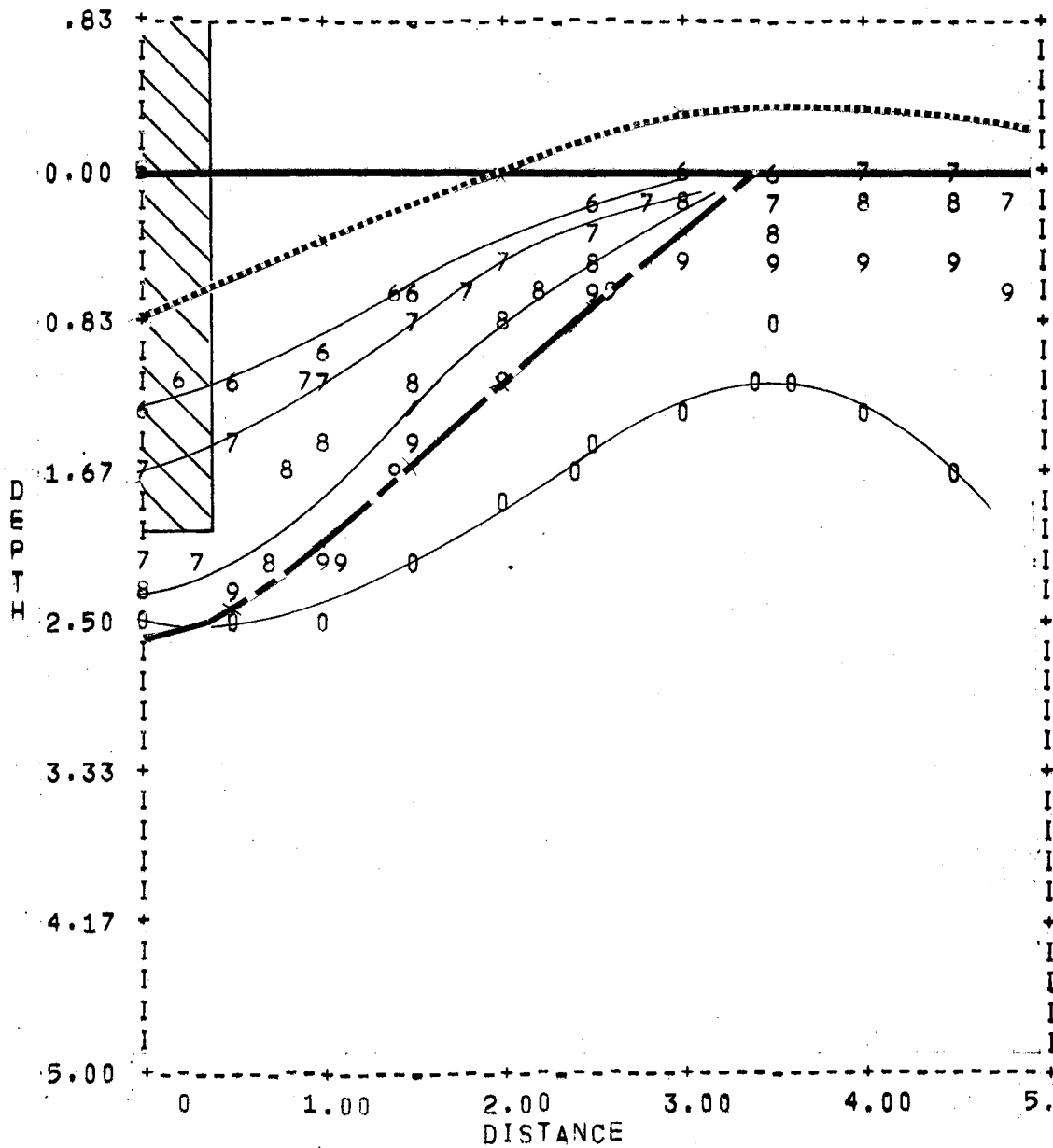
	Original ground surface
	Final ground surface
	Boundary of the reduced density zone

APPENDIX A-I



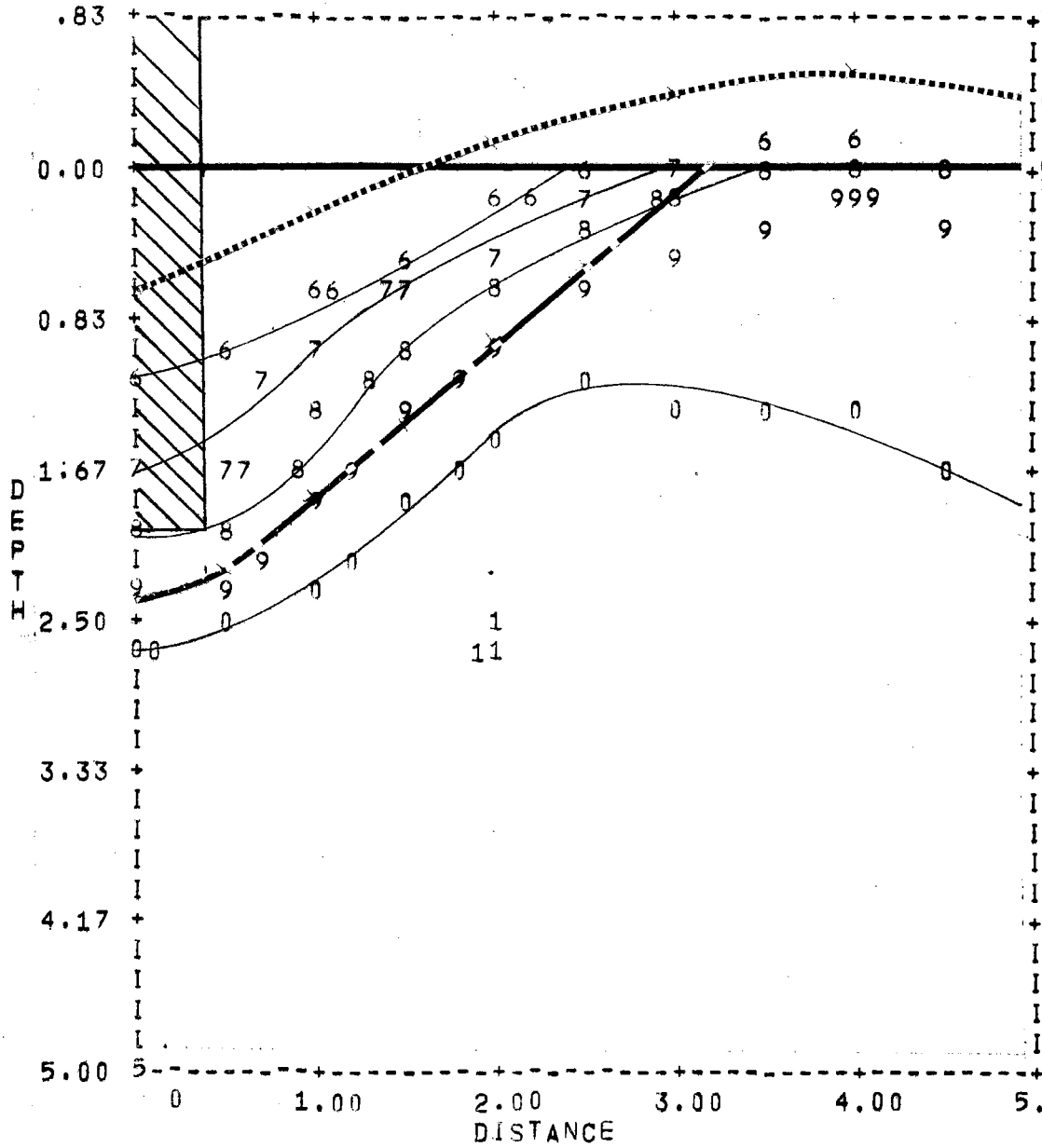
DENSITY PATTERN IN AN UNDISTURBED SAMPLE OF ARTIFICIAL FINE SOIL, TWO REPLICATIONS

APPENDIX A-II



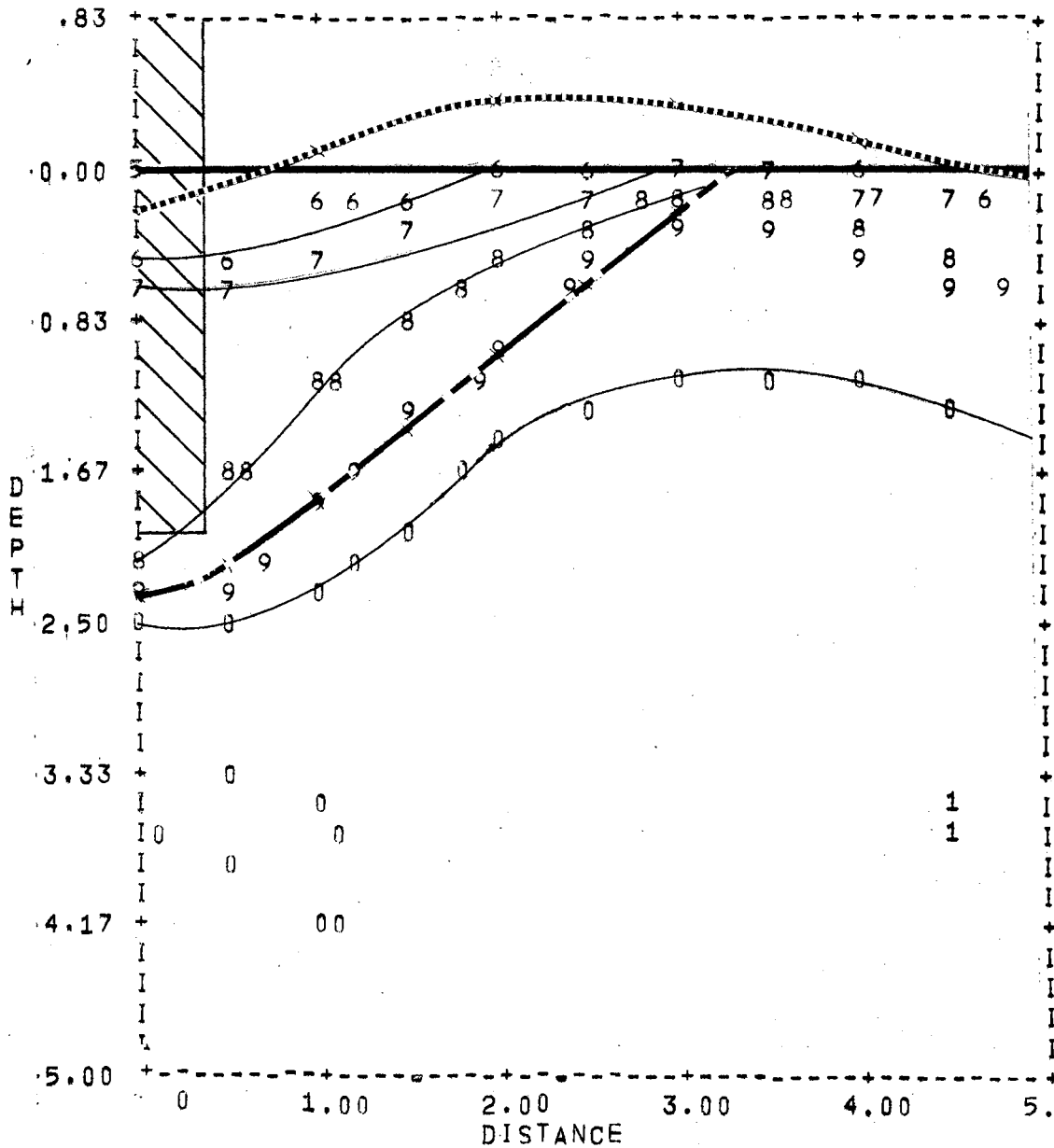
DENSITY PATTERN FOR OPENER 0-60 IN ARTIFICIAL FINE SOIL, TWO REPLICATIONS

APPENDIX A-III



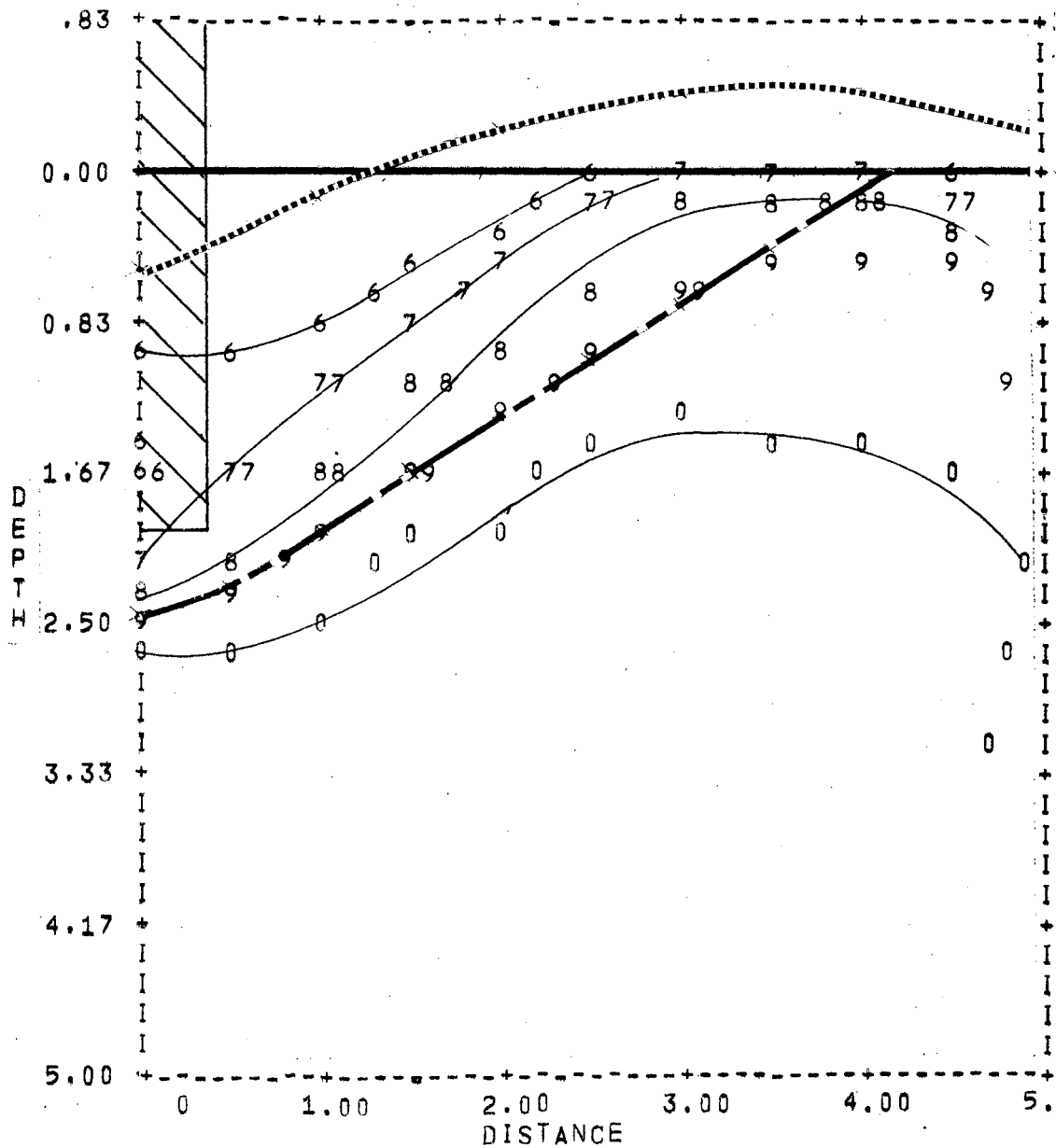
DENSITY PATTERN FOR OPENER 0-75 IN
ARTIFICIAL FINE SOIL, TWO REPLICATIONS

APPENDIX A-IV



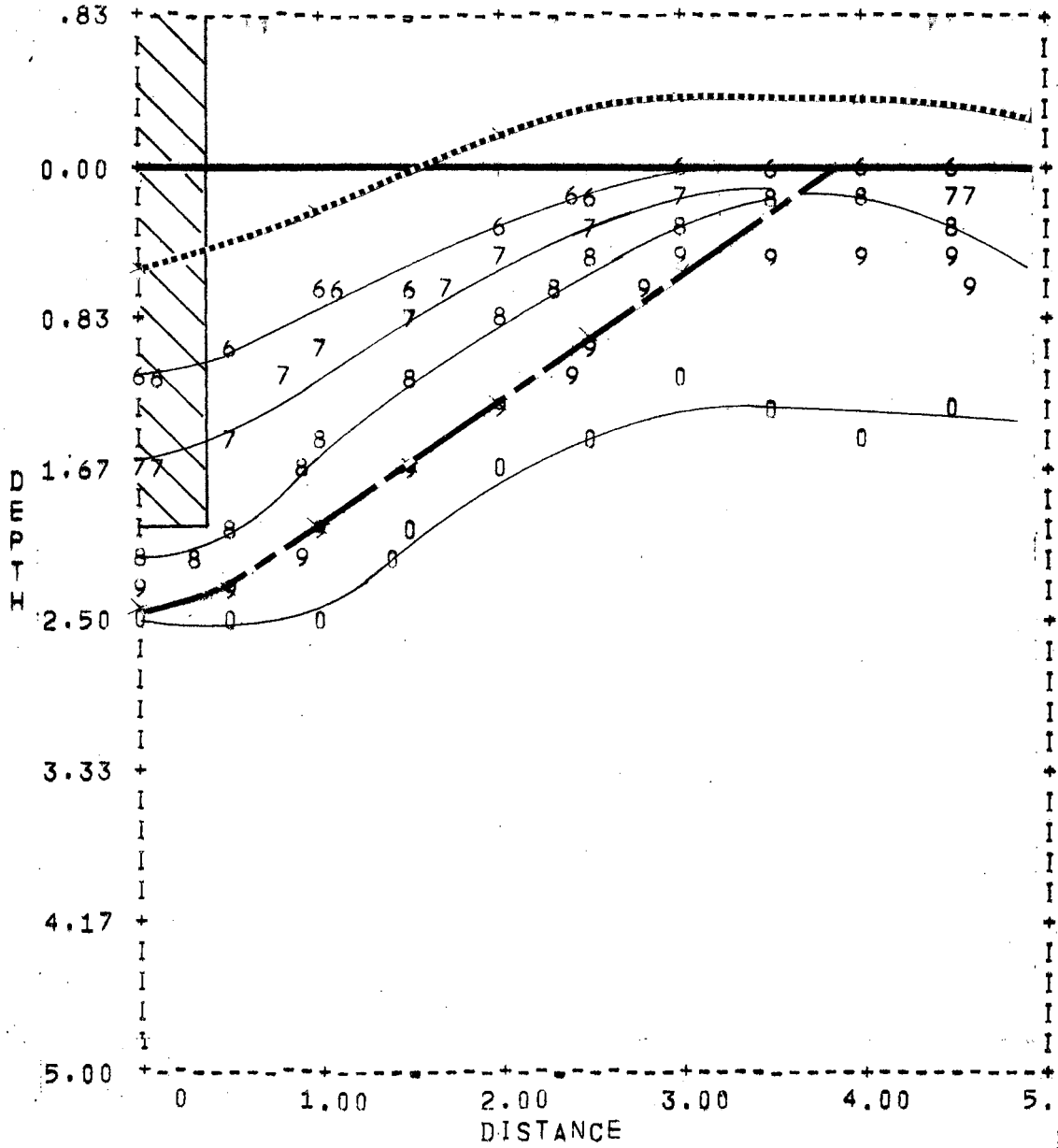
DENSITY PATTERN FOR OPENER 0-82 1/2 IN
ARTIFICIAL FINE SOIL, TWO REPLICATIONS

APPENDIX A-V



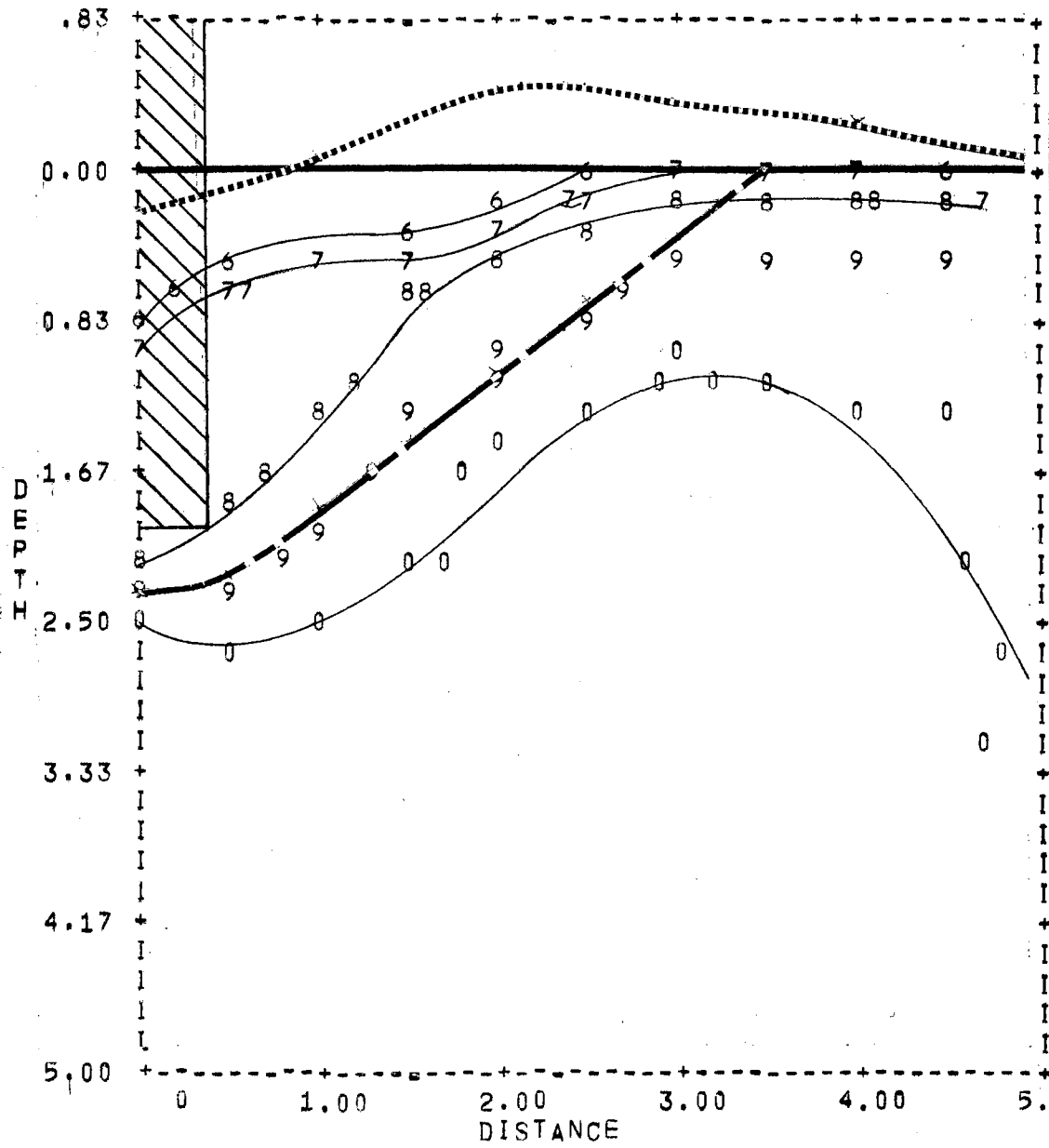
DENSITY PATTERN FOR OPENER 45-60 IN
ARTIFICIAL FINE SOIL, TWO REPLICATIONS

APPENDIX A-VI



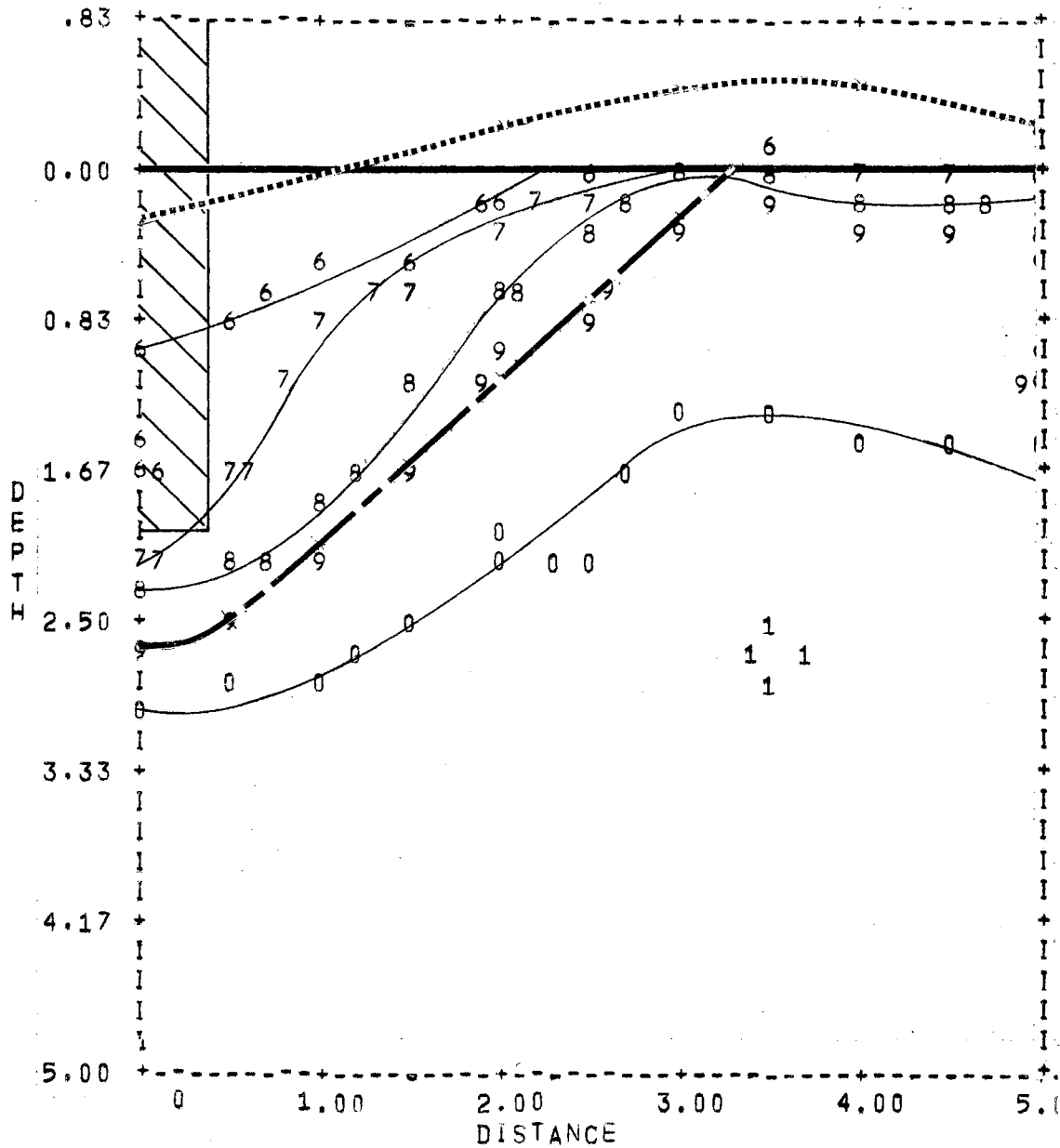
DENSITY PATTERN FOR OPENER 45-75 IN
ARTIFICIAL FINE SOIL, TWO REPLICATIONS

APPENDIX A-VII



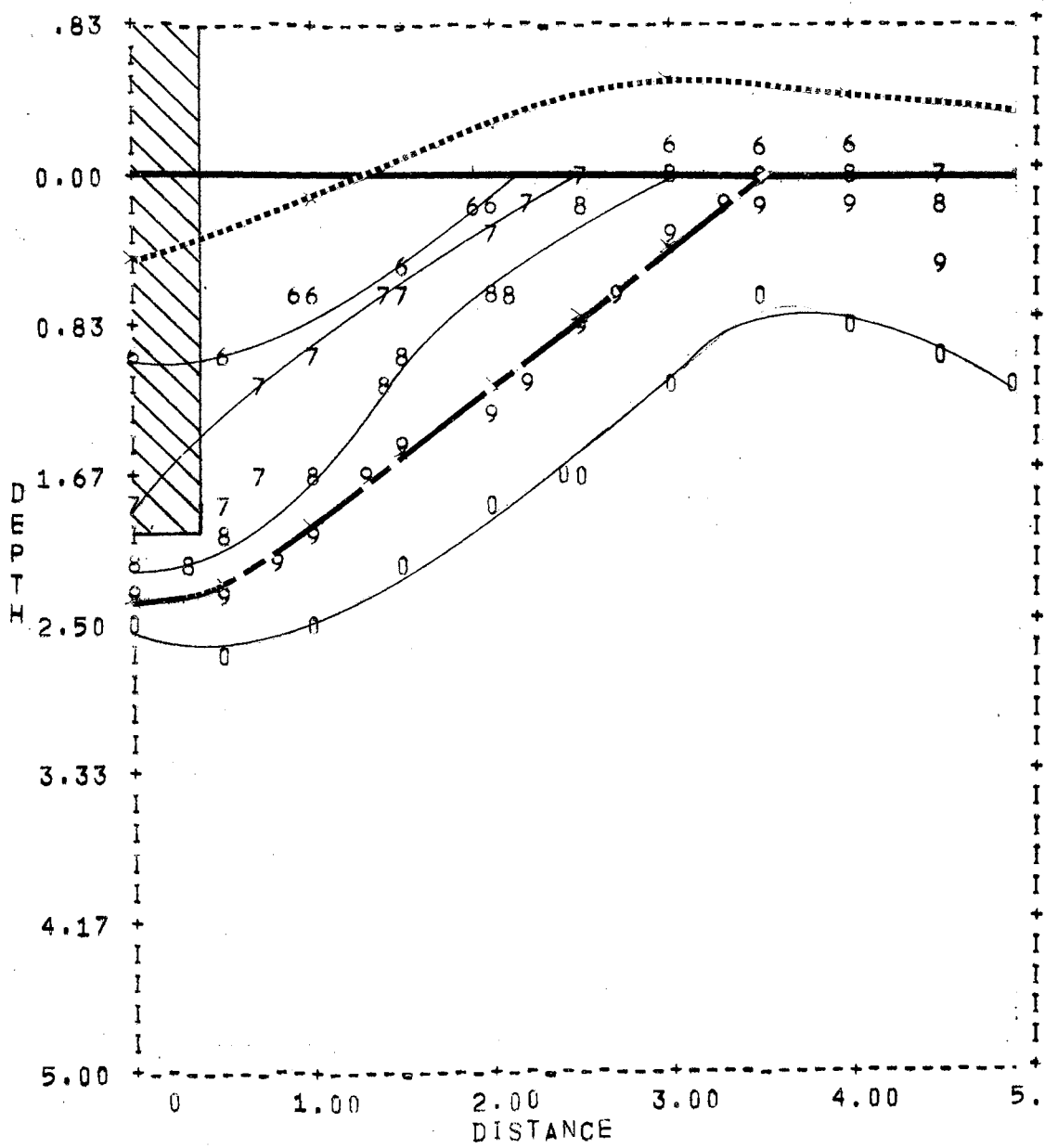
DENSITY PATTERN FOR OPENER 45-82 1/2 IN
ARTIFICIAL FINE SOIL, TWO REPLICATIONS

APPENDIX A-VIII



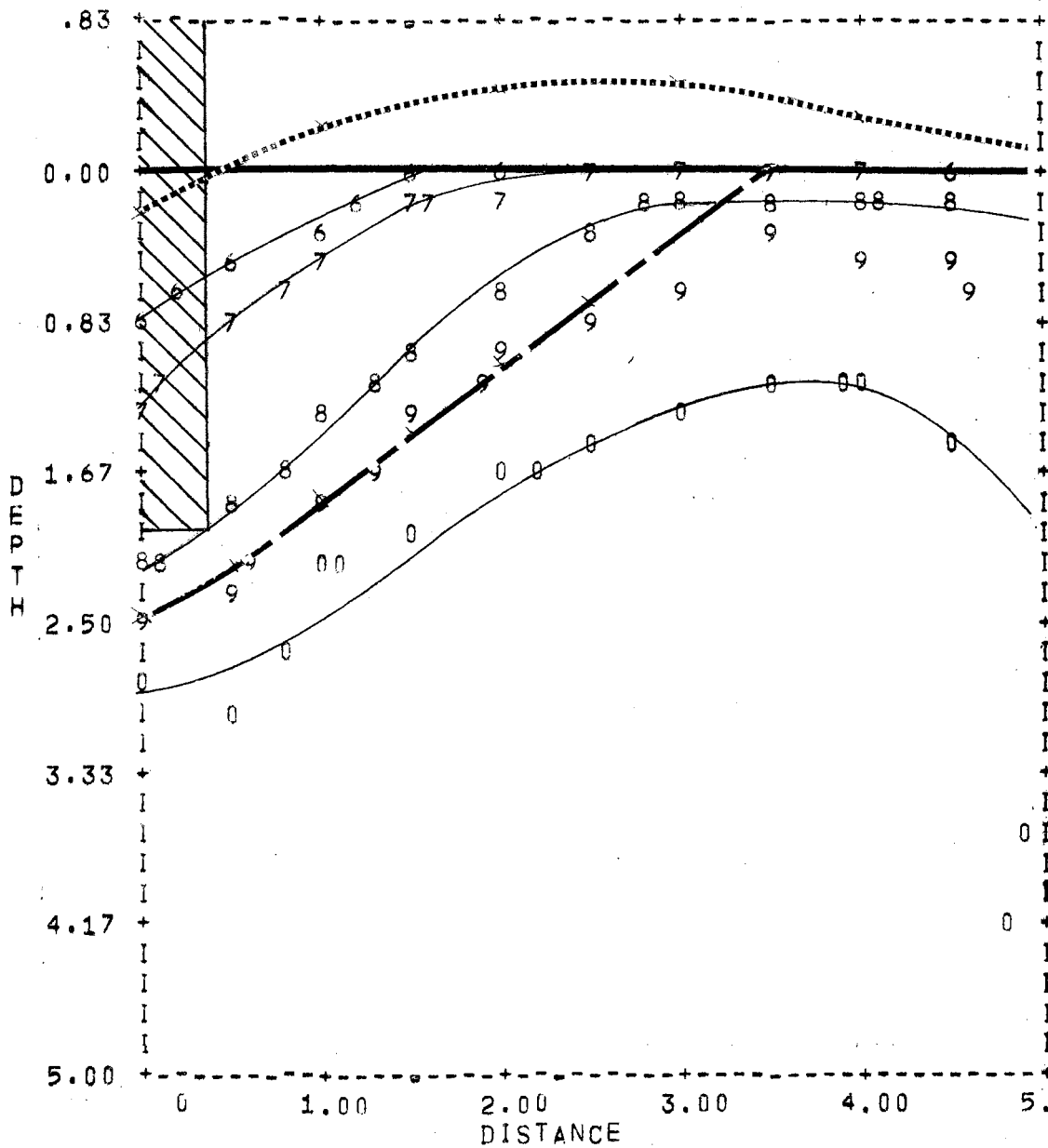
DENSITY PATTERN FOR OPENER 60-60 IN
ARTIFICIAL FINE SOIL, TWO REPLICATIONS

APPENDIX A-IX



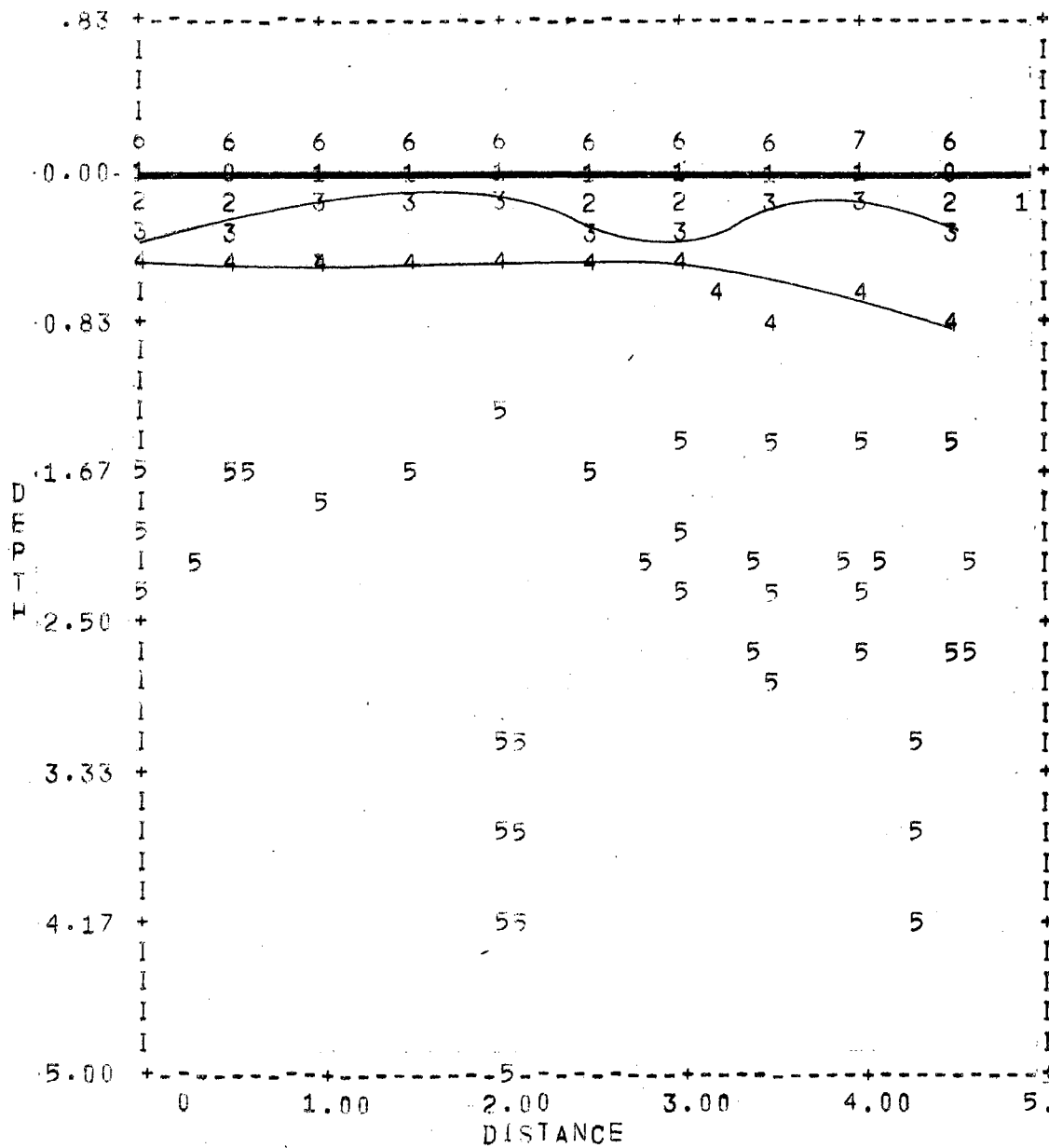
DENSITY PATTERN FOR OPENER 60-75 IN
ARTIFICIAL FINE SOIL, TWO REPLICATIONS

APPENDIX A-X



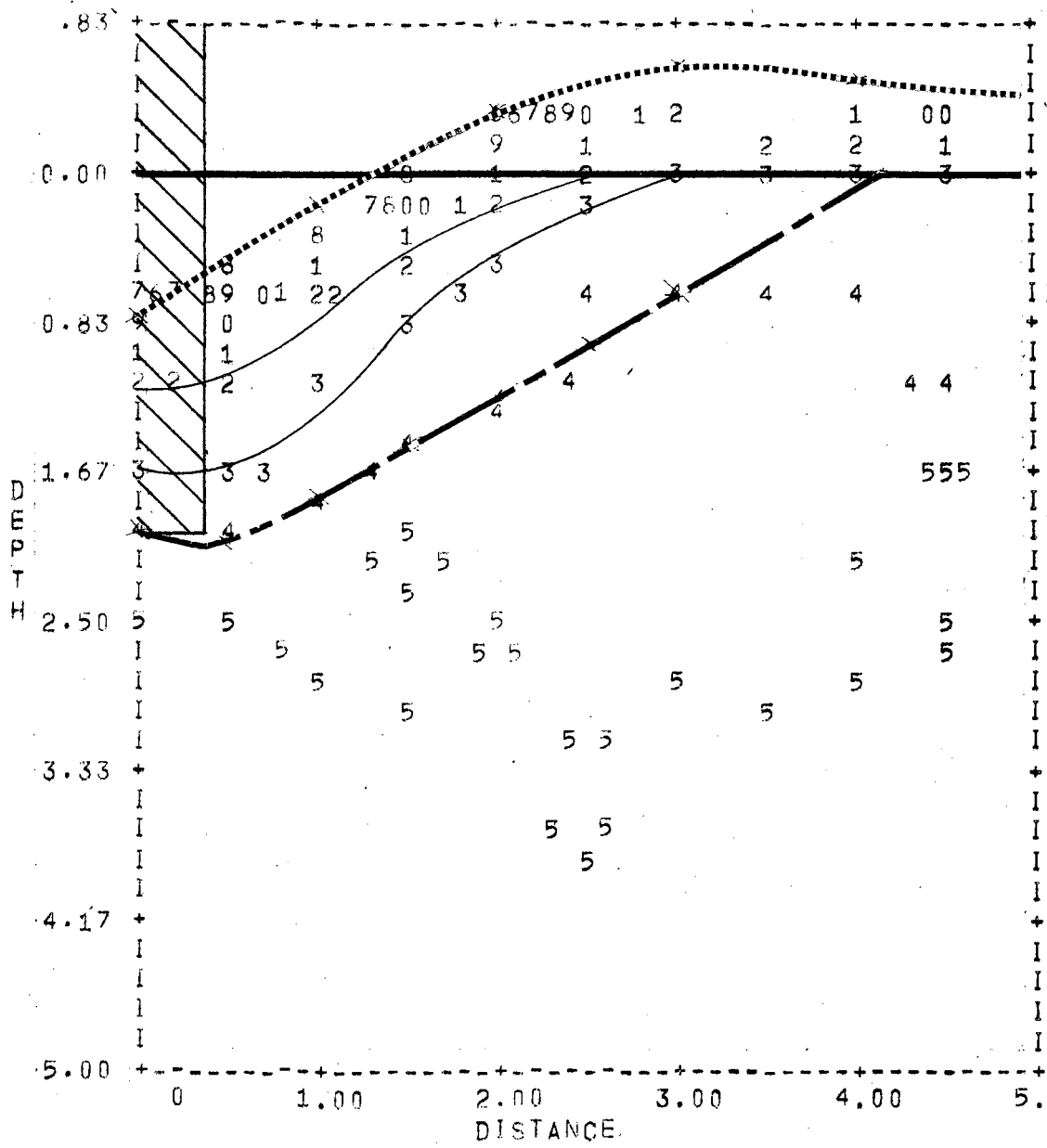
DENSITY PATTERN FOR OPENER 60-82 1/2 IN
ARTIFICIAL FINE SOIL, TWO REPLICATIONS

APPENDIX A-XI



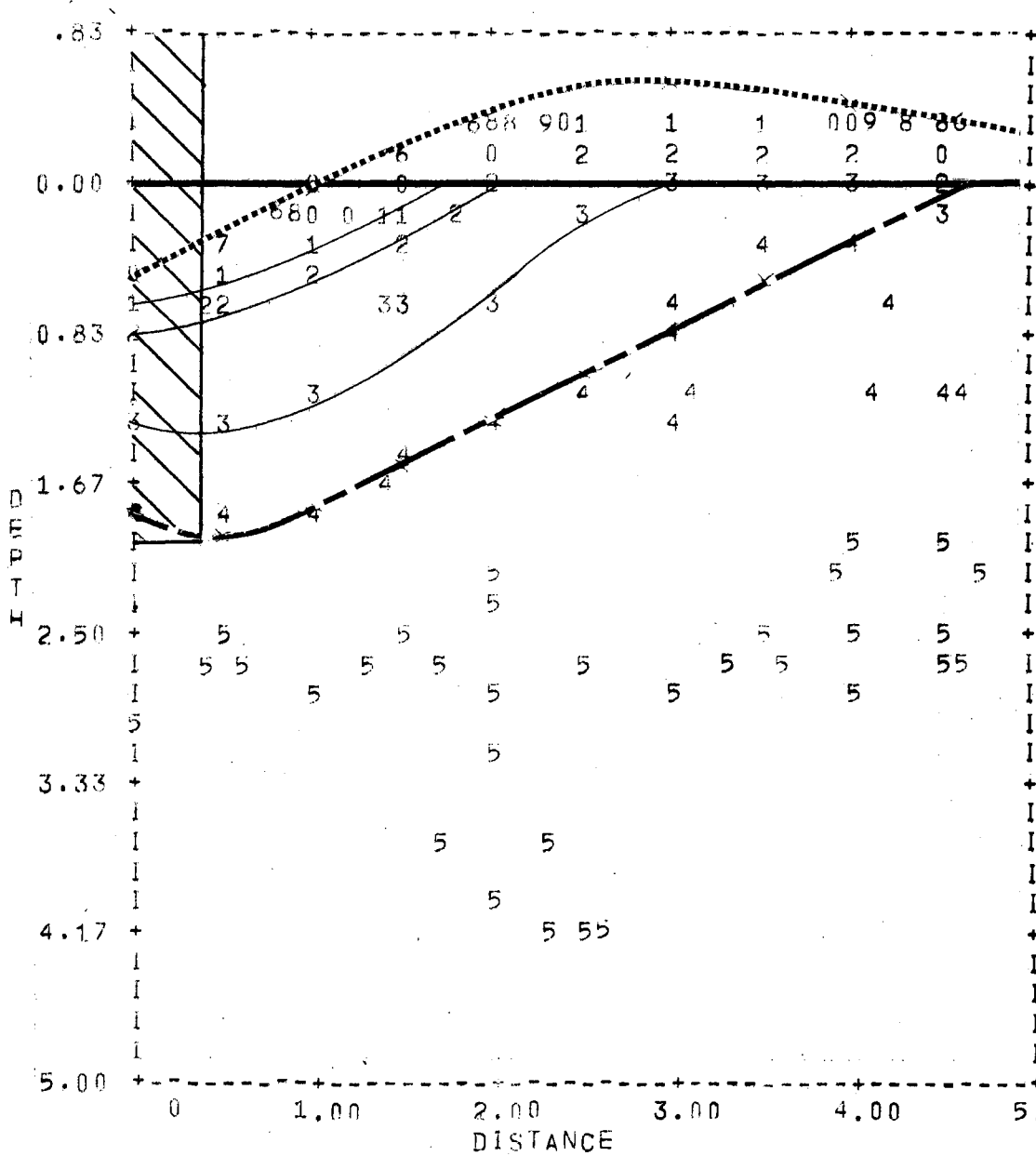
DENSITY PATTERN OF UNDISTURBED
ARTIFICIAL COARSE SOIL

APPENDIX A-XII



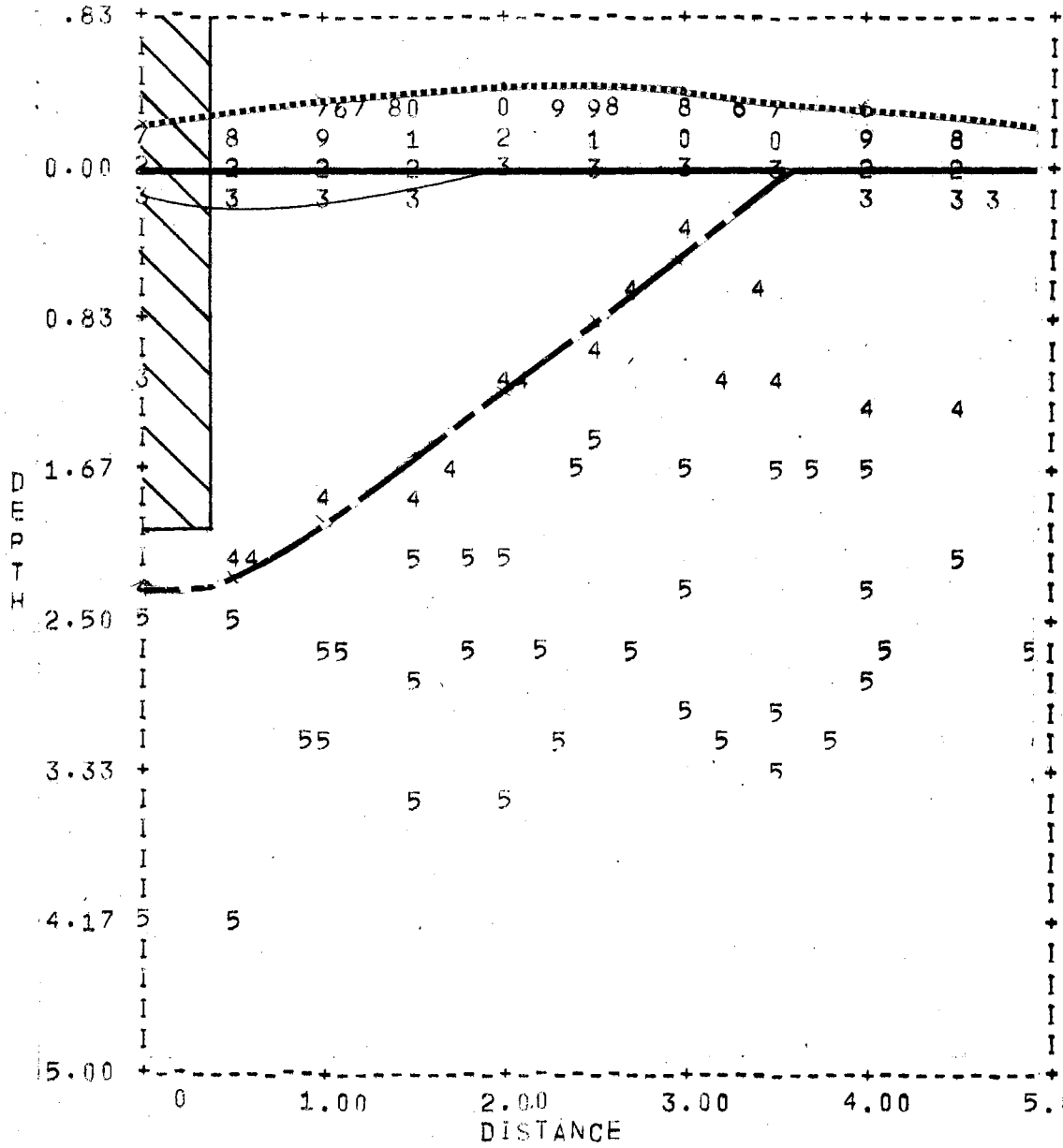
DENSITY PATTERN OF OPENER 0-60 IN ARTIFICIAL COARSE SOIL

APPENDIX A-XIII



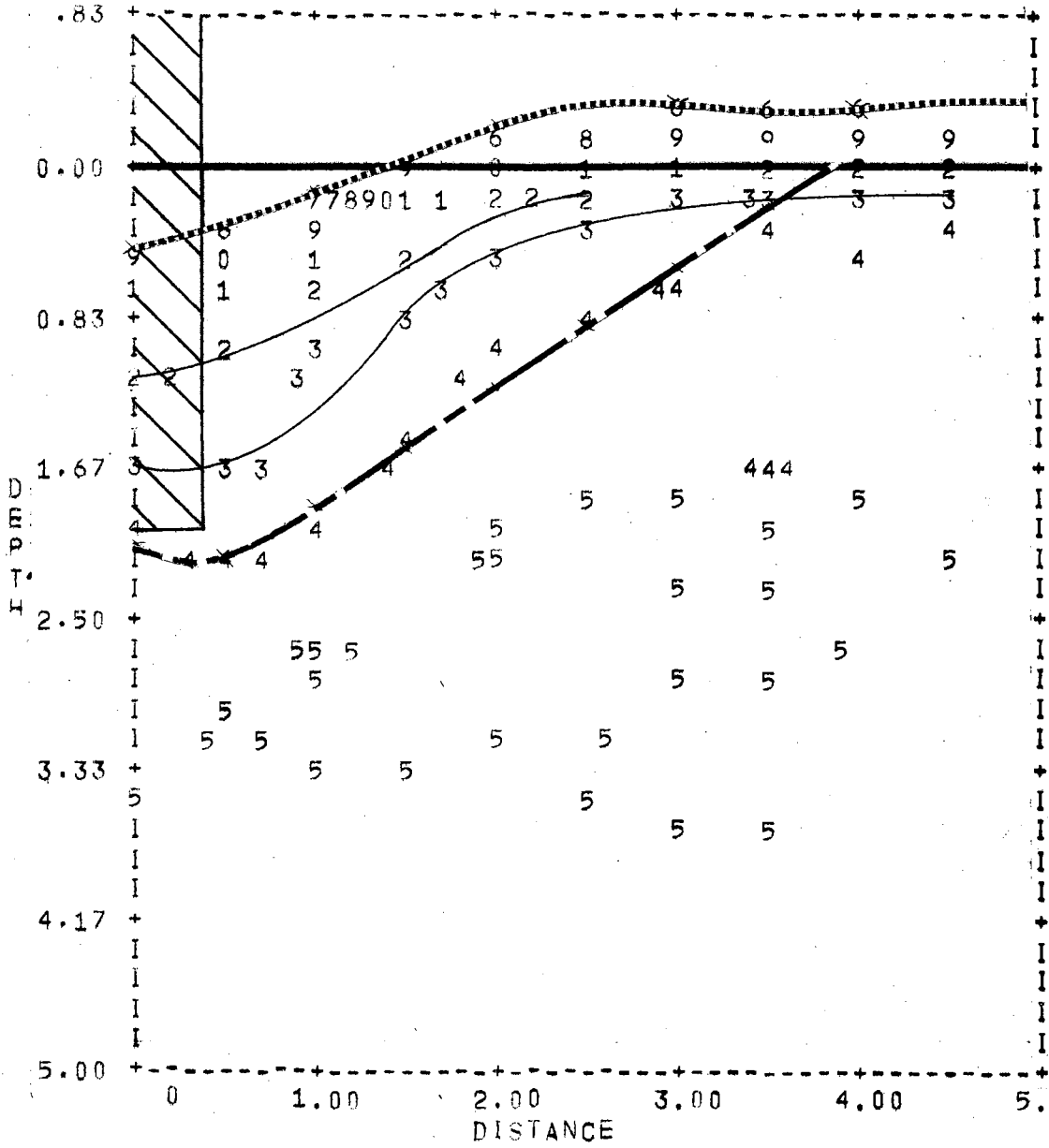
DENSITY PATTERN OF OPENER 0-75 IN
ARTIFICIAL COARSE SOIL

APPENDIX A-XIV



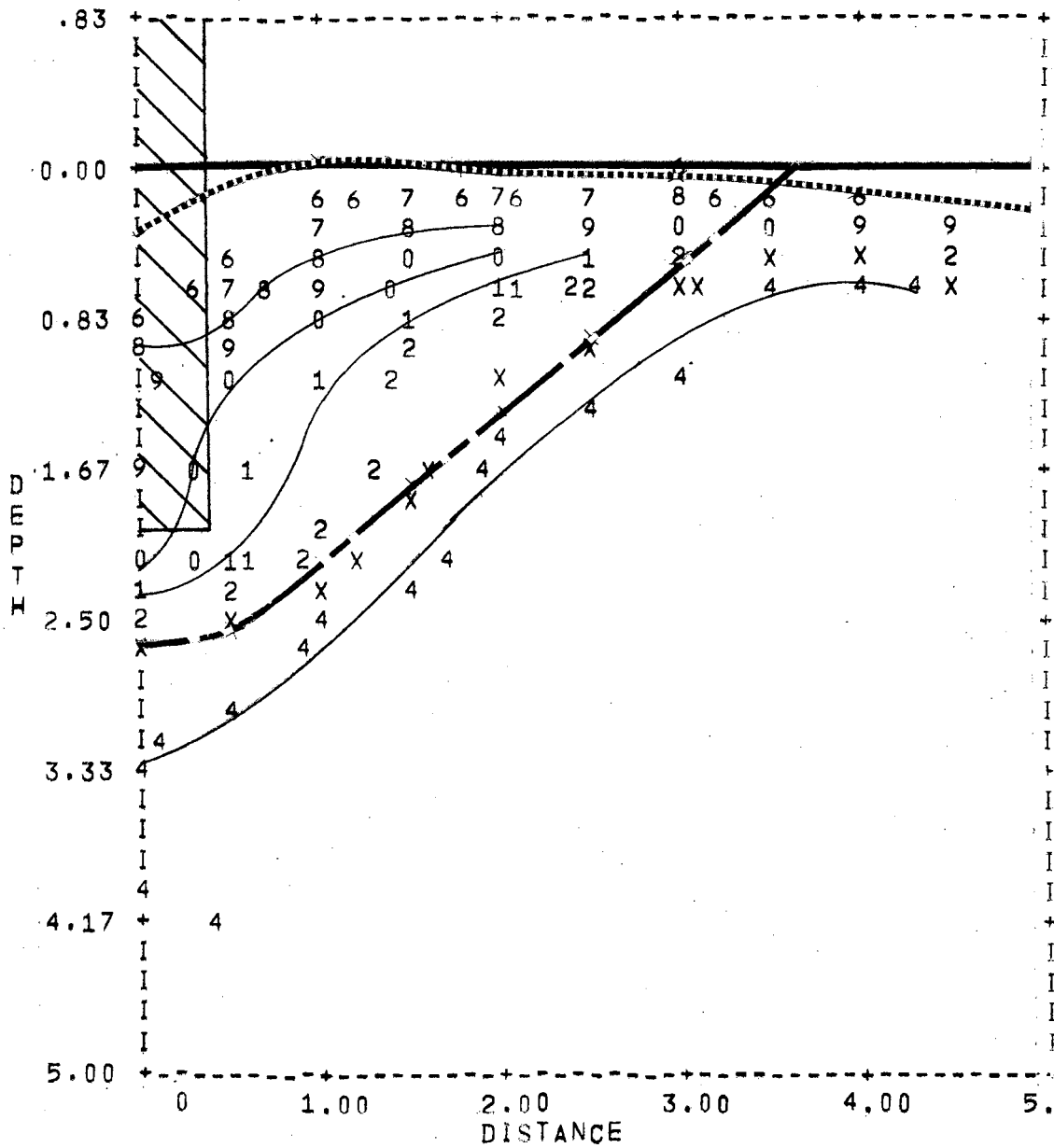
DENSITY PATTERN OF OPENER 0-82 1/2 IN
ARTIFICIAL COARSE SOIL

APPENDIX A-XV



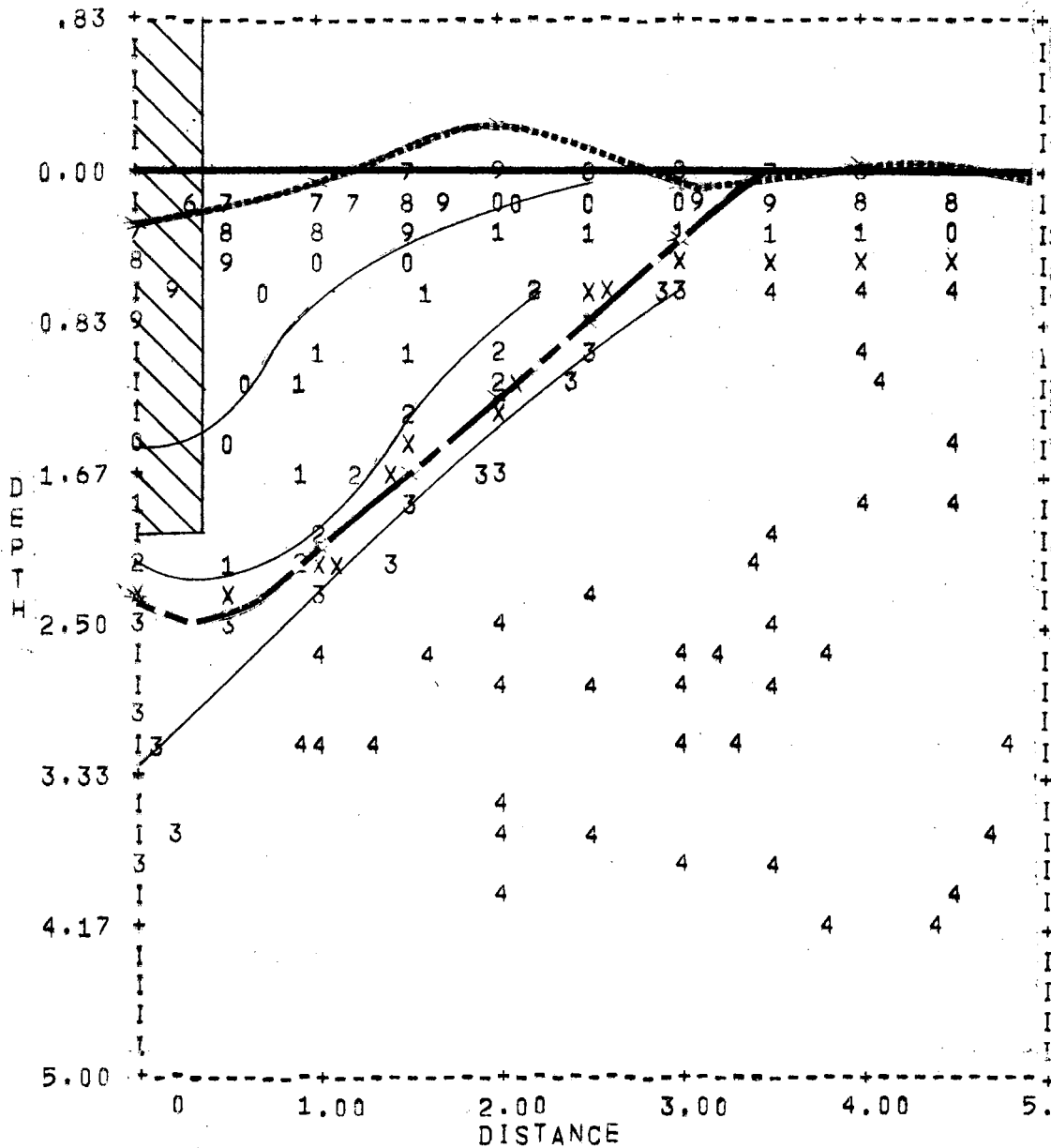
DENSITY PATTERN OF OPENER 45-60 IN
ARTIFICIAL COARSE SOIL

APPENDIX A-XVI



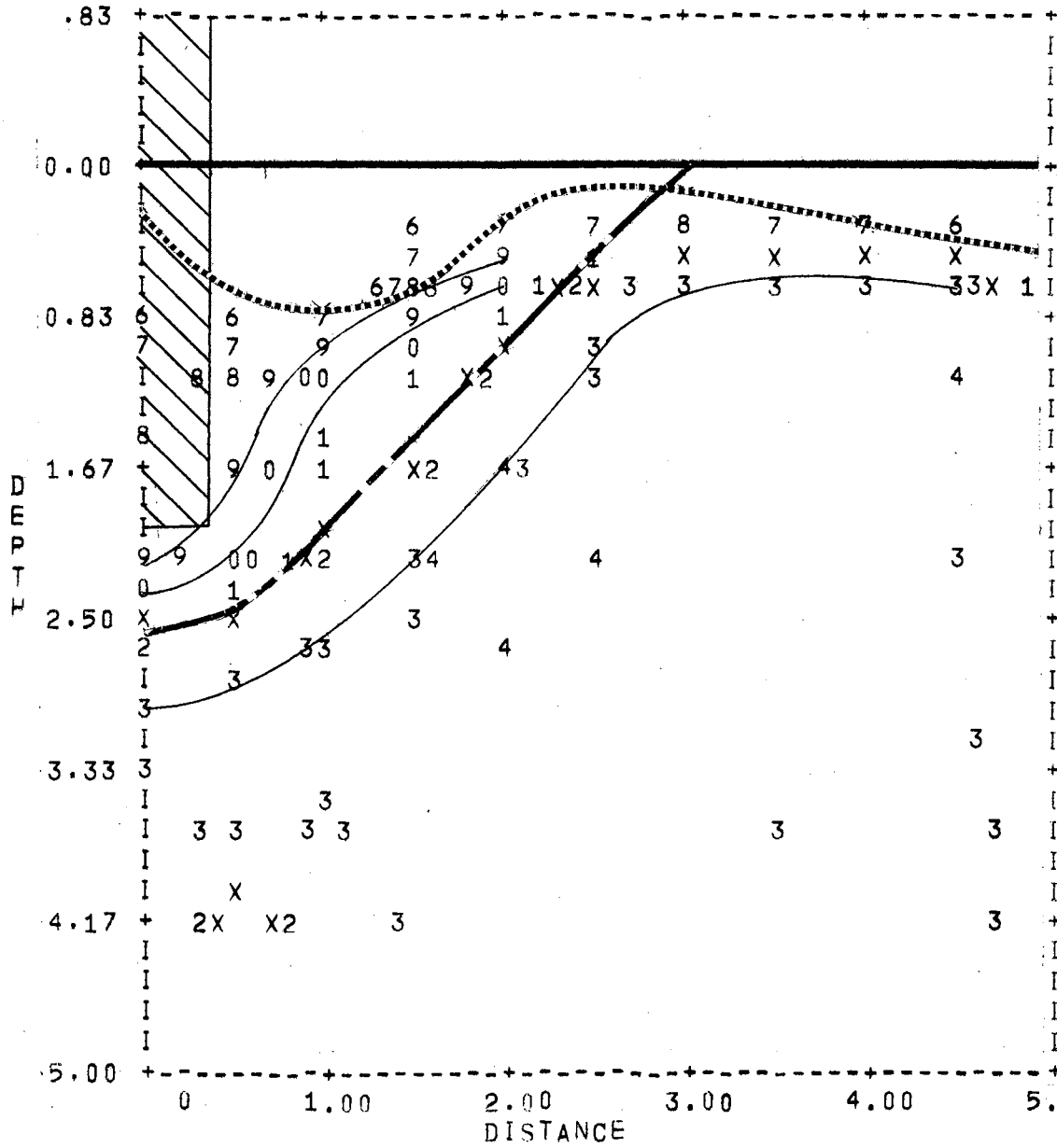
DENSITY PATTERN OF OPENER 0-75 IN NATURAL MEDIUM SOIL

APPENDIX A-XVII



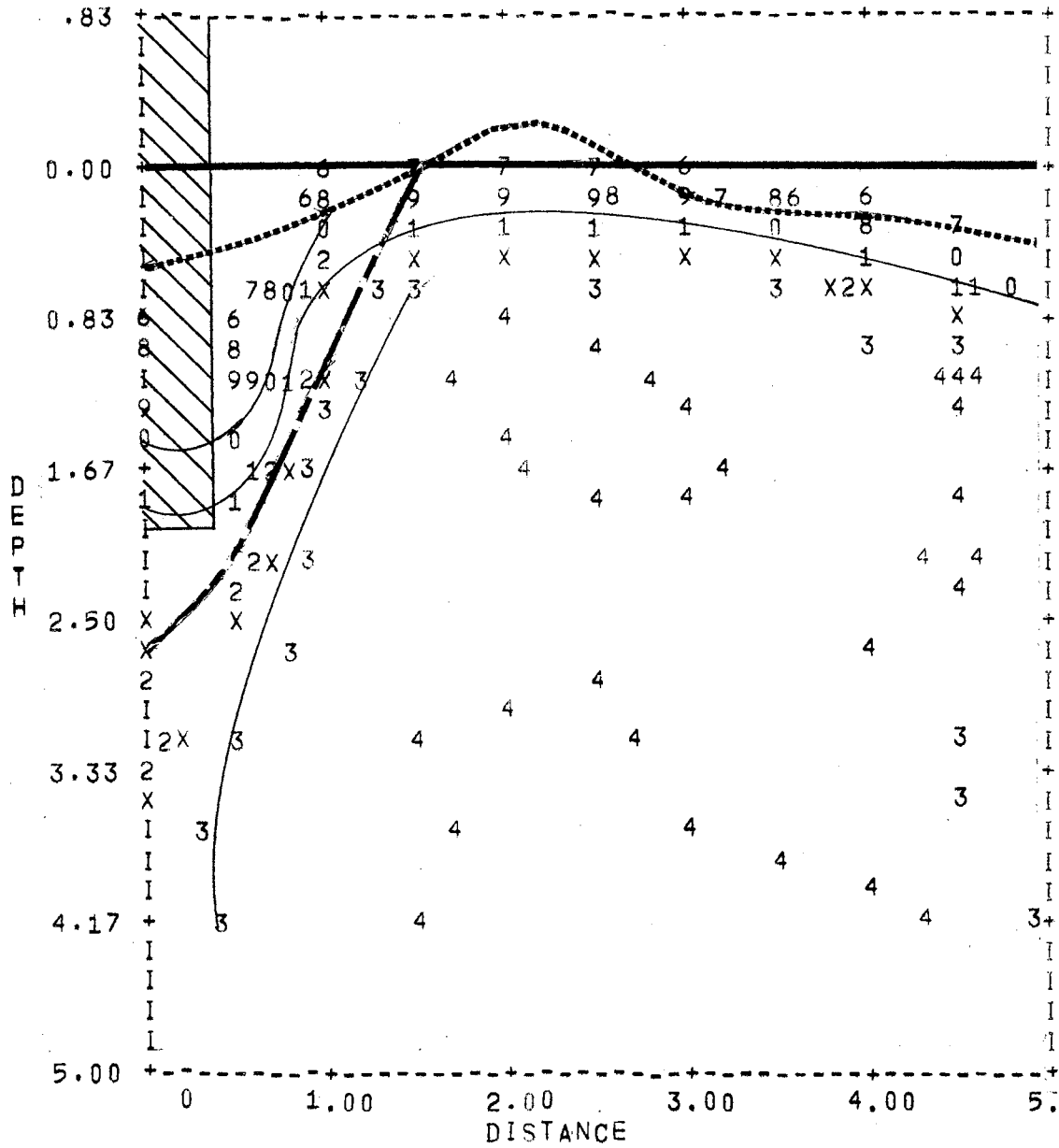
DENSITY PATTERN OF OPENER 0-82 1/2 IN' NATURAL MEDIUM SOIL

APPENDIX A-XVIII



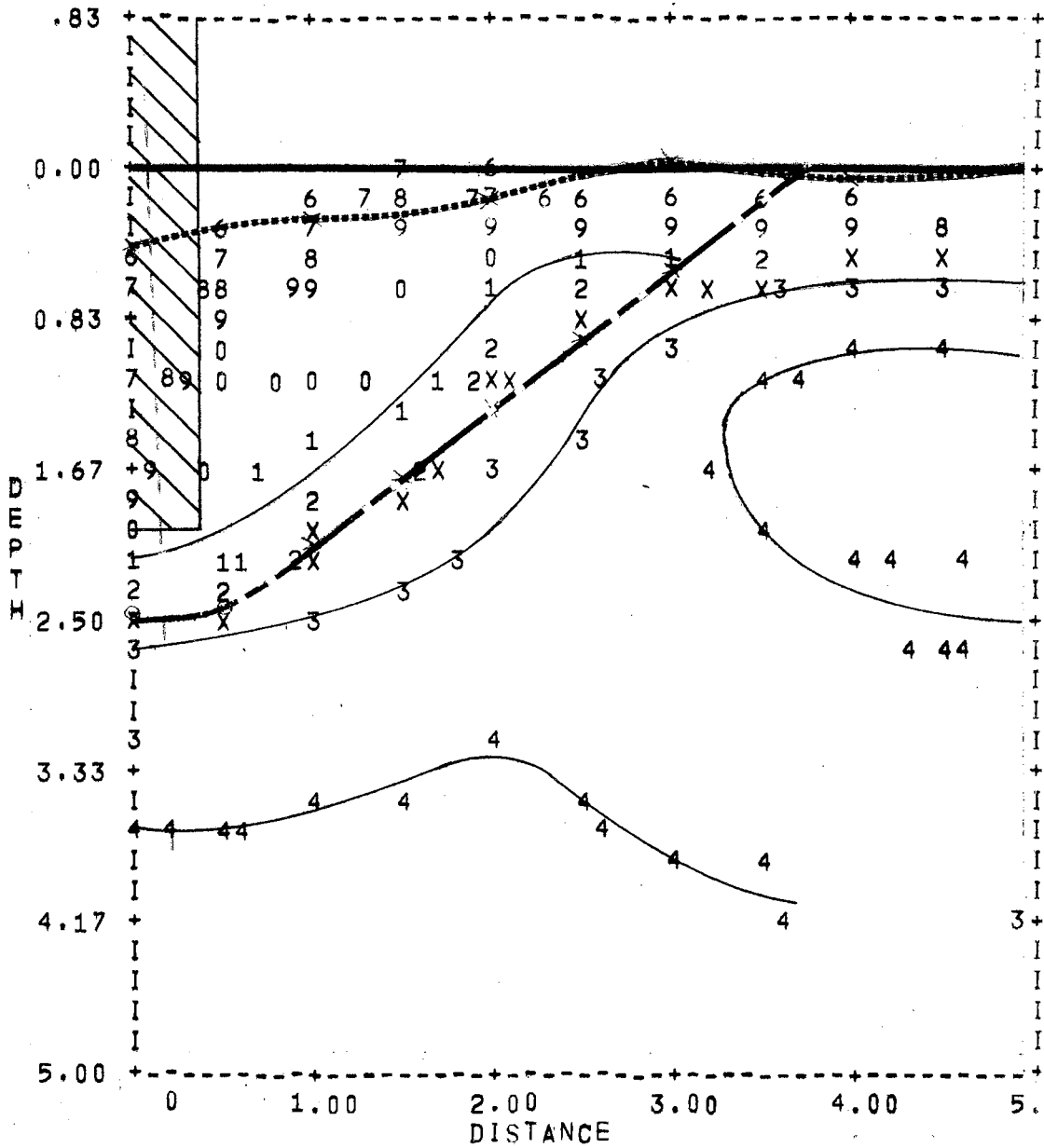
DENSITY PATTERN OF OPENER 45-60 IN
NATURAL MEDIUM SOIL

APPENDIX A-XIX



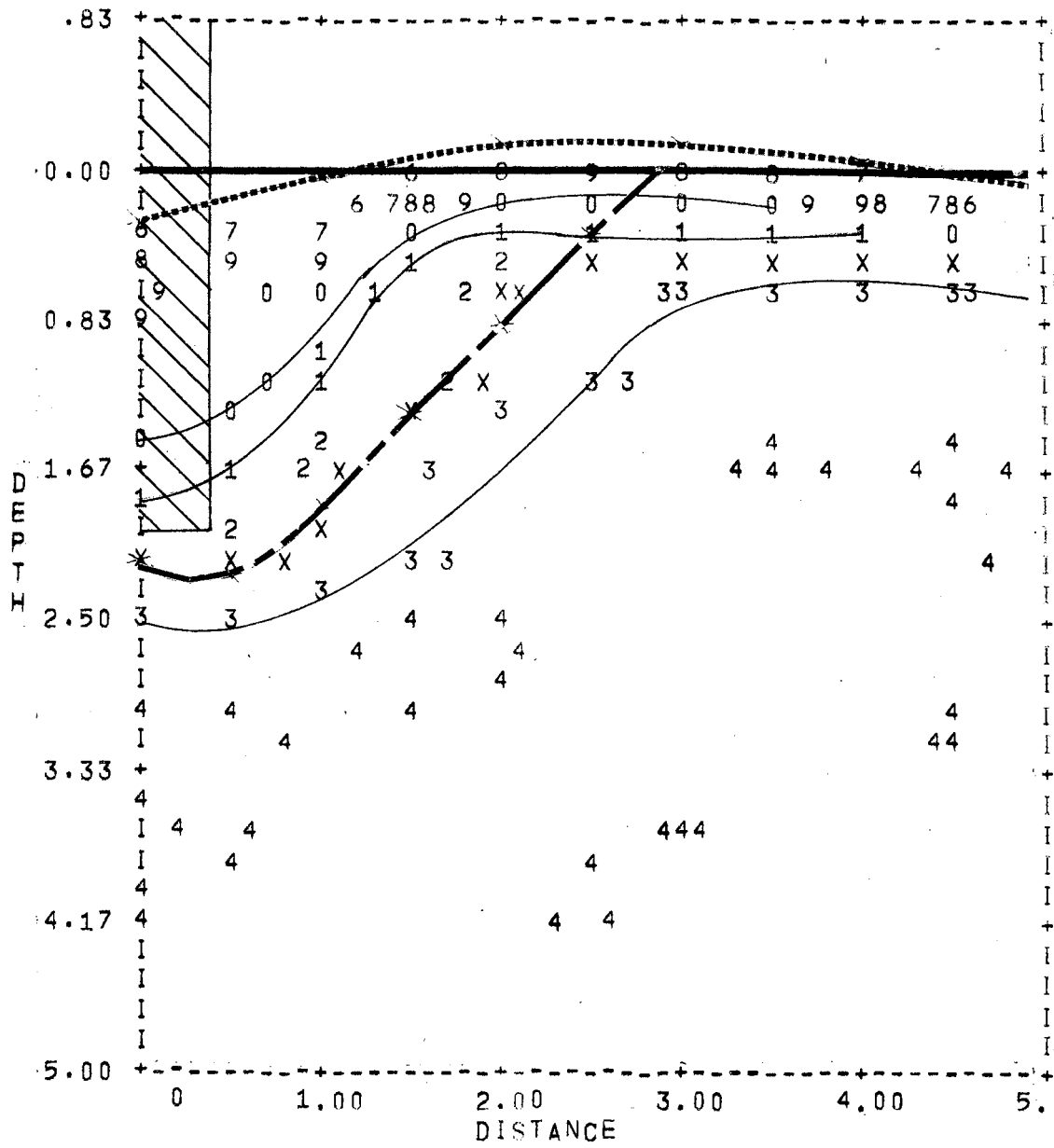
DENSITY PATTERN OF OPENER 45-75 IN
NATURAL MEDIUM SOIL

APPENDIX A-XX



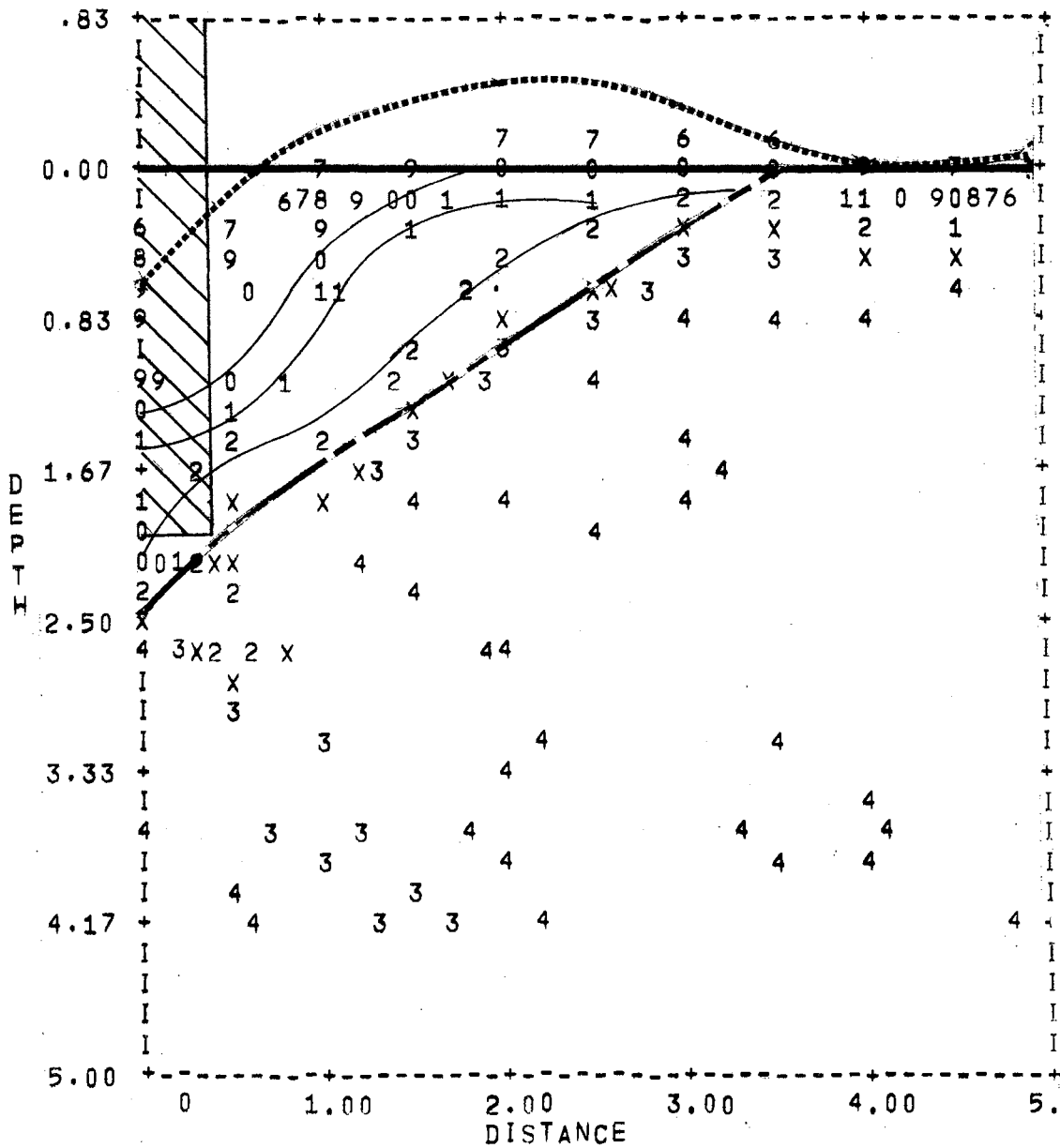
DENSITY PATTERN OF OPENER 45-82 1/2 IN NATURAL MEDIUM SOIL

APPENDIX A-XXI



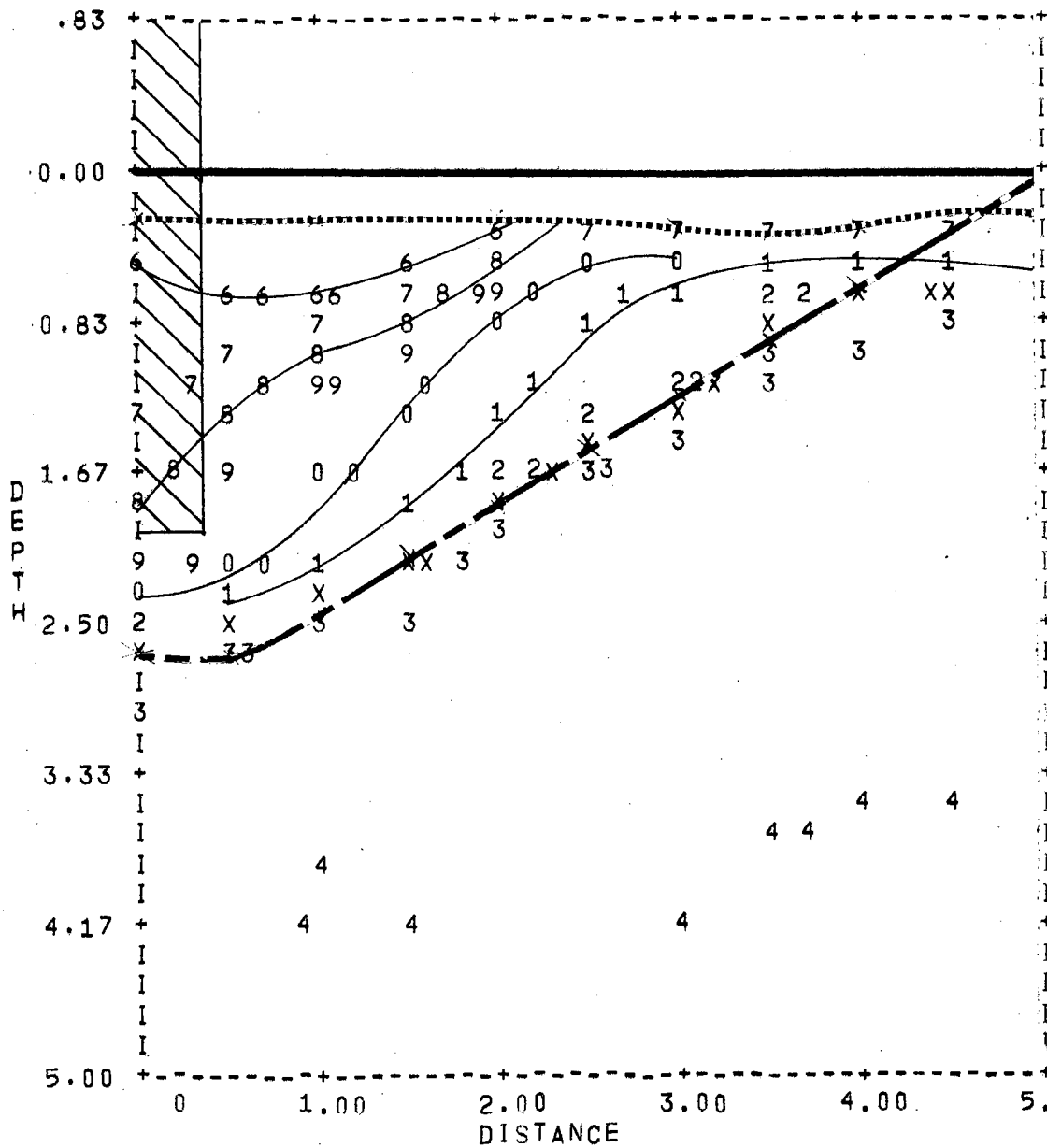
DENSITY PATTERN OF OPENER 60-60 IN NATURAL MEDIUM SOIL

APPENDIX A-XXII



DENSITY PATTERN OF OPENER 60-75 IN NATURAL MEDIUM SOIL

APPENDIX A-XXIII



DENSITY PATTERN OF OPENER 60-82 1/2 IN NATURAL MEDIUM SOIL

VITA

George Henry Abernathy

Candidate for the Degree of

Doctor of Philosophy

Thesis: SOIL DENSITY MODIFICATION WITH FURROW OPENERS OF SIMPLE GEOMETRIC SHAPE

Major Field: Engineering

Biographical:

Personal Data: Born at West Newton, Pennsylvania, November 9, 1929 the son of Ellis H. and Lasca G. Abernathy; moved to Roy, New Mexico soon thereafter.

Education: Graduated from high school at Roy, New Mexico in 1948; received Bachelor of Science degree from the New Mexico State University, with a major in Agricultural Engineering, in June, 1952; received Master of Engineering degree from the University of California, Davis, in June, 1956; completed requirements for the Doctor of Philosophy degree in May, 1967.

Professional Experience: Entered the United States Army, Corps of Engineers, in 1952 as Second Lieutenant; served in Japan and Korea, supervised road construction and became company executive officer; summer employment, 1955, as Test Engineer with International Harvester, Combine Division; became Assistant Research Specialist at University of California in September, 1955, designing experimental fruit harvesting machinery; accepted present position of Assistant Professor of Agricultural Engineering, performing research on cotton production machinery at New Mexico State University in 1957.